MOTOROLA SOLUTIONS

ACCREDITED
TESTING CERT # 2518.01

DECLARATION OF COMPLIANCE: MPE/SAR ASSESSMENT
Part 1 of 2

EME Test Laboratory
8000 West Sunrise Blvd
Fort Lauderdale, FL. 33322

Date of Report: March 11, 2013
Report Revision: O
Report ID: SR10953 Full PCII_MPE_Report: DVR700 with Companion Mobile APX Dual Bands VHF HP and UHF R1 HP Rev.O_130311.

Responsible Engineer:	Kim Uong (Principal Staff EME Test Engineer)
Report author:	Kim Uong (Principal Staff EME Test Engineer)
Date(s) Tested:	DVR: 10/12/2012 Companion Mobile: 9/15/2012 – 9/17/2012 (VHF Test Dates)
Manufacturer/Location:	Futurecom Systems Group Inc., Concord, Ontario, Canada
Date submitted for test:	10/1/2012
DUT Description:	DVR: 764-806 MHz, Digital Vehicular Repeater. Companion Mobile: APX7500 Dual Band VHF 100W and UHF 100W
Test TX mode(s):	CW
Max. Power output:	DVR: 5W (100% duty cycle) Companion Mobile: 120W (50% duty cycle, PTT)
TX Frequency Bands:	DVR: 764-776MHz (talk around); 794-806 MHz (repeater) Companion Mobile: 136-174 MHz (VHF) and 380-470MHz (UHF R1)
Signaling type:	FM; APCO 25
Model(s) Tested:	DVR: DQPMDVR7000P Companion Mobile: M30TXS9PW1AN (VHF: M30KTS9PW1AN)
Model(s) Certified:	DQPMDVR7000P (DVR)
Serial Number(s):	5060955 (DVR); 123ABC4567 (Companion Mobile, VHF)
Classification:	Occupational/Controlled Environment
FCC ID:	LO6-DVRS700 Part 22 & 90: 763-775MHz, 793-805MHz, 806-809MHz; 150.8-173.4MHz; 406.1-470MHz; Results outside FCC bands are not applicable for FCC compliance demonstration.

Based on the information and the testing results provided herein, the undersigned certifies that when used as stated in the operating instructions supplied, said product complies with the national and international reference standards and guidelines listed in section 3.0 of this report. This report shall not be reproduced without written approval from an officially designated representative of the Motorola Solutions Inc. EME Laboratory.
I attest to the accuracy of the data and assume full responsibility for the completeness of these measurements.
This reporting format is consistent with the suggested guidelines of the TIA TSB-159 April 2006
The results and statements contained in this report pertain only to the device(s) evaluated herein.

Deanna Zakharia

Deanna Zakharia
EME Lab Senior Resource Manager and Laboratory Director

Approval Date: 3/18/2013

Document Revision History

Date	Revision	Comments
3/11/2013	O	Initial release

Part 1 of 2: MPE Assessment for VHF (136-174MHz) 100W
Part 2 of 2: MPE Assessment for UHF (380-470MHz) 100W

Part 1 of 2

1.0 Introduction

This report details the test setup, test equipment and test results of Maximum Permissible Exposure (MPE) performed at Motorola Solutions' outside test site and Specific Absorption Rate (SAR) simulations for DVR product FCC ID: LO6-DVRS700 (Model # DQPMDVR7000P) when used with Companion Mobile FCC ID: AZ492FT4898 (Model # M30TXS9PW1AN).

2.0 Abbreviations / Definitions

APCO: Association of Public-Safety Communications Officials
BS: Bystander
C4FM: Compatible 4-Level Frequency Modulation
CNR: Calibration Not Required
CQPSK: Compatible Quadrature Phase Shift Keying
CW: Continuous Wave
DUT: Device Under Test
DVR: Digital Vehicular Repeater
EME: Electromagnetic Energy
F2: 2 slot Time Division Multiple Access
FM: Frequency Modulation
MPE: Maximum Permissible Exposure
NA: Not Applicable
PB: Passenger Backseat
PF: Passenger Front seat
PTT: Push to Talk
SAR: Specific Absorption Rate
TDMA: Time Division Multiple Access

3.0 Referenced Standards and Guidelines

This product is designed to comply with the following applicable national and international standards and guidelines.

- United States Federal Communications Commission, Code of Federal Regulations; Rule Part 47CFR § 1.1310, § 2.1091 (d) and § 2.1093 for RF Exposure, where applicable.
- Federal Communications Commission, "Evaluating Compliance with FCC Guidelines for Human Exposure to Radio frequency Electromagnetic Fields", OET Bulletin 65, Supplement C (Edition 01-01), FCC, Washington, D.C.: June 2001.
- American National Standards Institute (ANSI) / Institute of Electrical and Electronics Engineers (IEEE) C95. 1-1999
- American National Standards Institute (ANSI) / Institute of Electrical and Electronics Engineers (IEEE) C95. 1-1992. Specific to FCC rules and regulations.
- Institute of Electrical and Electronics Engineers (IEEE) C95.3-2002
- Ministry of Health (Canada) Safety Code 6 (2009), Limits of Human Exposure to Radio frequency Electromagnetic Fields in the Frequency Range from 3 kHz to 300 GHz

4.0 Power Density Limits

Table 1 – Occupational / Controlled Exposure Limits

Frequency Range (MHz)	FCC OET Bulletin 65 Supplement C mW/cm^2	ICNIRP W/m^2	IEEE C95.1 1992/1999 mW/cm^2	IEEE C95.1 2005 W/m^2	RSS 102 issue 4 - 2010 W/m^2
30 - 300	1.0				*10.0
10 - 400		10.0			
100 - 300			1.0	10.0	
300 - 1,500	f/300				f/30
300 - 3,000			f/300	f/30	
400 - 2,000		f/40			
1,500 - 15,000					50.0
1,500 - 100,000	5.0				
2,000 – 300,000		50.0			
3,000 - 300,000			10.0	100.0	

*Power density limit is applicable at frequencies greater than 100MHz

Table 2 – General Population / Uncontrolled Exposure Limits

Frequency Range (MHz)	FCC OET Bulletin 65 Supplement C mW/cm^2	ICNIRP W/m^2	IEEE C95.1 1992/1999 mW/cm^2	IEEE C95.1 2005 W/m^2	RSS 102 issue 4 – 2010 W/m^2
30 – 300	0.2				*2.0
10 – 400		2.0			
100 – 300			0.2		
100 – 400				2.0	
300 – 1,500	f/1,500				f/150
400 – 2,000		f/200		f/200	
300 – 15,000			f/1,500		
1,500 – 15,000					10.0
1,500 – 100,000	1.0				
2,000 – 100,000				10.0	
2,000 – 300,000		10.0			

*Power density limit is applicable at frequencies greater than 100MHz

5.0 N_c Test Channels

The number of test channels are determined by using Equation 1 below. This equation is available in FCC's KDB 447498. The test channels are appropriately spaced across the antenna's frequency range.

Equation 1 – Number of test channels
$N_c = \text{Round}\{[100(f_{high} - f_{low})/f_c]^{0.5} \text{ x } (f_c / 100)^{0.2}\}$

where N_c is the number of test channels, f_{high} and f_{low} are the highest and lowest frequencies within the transmission band, f_c is the mid-band frequency, and frequencies are in MHz.

6.0 Measurement Equipment

Table 3 - Equipment

Equipment Type	Model #	SN	Calibration Date	Calibration Due Date
Automobile	2003 Ford Crown Victoria, 4-Door	NA	NA	NA
Survey Meter Probe – E-Field	ETS Model HI-2200 ETS Model E100	00086887 00126277	6/11/2012	6/11/2013
Survey Meter Probe – H-Field	ETS Model HI-2200 ETS Model H200	00086887 00084225	6/11/2012	6/11/2013

E-field measurements are in mW/cm^2.
H-field measurements are in A/m.

7.0 Measurement System Uncertainty Levels

Table 4 - Uncertainty Budget for Near Field Probe Measurements

	Tol. (± %)	Prob. Dist.	Divisor	u_i (±%)	v_i
Measurement System					
Probe Calibration	6.0	N	1.00	6.0	∞
Survey Meter Calibration	3.0	N	1.00	3.0	∞
Hemispherical Isotropy	8.0	R	1.73	4.6	∞
Linearity	5.0	R	1.73	2.9	∞
Pulse Response	1.0	R	1.73	0.6	∞
RF Ambient Noise	3.0	R	1.73	1.7	∞
RF Reflections	8.0	R	1.73	4.6	∞
Probe Positioning	10.0	R	1.73	5.8	∞
Test sample Related					
Antenna Positioning	3.0	N	1.00	3.0	∞
Power drift	5.0	R	1.73	2.9	∞
Combined Standard Uncertainty		RSS		12.2	∞
Expanded Uncertainty (95% CONFIDENCE LEVEL)		k=2		24	

8.0 Product and System Description

This device (FCC ID: LO6-DVRS700, Model # DQPMDVR7000P) is a MOBEXCOM Digital Vehicular Repeater (DVR) manufactured by FUTURECOM Systems Group. The DVR, in addition to standalone operation, is capable of interfacing to a companion mobile radio using serial data protocol for audio and control. The full duplex DVR provides local area coverage for portable to portable communication in the DVR's operating band while the Companion Mobile radio provides wide-area coverage extension.

The system can operate in the following modes: Mobile mode - where the vehicular repeat function is off but receives emergency and mode change commands from portable devices; Local mode - with portable to portable repeat and network monitoring capabilities; and System mode - with portable to portable repeat functions with full network interconnect. Furthermore, the DVRS offers a busy lockout feature where a simulcast prevention algorithm is used for seamless multi-vehicle operation on the same channel. Moreover, the system supports emergency calls in the MDC1200 signaling format. Other system features include field programmability, seamless interface to a mobile radio through the control head bus, controllability via a mobile radio control head, as well as remotely by a dispatcher or portable user. The DVR supports up to 64 channels and 255 talk groups, MDC1200, DTMF, EIA, CCIR signaling as well as PL and DPL. The DVR supports programmability of leading and/or trailing tones, and audio and TX priorities per mode as well as talk group steering.

This test report covers the RF Exposure performance of the DVR FCC ID: LO6-DVRS700 (700MHz 5watts) interfaced with, and transmitting simultaneously with a Companion Mobile radio FCC ID: AZ492FT4898 (VHF 100 watts), and with both units installed in a typical vehicle.

The DVR transmit frequency ranges are 764-775MHz (talk around) and 794-806MHz (repeater) at transmit duty cycle up to 100%. The Companion Mobile transmit frequency range is 136-174MHz at transmit duty cycle up to 50% (PTT). The DVR antenna is limited to ¼ wave (0dBd gain) mounted at the center of the trunk, and the Companion Mobile VHF antennas are limited to ¼ wave (0dBd gain) mounted at the side of the roof (45cm from the center of the roof). The maximum conducted power delivered to the DVR antenna is 5 watts, due to the filter losses, while the maximum conducted power delivered to the Companion Mobile is 120 watts.

This device will be marketed to and used by employees solely for work-related operations, such as public safety agencies, e.g. police, fire and emergency medical. User training is the responsibility of these agencies which can be expected to employ the usage instructions, safety information and operational cautions set forth in the user's manual, instructional sessions or other means.

Accordingly this product is classified as Occupational/Controlled Exposure. However, in accordance with FCC requirements, the passengers inside the vehicle and the bystanders external to the vehicle are evaluated to the General Population/Uncontrolled Exposure Limits.

(Note that "Bystanders" as used herein are people other than operator)

9.0 Options and Accessories

The offered antennas for the DVR and the Companion Mobile are listed on the table 5.

Table 5

FCC ID	Model/Description	Antennas
LO6-DVRS700	DQPMDVR7000P 764-806MHz, 5 watt, vehicular repeater	HAF4016A (764-870 MHz, 1/4 wave Trunk mount, 0dBd gain)
AZ492FT4898	M30TXS9PW1AN Companion Mobile: APX7500 Dual Band VHF 100W - UHF 100W (136-174MHz & 380-470MHz)	HAD4008A (150.8-162 MHz, 1/4 wave Roof mount, 0dBd gain) HAD4009A (162-174 MHz, 1/4 wave Roof mount, 0dBd gain) HAD4021A (136-174 MHz, 1/4 Wave Roof mount, 0dBd gain)

10.0 Test Set-Up Description

Assessments were performed with DVR and the companion mobile radio installed in the test vehicle while engine was at idle, at the specified distances and test locations indicated in sections 11.0, 12.0 and Appendix A.

- DVR: the ¼ wave 0dBd gain antenna (HAF4016A) was assessed while mounted at the trunk.

- Companion mobile: the ¼ wave 0dBd gain antennas (HAD4008A, HAD4009A, HAD4021A) were assessed while mounted at the side of the roof (driver side) of the test vehicle.

All antennas described in Table 5 were considered in order to develop the test plan for this product. Antennas were installed and tested per their appropriate mount locations (Roof / Trunk) and defined test channels.

11.0 Method of Measurement for DVR with trunk mounted antenna(s)

(Referenced Appendix A for illustration of antenna location and test distances).

11.1. External/Bystander vehicle MPE measurements

The DVR antenna is located at the center of the trunk. Refer to Appendix A for antenna location and distance.

MPE measurements for bystander (BS) conditions are determined by taking the average of (10) measurements in a 2 m vertical line for each of the (5) bystander test locations indicated in Appendix A with 20cm height increments at the test distance of 90cm from the test vehicle's body, as stated in the user manual. The measurement probe is positioned orthogonal to antenna (typically parallel to ground with a vertically mounted antenna) and aimed directly at the antenna's axis. These measurements are representative of persons other than the operator standing next to the vehicle.

11.2. Internal/Passenger vehicle MPE measurements

The DVR antenna is located toward the center of the trunk at a minimum 85cm from backseat passenger. Refer to Appendix A for antenna location and distance.

MPE measurements for passenger front seat (PF) and backseat (PB) conditions are determined by taking the average of the (3) measurements (Head, Chest, and Lower Trunk) inside the vehicle for both the front and back seats.

The backseat is a bench seat and therefore each position (Head, Chest & Lower Trunk) were scanned across (horizontally) the seat starting from the middle of the seat to the edge of the seat stopping 20cm from the vehicle door. Similar process was used in the front bucket seat.

The probe handle is oriented parallel (horizontal) to the ground and pointed towards the back of the vehicle. The probe handle is not oriented normal to the seat surface. The probe head (incorporating the field sensors) is scanned continuously (using the max-hold function available in the meter) along three test axes which are parallel to the seat angle (intended as the line determined by the intersection of the plane of the seat and the plane of the backrest) and are 20cm from the seat surface. One test axis is at the Head height, another is at the Chest height, and another is at the Lower Trunk height. The maximum field level value recorded for each test axis is logged. The MPE is determined by averaging these three maximum values regardless of the geometrical location where they were observed. For instance, the locations of the three maxima may lie on different vertical (relative to ground) lines.

This approach leads to results that are representative of the exposure of vehicle occupants since it is based on an average across the body portions closest to the antenna for trunk mount position, and is conservatively biased because the highest results for each test axis are combined, e.g. the highest head exposure could be in the middle of the seat while the highest lower trunk exposure could be closer to the door.

12.0 Method of Measurement for Companion Mobile with roof mounted antenna(s)

(Referenced Appendix A for illustration of antenna location and test distances).

12.1. External/Bystander vehicle MPE measurements

The Companion Mobile antennas are located at the side of the roof (45cm from the center of the roof, along the width of the vehicle, driver side). Refer to Appendix A for antenna location and distance.

MPE measurements for bystander (BS) conditions are determined by taking the average of (10) measurements in a 2 m vertical line for each of the (5) bystander test locations indicated in Appendix A with 20cm height increments at the test distance of 90cm from the test vehicle's body, as stated in the user manual. The measurement probe is positioned orthogonal to antenna (typically parallel to ground with a vertically mounted antenna) and aimed directly at the antenna's axis. These measurements are representative of persons other than the operator standing next to the vehicle.

12.2. Internal/Passenger vehicle MPE measurements

The Companion Mobile antennas are located at the side of the roof (45cm from the center of the roof, along the width of the vehicle, driver side). Refer to Appendix A for antenna location and distance.

MPE measurements for passenger front seat (PF) and backseat (PB) conditions are determined by taking the average of the (3) measurements (Head, Chest, and Lower Trunk) inside the vehicle for both the front and back seats.

The backseat is a bench seat and therefore each position (Head, Chest & Lower Trunk) were scanned across (horizontally) the seat starting from the middle of the seat to the edge of the seat stopping 20cm from the vehicle door. Similar process was used in the front bucket seat.

The probe handle is oriented parallel (horizontal) to the ground and pointed towards the back of the vehicle. The probe handle is not oriented normal to the seat surface. The probe head (incorporating the field sensors) is scanned continuously (using the max-hold function available in the meter) along three test axes which are parallel to the seat angle (intended as the line determined by the intersection of the plane of the seat and the plane of the backrest) and are 20cm from the seat surface. One test axis is at the Head height, another is at the Chest height, and another is at the Lower Trunk height. The maximum field level value recorded for each test axis is logged. The MPE is determined by averaging these three maximum values regardless of the geometrical location where they were observed. For instance, the locations of the three maxima may lie on different vertical (relative to ground) lines.

This approach leads to results that are representative of the exposure of vehicle occupants since it is based on an average across the body portions closest to the antenna for roof mount position, and is conservatively biased because the highest results for each test axis are combined, e.g. the highest head exposure could be in the middle of the seat while the highest lower trunk exposure could be closer to the door.

13.0 MPE Calculations

The final MPE results for this mobile radio are presented in section 15.1 Tables 7 - 10. The results for the DVR are based on the 100% duty cycle while the results for the Companion Mobile are based on 50% duty cycle for PTT.

Below is an explanation of how the MPE results are calculated. Refer to Appendix D for MPE measurement results and calculations.

External to vehicle (Bystander) - 10 measurements are averaged over the body (*Avg_over_body*).
Internal to vehicle (Passengers) - 3 measurements are averaged over the body (*Avg_over_body*).

The Average over Body test methodology is consistent with IEEE/ANSI C95.3-2002 guidelines.

Therefore;

Equation 2 – Power Density Calculation *(Calc._P.D.)*

$$Calc.\_P.D. = (Avg\_over\_body) * (probe\_frequency\_cal\_factor) * (duty\_cycle)$$

Note1: The highest "average" cal factors from the calibration certificates were selected for the applicable frequency range. Linear interpretation was used to determine "probe_frequency_cal_factor" for the specific test frequencies.

Note 2: The E-field probe calibration certificate's frequency cal factors were determined by measuring V/m. The survey meter's results were measured in power density (mW/cm^2) and therefore the "probe_frequency_cal_factor" was squared in equation 2 to account for these results.

Note 3: The H-field probe calibration certificate's frequency cal factors were determined by measuring A/m. The survey meter's results were measured in A/m and therefore the "Avg_over_body" A/m results were converted to power density (mW/cm^2) using the equation 3. H-field measurements are only applicable to frequencies below 300MHz.

Equation 3 – Converting A/m to mW/cm^2

$$mW/cm\hat{}2 = (A/m)\hat{}2 * 37.699$$

Equation 4 – Power Density Maximum Calculation

$$Max\_Calc.\_P.D. = P.D.\_calc * \frac{\max\_output\_power}{initial\_output\_power}$$

Note 4: For initial output power> max_output_power; max_output_power / initial output power = 1

14.0 Antenna Summary

Table 6 below summarizes the tested antennas and their descriptions, mount location (roof/trunk), overlap of FCC bands, number of test channels per FCC KDB 447498 (FCC N_c) and actual number of tested channels (Actual N_c). This information was used to determine the test configurations presented in this report.

Table 6

#	DUT FCC ID (Model #)	Antenna Model	Frequency Range (MHz)	Physical Length (cm)	Gain (dBi)	Remarks	Mount Location (Roof/Trunk)	Overlap FCC Bands (MHz)	FCC N_c	Actual N_c
1	LO6-DVRS700 (DQPMDVR7000P)	HAF4016A	764-870	9.0	2.15	1/4 wave, wire	Trunk (center)	764-775	3	3
								794-806	3	3
2	AZ492FT4898 (M30TXS9PW1AN)	HAD4008A	150.8-162	45.5	2.15	1/4 wave, wire	Roof (45cm from center of the roof, Driver side)	150.8-162	3	3
3		HAD4009A	162-174	43.0	2.15	1/4 wave, wire		162-173.4	3	3
4		HAD4021A	136-174	51.7	2.15	1/4 wave, wire		150.8-173.4	4	7

15.0 Test Results Summary

The following tables below summarize the MPE results for each test configuration: antenna location, test positions (BS1: Bystander test location # 1, BS2: Bystander test location # 2, BS3: Bystander test location # 3, BS4: Bystander test location # 4, BS5: Bystander test location # 5, PB-Passenger Backseat, PF-Passenger Front seat), E/H field measurements, antenna model & freq. range, maximum output power, initial power, TX frequency, max calculated power density results, applicable FCC specification limits and % of the applicable specification limits.

15.1. MPE Test Results

Table 7 – DVR (700MHz 5W)

Bystander - MPE assessment for trunk mounted antenna

Trunk/ Roof	Test Location	E/H Field	Ant. Model	Max Pwr (W)	Initial Pwr (W)	Tx Freq (MHz)	Max Calc. P.D. (mW/ cm^2)	FCC Limit	% To Spec Limit
Trunk	BS1	E	HAF4016A (764-870MHz)	5.0	5.0	764.000	0.00	0.51	0.4
						770.000	0.00	0.51	0.2
						775.000	0.00	0.52	0.2
						794.000	0.00	0.53	0.2
						800.000	0.00	0.53	0.2
						806.000	0.00	0.54	0.3
	BS2	E	HAF4016A (764-870MHz)	5.0	5.0	764.000	0.00	0.51	0.9
						770.000	0.00	0.51	0.6
						775.000	0.00	0.52	0.7
						794.000	0.00	0.53	0.8
						800.000	0.00	0.53	0.9
						806.000	0.01	0.54	1.3
	BS3	E	HAF4016A (764-870MHz)	5.0	5.0	764.000	0.01	0.51	1.7
						770.000	0.01	0.51	1.2
						775.000	0.01	0.52	1.3
						794.000	0.01	0.53	1.0
						800.000	0.01	0.53	1.1
						806.000	0.01	0.54	1.7
	BS4	E	HAF4016A (764-870MHz)	5.0	5.0	764.000	0.01	0.51	1.6
						770.000	0.01	0.51	1.2
						775.000	0.01	0.52	1.4
						794.000	0.01	0.53	1.0
						800.000	0.01	0.53	1.0
						806.000	0.01	0.54	1.5
	BS5	E	HAF4016A (764-870MHz)	5.0	5.0	764.000	0.02	0.51	3.1
						770.000	0.01	0.51	2.7
						775.000	0.02	0.52	3.1
						794.000	0.01	0.53	2.3
						800.000	0.01	0.53	2.5
						806.000	0.02	0.54	3.3

Table 8 – DVR (700MHz 5W)

Passenger - MPE assessment for trunk mounted antenna

Trunk/ Roof	Test Location	E/H Field	Ant. Model	Max Pwr (W)	Initial Pwr (W)	Tx Freq (MHz)	Max Calc. P.D. (mW/ cm^2)	FCC Limit	% To Spec Limit
Trunk	PB	E	HAF4016A (764-870MHz)	5.0	5.0	764.000	0.03	0.51	5.8
						770.000	0.02	0.51	4.6
						775.000	0.04	0.52	7.1
						794.000	0.02	0.53	4.6
						800.000	0.02	0.53	4.5
						806.000	0.04	0.54	8.2
	PF	E	HAF4016A (764-870MHz)	5.0	5.0	764.000	0.01	0.51	2.8
						770.000	0.01	0.51	2.4
						775.000	0.02	0.52	2.9
						794.000	0.02	0.53	3.6
						800.000	0.02	0.53	3.3
						806.000	0.02	0.54	4.2

Table 9 – Companion Mobile (VHF 100W)
Bystander - MPE assessment for roof mounted antennas

Trunk/ Roof	Test Location	E/H Field	Ant. Model	Max Pwr (W)	Initial Pwr (W)	Tx Freq (MHz)	Max Calc. P.D. (mW/cm^2)	FCC Limit	% To Spec Limit
Roof	BS1	E	HAD4008A (150.8-162MHz)	120	116.0	150.800	0.09	0.20	43.2
					117.0	156.400	0.09	0.20	45.3
					117.0	162.000	0.10	0.20	48.8
			HAD4009A (162-174MHz)	120	117.0	162.000	0.08	0.20	40.9
					117.0	167.700	0.11	0.20	56.7
					118.0	173.400	0.14	0.20	68.9
			HAD4021A (136-174MHz)	120	116.0	136.000	0.07	0.20	35.2
					116.0	140.900	0.05	0.20	27.1
					116.0	145.900	0.06	0.20	29.4
					116.0	150.800	0.08	0.20	40.0
					116.0	158.300	0.09	0.20	43.1
					118.0	165.900	0.09	0.20	43.6
					118.0	173.400	0.11	0.20	56.4
	BS2	E	HAD4008A (150.8-162MHz)	120	116.0	150.800	0.12	0.20	58.2
					117.0	156.400	0.13	0.20	62.7
					117.0	162.000	0.14	0.20	69.1
			HAD4009A (162-174MHz)	120	117.0	162.000	0.12	0.20	61.3
					117.0	167.700	0.17	0.20	86.0
					118.0	173.400	0.18	0.20	89.2
			HAD4021A (136-174MHz)	120	116.0	136.000	0.09	0.20	47.1
					116.0	140.900	0.08	0.20	38.9
					116.0	145.900	0.10	0.20	50.4
					116.0	150.800	0.11	0.20	55.1
					116.0	158.300	0.12	0.20	57.8
					118.0	165.900	0.12	0.20	61.4
					118.0	173.400	0.14	0.20	70.7

Table 9 – Companion Mobile (VHF 100W) (cont'd)
Bystander - MPE assessment for roof mounted antennas

Trunk/ Roof	Test Location	E/H Field	Ant. Model	Max Pwr (W)	Initial Pwr (W)	Tx Freq (MHz)	Max Calc. P.D. (mW/cm^2)	FCC Limit	% To Spec Limit
Roof	BS3	E	HAD4008A (150.8-162MHz)	120	116.0	150.800	0.10	0.20	49.0
					117.0	156.400	0.11	0.20	55.8
					117.0	162.000	0.12	0.20	60.3
			HAD4009A (162-174MHz)	120	117.0	162.000	0.11	0.20	56.2
					117.0	167.700	0.12	0.20	62.3
					118.0	173.400	0.11	0.20	57.5
			HAD4021A (136-174MHz)	120	116.0	136.000	0.08	0.20	38.7
					116.0	140.900	0.07	0.20	33.3
					116.0	145.900	0.09	0.20	43.4
					116.0	150.800	0.10	0.20	48.4
					116.0	158.300	0.11	0.20	54.1
					118.0	165.900	0.09	0.20	46.4
					118.0	173.400	0.08	0.20	42.1
	BS4	E	HAD4008A (150.8-162MHz)	120	116.0	150.800	0.08	0.20	41.5
					117.0	156.400	0.07	0.20	33.8
					117.0	162.000	0.07	0.20	36.1
			HAD4009A (162-174MHz)	120	117.0	162.000	0.06	0.20	32.3
					117.0	167.700	0.06	0.20	30.7
					118.0	173.400	0.07	0.20	34.2
			HAD4021A (136-174MHz)	120	116.0	136.000	0.08	0.20	37.7
					116.0	140.900	0.06	0.20	31.4
					116.0	145.900	0.07	0.20	34.9
					116.0	150.800	0.08	0.20	39.3
					116.0	158.300	0.05	0.20	27.2
					118.0	165.900	0.05	0.20	24.5
					118.0	173.400	0.06	0.20	27.9

Table 9 – Companion Mobile (VHF 100W) (cont'd)
Bystander - MPE assessment for roof mounted antennas

Trunk/ Roof	Test Location	E/H Field	Ant. Model	Max Pwr (W)	Initial Pwr (W)	Tx Freq (MHz)	Max Calc. P.D. (mW/cm^2)	FCC Limit	% To Spec Limit
Roof	BS5	E	HAD4008A (150.8-162MHz)	120	116.0	150.800	0.03	0.20	16.3
					117.0	156.400	0.03	0.20	17.1
					117.0	162.000	0.03	0.20	15.2
			HAD4009A (162-174MHz)	120	117.0	162.000	0.03	0.20	13.4
					117.0	167.700	0.03	0.20	13.0
					118.0	173.400	0.03	0.20	14.4
			HAD4021A (136-174MHz)	120	116.0	136.000	0.04	0.20	19.3
					116.0	140.900	0.04	0.20	18.7
					116.0	145.900	0.04	0.20	18.3
					116.0	150.800	0.03	0.20	15.1
					116.0	158.300	0.03	0.20	12.9
					118.0	165.900	0.02	0.20	12.4
					118.0	173.400	0.02	0.20	10.8
	BS1	H	HAD4008A (150.8-162MHz)	120	116.0	150.800	0.08	0.20	42.4
					117.0	156.400	0.09	0.20	44.7
					117.0	162.000	0.09	0.20	45.9
			HAD4009A (162-174MHz)	120	117.0	162.000	0.08	0.20	39.6
					117.0	167.700	0.11	0.20	56.1
					118.0	173.400	0.14	0.20	68.7
			HAD4021A (136-174MHz)	120	116.0	136.000	0.07	0.20	35.9
					116.0	140.900	0.06	0.20	30.6
					116.0	145.900	0.07	0.20	33.9
					116.0	150.800	0.08	0.20	40.9
					116.0	158.300	0.09	0.20	43.5
					118.0	165.900	0.09	0.20	43.8
					118.0	173.400	0.11	0.20	55.4

Table 9 – Companion Mobile (VHF 100W) (cont'd)
Bystander - MPE assessment for roof mounted antennas

Trunk/ Roof	Test Location	E/H Field	Ant. Model	Max Pwr (W)	Initial Pwr (W)	Tx Freq (MHz)	Max Calc. P.D. (mW/cm^2)	FCC Limit	% To Spec Limit
Roof	BS2	H	HAD4008A (150.8-162MHz)	120	116.0	150.800	0.11	0.20	54.5
					117.0	156.400	0.12	0.20	60.1
					117.0	162.000	0.13	0.20	66.4
			HAD4009A (162-174MHz)	120	117.0	162.000	0.12	0.20	60.0
					117.0	167.700	0.17	0.20	84.5
					118.0	173.400	0.17	0.20	82.6
			HAD4021A (136-174MHz)	120	116.0	136.000	0.09	0.20	44.1
					116.0	140.900	0.07	0.20	36.4
					116.0	145.900	0.10	0.20	48.2
					116.0	150.800	0.10	0.20	50.8
					116.0	158.300	0.11	0.20	57.1
					118.0	165.900	0.13	0.20	64.5
					118.0	173.400	0.13	0.20	64.8
	BS3	H	HAD4008A (150.8-162MHz)	120	116.0	150.800	0.09	0.20	44.7
					117.0	156.400	0.10	0.20	50.1
					117.0	162.000	0.11	0.20	55.6
			HAD4009A (162-174MHz)	120	117.0	162.000	0.10	0.20	52.3
					117.0	167.700	0.12	0.20	57.6
					118.0	173.400	0.12	0.20	58.1
			HAD4021A (136-174MHz)	120	116.0	136.000	0.07	0.20	36.1
					116.0	140.900	0.06	0.20	28.0
					116.0	145.900	0.07	0.20	35.3
					116.0	150.800	0.08	0.20	39.3
					116.0	158.300	0.09	0.20	45.4
					118.0	165.900	0.08	0.20	41.6
					118.0	173.400	0.09	0.20	44.3

Table 9 – Companion Mobile (VHF 100W) (cont'd)
Bystander - MPE assessment for roof mounted antennas

Trunk/ Roof	Test Location	E/H Field	Ant. Model	Max Pwr (W)	Initial Pwr (W)	Tx Freq (MHz)	Max Calc. P.D. (mW/cm^2)	FCC Limit	% To Spec Limit
Roof	BS4	H	HAD4008A (150.8-162MHz)	120	116.0	150.800	0.08	0.20	41.7
					117.0	156.400	0.07	0.20	34.6
					117.0	162.000	0.08	0.20	40.9
			HAD4009A (162-174MHz)	120	117.0	162.000	0.07	0.20	36.4
					117.0	167.700	0.07	0.20	34.1
					118.0	173.400	0.08	0.20	39.1
			HAD4021A (136-174MHz)	120	116.0	136.000	0.07	0.20	36.5
					116.0	140.900	0.06	0.20	30.7
					116.0	145.900	0.07	0.20	36.5
					116.0	150.800	0.08	0.20	39.0
					116.0	158.300	0.06	0.20	29.7
					118.0	165.900	0.06	0.20	28.1
					118.0	173.400	0.06	0.20	30.5
	BS5	H	HAD4008A (150.8-162MHz)	120	116.0	150.800	0.04	0.20	20.2
					117.0	156.400	0.04	0.20	19.9
					117.0	162.000	0.03	0.20	16.8
			HAD4009A (162-174MHz)	120	117.0	162.000	0.03	0.20	15.2
					117.0	167.700	0.03	0.20	16.9
					118.0	173.400	0.03	0.20	17.2
			HAD4021A (136-174MHz)	120	116.0	136.000	0.05	0.20	22.9
					116.0	140.900	0.05	0.20	23.0
					116.0	145.900	0.04	0.20	22.5
					116.0	150.800	0.04	0.20	20.1
					116.0	158.300	0.03	0.20	15.1
					118.0	165.900	0.03	0.20	14.0
					118.0	173.400	0.03	0.20	14.1

Table 10 – Companion Mobile (VHF 100W)
Passenger - MPE assessment for roof mounted antennas

Trunk/ Roof	Test Location	E/H Field	Ant. Model	Max Pwr (W)	Initial Pwr (W)	Tx Freq (MHz)	Max Calc. P.D. (mW/cm^2)	FCC Limit	% To Spec Limit
MPE measurements for the Back Passenger									
Roof	PB	E	HAD4008A (150.8-162MHz)	120	116.0	150.800	0.09	0.20	45.4
					117.0	156.400	0.03	0.20	13.1
					117.0	162.000	0.11	0.20	56.6
			HAD4009A (162-174MHz)	120	117.0	162.000	0.12	0.20	61.5
					117.0	167.700	0.10	0.20	52.4
					118.0	173.400	0.05	0.20	26.5
			HAD4021A (136-174MHz)	120	116.0	136.000	0.13	0.20	63.6
					116.0	140.900	0.10	0.20	48.4
					116.0	145.900	0.07	0.20	36.9
					116.0	150.800	0.08	0.20	40.3
					116.0	158.300	0.04	0.20	19.6
					118.0	165.900	0.09	0.20	43.3
					118.0	173.400	0.04	0.20	19.3
MPE measurements for the Front Passenger									
Roof	PF (Driver side)	E	HAD4008A (150.8-162MHz)	120	116.0	150.800	0.27	0.20	**136.6**
					117.0	156.400	0.15	0.20	74.7
					117.0	162.000	0.12	0.20	58.5
			HAD4009A (162-174MHz)	120	117.0	162.000	0.10	0.20	51.2
					117.0	167.700	0.12	0.20	60.2
					118.0	173.400	0.12	0.20	60.8
			HAD4021A (136-174MHz)	120	116.0	136.000	0.09	0.20	44.5
					116.0	140.900	0.17	0.20	84.6
					116.0	145.900	0.26	0.20	**130.7**
					116.0	150.800	0.28	0.20	**138.5**
					116.0	158.300	0.09	0.20	46.6
					118.0	165.900	0.09	0.20	45.3
					118.0	173.400	0.09	0.20	45.0

Note: Results in bold require SAR simulation.

Table 10 – Companion Mobile (VHF 100W) (cont'd)
Passenger - MPE assessment for roof mounted antennas

Trunk/ Roof	Test Location	E/H Field	Ant. Model	Max Pwr (W)	Initial Pwr (W)	Tx Freq (MHz)	Max Calc. P.D. (mW/cm^2)	FCC Limit	% To Spec Limit
MPE measurements for the Back Passenger									
Roof	PB	H	HAD4008A (150.8-162MHz)	120	116.0	150.800	0.07	0.20	33.0
					117.0	156.400	0.03	0.20	16.1
					117.0	162.000	0.04	0.20	17.9
			HAD4009A (162-174MHz)	120	117.0	162.000	0.03	0.20	17.2
					117.0	167.700	0.08	0.20	41.4
					118.0	173.400	0.05	0.20	26.3
			HAD4021A (136-174MHz)	120	116.0	136.000	0.09	0.20	46.3
					116.0	140.900	0.08	0.20	41.1
					116.0	145.900	0.10	0.20	50.8
					116.0	150.800	0.06	0.20	31.7
					116.0	158.300	0.02	0.20	9.3
					118.0	165.900	0.05	0.20	24.9
					118.0	173.400	0.04	0.20	20.2
MPE measurement for the Front Passenger									
Roof	PF (Driver side)	H	HAD4008A (150.8-162MHz)	120	116.0	150.800	0.22	0.20	**110.3**
					117.0	156.400	0.11	0.20	55.7
					117.0	162.000	0.06	0.20	29.8
			HAD4009A (162-174MHz)	120	117.0	162.000	0.05	0.20	26.8
					117.0	167.700	0.06	0.20	28.6
					118.0	173.400	0.08	0.20	38.0
			HAD4021A (136-174MHz)	120	116.0	136.000	0.11	0.20	54.1
					116.0	140.900	0.15	0.20	73.8
					116.0	145.900	0.29	0.20	**144.0**
					116.0	150.800	0.20	0.20	**100.4**
					116.0	158.300	0.08	0.20	40.0
					118.0	165.900	0.06	0.20	29.3
					118.0	173.400	0.06	0.20	30.4

Note: Results in bold require SAR simulation.

15.2. Combined MPE Results

The combined MPE results for DVR and it's Companion Mobile were calculated base on the percent of MPE limit for each of the applicable test channels according to the formula below. This is due to the signals emitted by each individual transmitter are statistically uncorrelated, the collective compliance of the transmitters is determined by summing the individual ratios between actual (S) and maximum allowed MPE exposure. Compliance is achieved if the total exposure level (T) is less than one.

Formula:

$$T = \frac{S_1}{MPE_1} + \frac{S_2}{MPE_2} + ... < 1$$

The highest combined power density percentage of the FCC MPE limits using the methodology and formula are indicated in the table 11 (referenced data from tables 7 thru 10 for highest calculated MPE % of limit for DVR and the Companion Mobile).

Table 11

	Percentage of Limit (%)		
Test Position	**DVR 700 (FCC ID: LO6-DVRS700)**	**Companion Mobile (FCC ID: AZ492FT4898)**	**Combined Percentages**
Passenger, Front seat (PF)	4.2	**144.0**	**148.2**
Passenger, Back seat (PB)	8.2	63.6	71.8
By-Stander #1 (BS-1)	0.4	68.9	69.3
By-Stander #2 (BS-2)	1.3	89.2	90.5
By-Stander #3 (BS-3)	1.7	62.3	64.0
By-Stander #4 (BS-4)	1.6	41.7	43.3
By-Stander #5 (BS-5)	3.3	23.0	26.3

Note: Results in bold require SAR simulation.

Table 12 – Highest Combined Calculated MPE % of limit for Passenger summary (Front seat)

(Reference tables 8 and 10)

					DVR (FCC ID: LO6-DVRS700) Trunk mount (%)					
					HAF4016A					
					764.000	770.000	775.000	794.000	800.000	806.000
				Highest Results (%)	2.8	2.4	2.9	3.6	3.3	4.2
Companion Mobile (FCC ID: AZ492FT4898) Roof Mount (%)	E	HAD4008A	150.800	**136.6**	**139.4**	**139.0**	**139.5**	**140.2**	**139.9**	**140.8**
			156.400	74.7	77.5	77.1	77.6	78.3	78.0	78.9
			162.000	58.5	61.3	60.9	61.4	62.1	61.8	62.7
		HAD4009A	162.000	51.2	54.0	53.6	54.1	54.8	54.5	55.4
			167.700	60.2	63.0	62.6	63.1	63.8	63.5	64.4
			173.400	60.8	63.6	63.2	63.7	64.4	64.1	65
		HAD4021A	136.000	44.5	47.3	46.9	47.4	48.1	47.8	48.7
			140.900	84.6	87.4	87.0	87.5	88.2	87.9	88.8
			145.900	**130.7**	**133.5**	**133.1**	**133.6**	**134.3**	**134.0**	**134.9**
			150.800	**138.5**	**141.3**	**140.9**	**141.4**	**142.1**	**141.8**	**142.7**
			158.300	46.6	49.4	49	49.5	50.2	49.9	50.8
			165.900	45.3	48.1	47.7	48.2	48.9	48.6	49.5
			173.400	45.0	47.8	47.4	47.9	48.6	48.3	49.2
	H	HAD4008A	150.800	**110.3**	**113.1**	**112.7**	**113.2**	**113.9**	**113.6**	**114.5**
			156.400	55.7	58.5	58.1	58.6	59.3	59.0	59.9
			162.000	29.8	32.6	32.2	32.7	33.4	33.1	34.0
		HAD4009A	162.000	26.8	29.6	29.2	29.7	30.4	30.1	31.0
			167.700	28.6	31.4	31.0	31.5	32.2	31.9	32.8
			173.400	38.0	40.8	40.4	40.9	41.6	41.3	42.2
		HAD4021A	136.000	54.1	56.9	56.5	57.0	57.7	57.4	58.3
			140.900	73.8	76.6	76.2	76.7	77.4	77.1	78.0
			145.900	**144.0**	**146.8**	**146.4**	**146.9**	**147.6**	**147.3**	**148.2**
			150.800	**100.4**	**103.2**	**102.8**	**103.3**	**104.0**	**103.7**	**104.6**
			158.300	40.0	42.8	42.4	42.9	43.6	43.3	44.2
			165.900	29.3	32.1	31.7	32.2	32.9	32.6	33.5
			173.400	30.4	33.2	32.8	33.3	34.0	33.7	34.6

Note: Results in bold require SAR simulation.

16.0 Conclusion

The DVR assessments were performed with an output power of 5 watts across the DVR transmit band. As for the Companion Mobile, depending on the test frequency, the Companion Mobile assessments were performed with an output power range as indicated in section 15.1, Tables 9-10. The highest power density results for DVR and the Companion Mobile devices scaled to the applicable maximum allowable power outputs are indicated in the Tables 13 and 14 for internal /passenger to the vehicle, and external/bystander for to the vehicle.

Table 13: Maximum MPE RF Exposure Summary for DVR (FCC ID: LO6-DVRS700)

Designator	Frequency (MHz)	Passenger (mW/cm²)	Bystander (mW/cm²)
Overall	764-776, 794-806	0.04	0.02
FCC	763-775, 793-805, 806-809	0.04	0.02

Table 14: Maximum MPE RF Exposure Summary for Companion Mobile (FCC ID: AZ492FT4898)

Designator	Frequency (MHz)	Passenger (mW/cm²)	Bystander (mW/cm²)
Overall	136 - 174	**0.29**	0.18
FCC	150.8 – 173.4	**0.28**	0.18

Table 15: Maximum Combined Calculated MPE % of limit

Designator	Frequency (MHz)		Percentage of Limit (%)	
	DVR (FCC ID: LO6-DVRS700)	Companion Mobile (FCC ID: AZ492FT4898)	Passenger	Bystander
Overall	764-776, 794-806	136 - 174	**148.2**	90.5
FCC	763-775, 793-805, 806-809	150.8 – 173.4	**142.7**	90.5

Note: Results in bold require SAR simulation.

The MPE results presented herein demonstrate compliance to the applicable FCC Occupational/ Controlled exposure limit. FCC rules require compliance for passengers and bystanders to the FCC General Population/ Uncontrolled limits. Although MPE is a convenient method of demonstrating compliance, SAR is recognized as the "basic restriction". For those configurations exceeding the MPE limit noted in section 15 tables 7 thru 12, compliance to the FCC/IEEE SAR General Population/Uncontrolled limit of 1.6mW/g is demonstrated in appendix E Computational EME Compliance Assessment via SAR computational analysis.

The computation results show that this m FCC ID: LO6-DVRS700 (Model # DQPMDVR7000P) device, when used with the Companion Mobile FCC ID: AZ492FT4898 (Model #M30TXS9PW1AN) and specified antennas, exhibit a maximum combined peak 1-g average SAR are indicated in the Table 16.

Table 16: Maximum Combined SAR results (Passenger)

Designator	Frequency (MHz)		Combined 1g-SAR (mW/g)
	DVR (FCC ID: LO6-DVRS700)	Companion Mobile (FCC ID: AZ492FT4898)	
Overall	764-776, 794-806	136 - 174	1.04
FCC	763-775, 793-805, 806-809	150.8 – 173.4	0.39

Appendix A - Antenna Locations and Test Distances

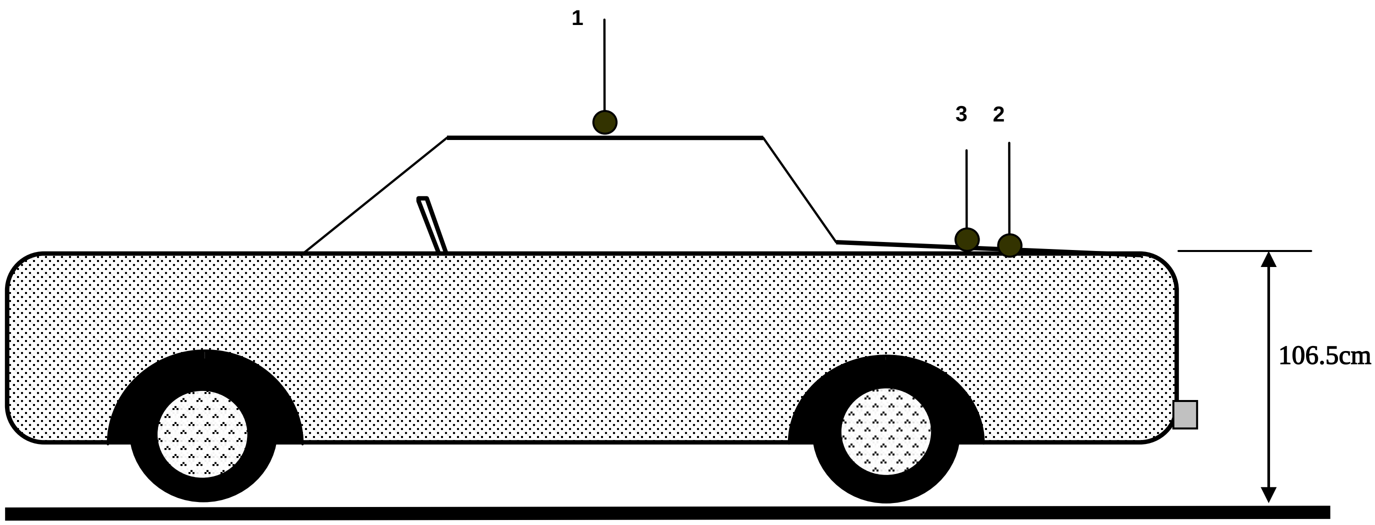

1 - Roof (45cm from center)
2 - Trunk (center)
3 - Trunk (85cm from back of the back seat)

Bystander Antenna mounting and test locations

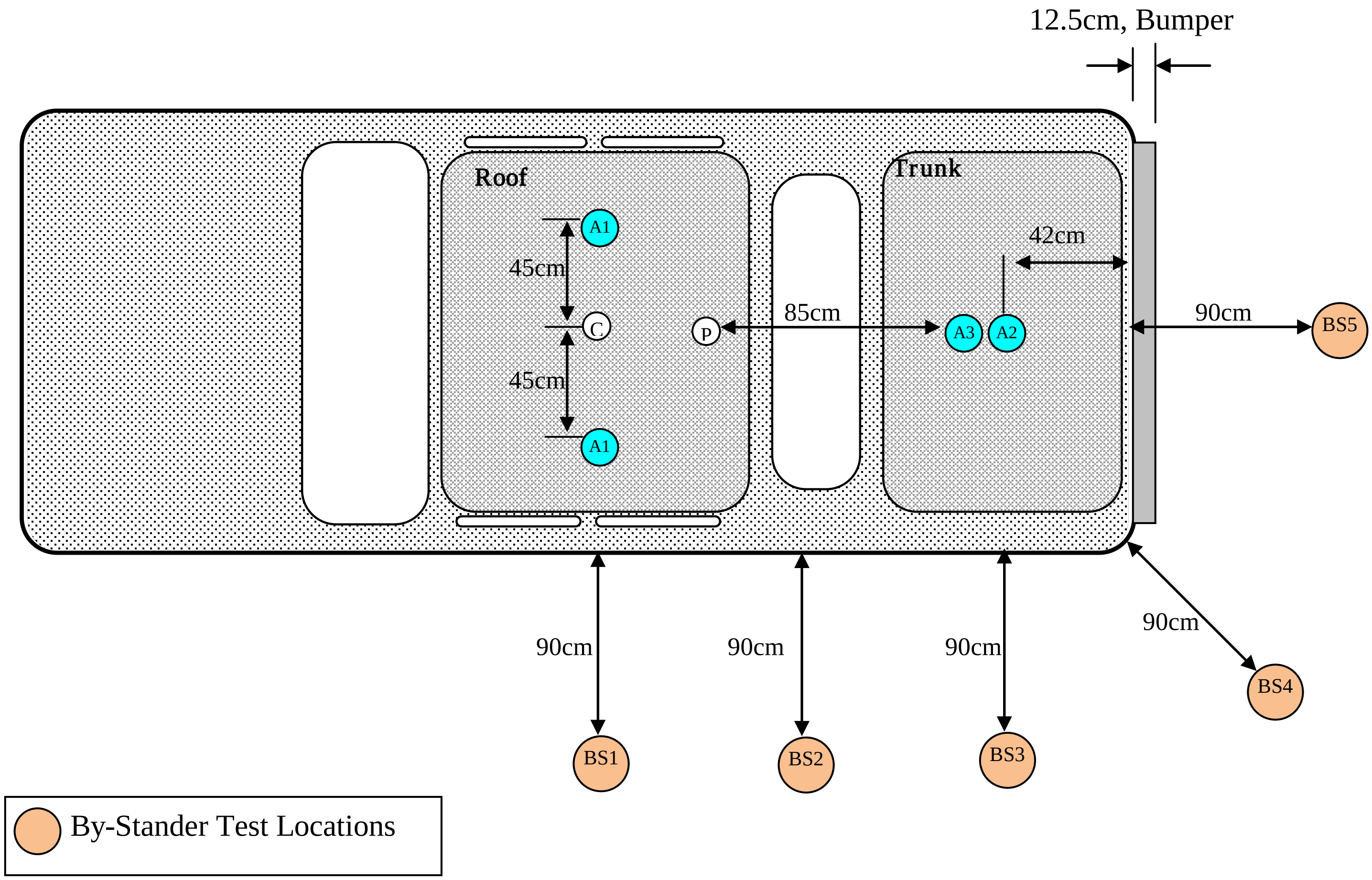

Notes:

1) Antenna location A1: APX7500 antenna mounting location(s) for Bystander and Passenger testing
2) Antenna location A2: DVR antenna mounting location for Bystander testing
3) Antenna location A3: DVR antenna mounting location for Passenger testing
4) Bystander test location #2 (BS2): Center point of the By-stander test location #1 and test location #3, which is by 88cm.
5) Bystander test location #3 (BS3): 90 degree angle from the trunk mount antenna
6) Bystander test location #4 (BS4): 45 degree angle from the trunk mount antenna
7) Assessments were performed at each test position for each of the offered antennas
8) Bystander positions (1-5) are 90cm from the vehicle body.
9) Total distance between bystander position 1 and roof mount antenna is 141cm
10) Total distance between bystander position 5 and trunk mount antenna is 131cm
11) Total distance between trunk mount antenna and rear passenger is 85cm

Seat scan areas
(Applicable to both front and back seats)

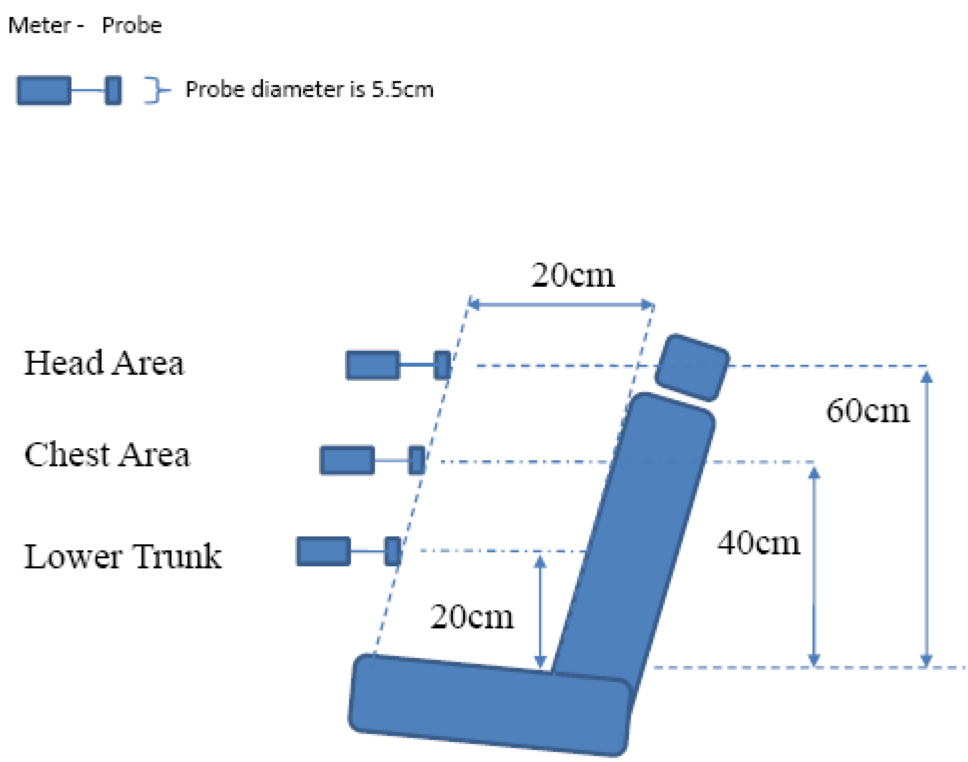

MPE Test Configuration

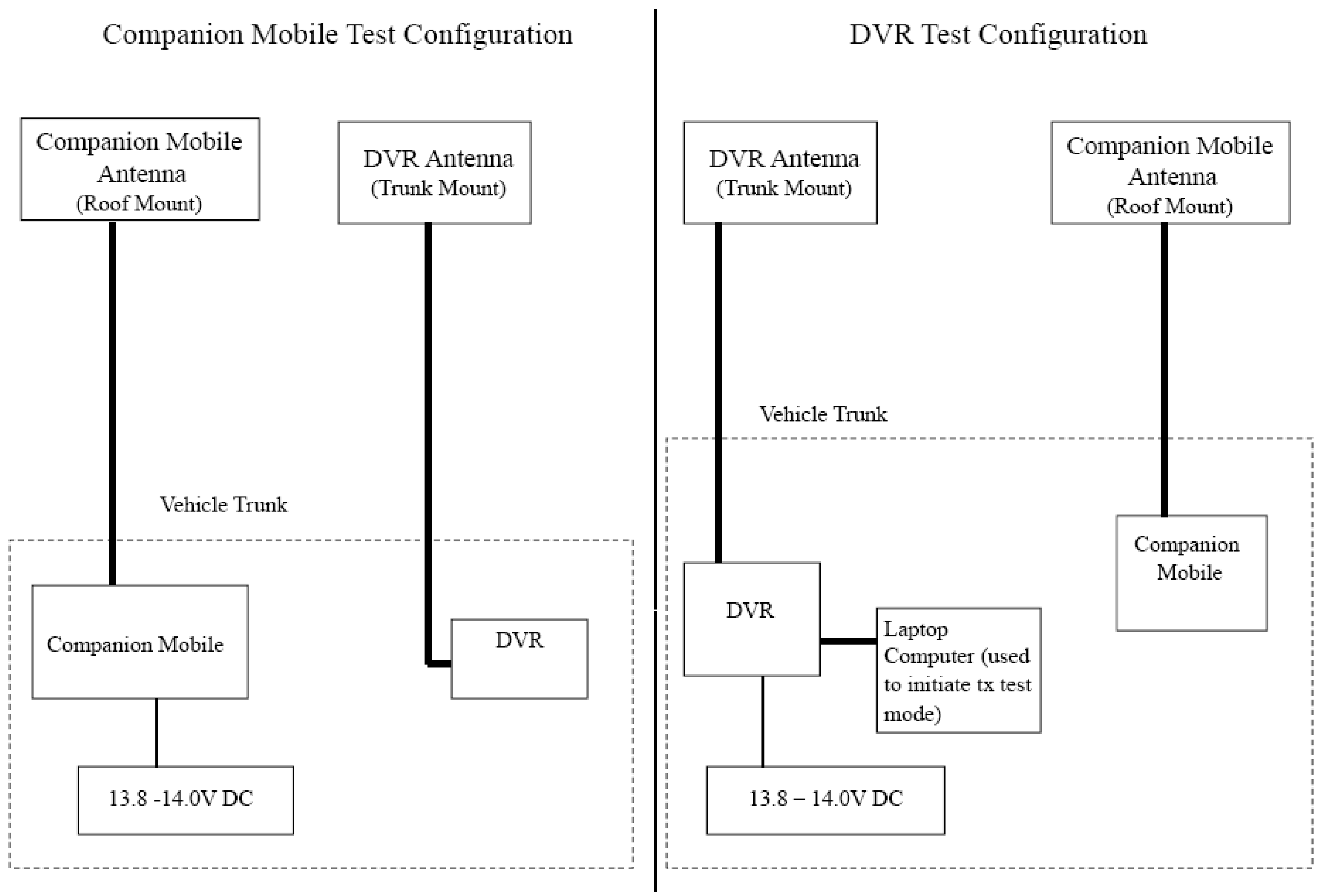

Appendix B - Probe Calibration Certificates

ilac-MRA ACCREDITED Calibration Laboratory Certificate 1387.01

ETS·LINDGREN
An ESCO Technologies Company
1301 Arrow Point Drive
Cedar Park, Texas 78613
(512) 531-6498

ETS·LINDGREN
Track# S000025288 Ltd Cal
By GC Date 11-Jun-12
Next Cal Due
www.ets-lindgren.com

Cert I.D.: 91609

Certificate of Calibration Conformance

Page 1 of 3

The instrument identified below has been individually calibrated in compliance with the following standard(s):

IEEE 1309 - 2005, Institute of Electrical and Electronics Engineers, Standard for Calibration of Electromagnetic Field Sensors and Probes, Excluding Antennas from 9 kHz to 40 GHz

Environment: Laboratory MTE is maintained in a temperature controlled environment with ambient conditions from 18 to 28 C, relative humidity less than 90%. The instrument under test has been calibrated in a suitable environment using an EMCO TEM Cell 5101C, GTEM! 5305 and an RF Shielded EMC Chamber which is conducive to maintaining accurate and reliable measurement quality.

Manufacturer:	ETS-Lindgren	**Operating Range:**	100kHz - 5GHz
Model Number:	E100	**Instrument Type:**	Isotropic Probe > 1 GHz
Serial Number/ ID:	*00126277*	**Date Code:**	
Tracking Number:	**S 000025288**	**Alternate ID:**	
Date Completed:	11-Jun-12	**Customer:**	AGILENT/MOTOROLA (FL)
Test Type:	Standard Field, Field Strength		

Calibration Uncertainty: Std Field Method 10kHz - 18000 MHz, +/-0.7 dB, 26.5GHz - 40GHz, +/- 0.95 dB
k=2, (95% Confidence Level)

Test Remarks: Probe tested with HI-2200 s/n 00086887. Special Calibration - Additional frequency points added per customer request.

Calibration Traceability: All Measuring and Test Equipment (M/TE) identified below are traceable to the SI units through the National Institute for Standards and Technology (NIST) or other recognized National Metrology Institute. Calibration Laboratory and Quality System controls are compliant with ISO/IEC 17025-2005 and ANSI/NCSL Z540-1-1994.

Standards and Equipment Used:
Make / Model / Name / S/N / Recall Date

Agilent/HP	8648C	Signal Generator	3623A03573	01-Feb-13
Agilent	E4419B	Power Meter	MY45104171	29-Sep-12
Agilent/HP	8648C	Signal Generator	3847A04406	01-Feb-13
Agilent	E4419B	Power Meter	MY45103242	01-Feb-13
Rohde & Schwarz	857.8008.02	Power Meter NRVD	100451	28-Mar-13
Hewlett Packard	83620B	Signal Generator	3722A00541	01-Feb-13
Fluke	6060B	RF Signal Generator	5690204	28-Jun-12

Condition of Instrument Upon Receipt:
In Tolerance to Internal Quality Standards

On Release:
In Tolerance to Internal Quality Standards

Calibration Completed By
George Cisneros, Calibration Technian

Attested and Issued on 11-Jun-12
Terry D. O'Neill, Calibration Manager

CALIBRATION REPORT

Electric Field Sensor

Model	*S/N*
E100	00126277
HI-2200	86887

Date: 11 June 2012

New Instrument
_ Other
_ Out of Tolerance
X Within Tolerance

Frequency Response

Frequency Response		*Nominal Field*	*Cal Factor**	*Deviation*
	MHz	*V/m*	(Eapplied/Eindicated)	*dB*
1	1	20	1.40	-2.93
2	15	20	1.10	-0.80
3	30	20	1.02	-0.21
4	75	20	0.98	0.14
5	100	20	0.99	0.05
6	150	20	1.00	0.00
7	200	20	1.00	0.00
8	250	20	0.98	0.15
9	300	20	0.99	0.05
10	400	20	1.00	0.00
11	500	20	1.00	-0.04
12	600	20	1.01	-0.06
13	700	20	1.01	-0.10
14	800	20	1.02	-0.15
15	900	20	1.02	-0.15
16	1000	20	0.98	0.21
17	2000	20	0.95	0.48
18	2450	20	1.01	-0.09
19	3000	20	1.02	-0.17
20	3500	20	0.97	0.30
21	4000	20	1.01	-0.11
22	5000	20	1.37	-2.76
23	5500	20	1.41	-2.95
24	6000	20	1.43	-3.10

* Corrected electric field values (V/m) can be obtained by multiplying the Cal Factor with the indicated E field readings.

Linearity

maximum linearity deviation is 0.1 dB
(measurements taken from 0.3 V/m to 800 V/m at 27.12 MHz)

Test Conditions

Calibration performed at ambient room temperature: 23 ±3°C

Page 2 of 3

ETS·LINDGREN
An ESCO Technologies Company

PROBE ROTATIONAL RESPONSE

Model	E100
S/N	00126277
Date	Date of Calibration 11 June 2012
Time	12:55:30 PM
Isotropy *	+ 0.304 dB/ -0.304 dB

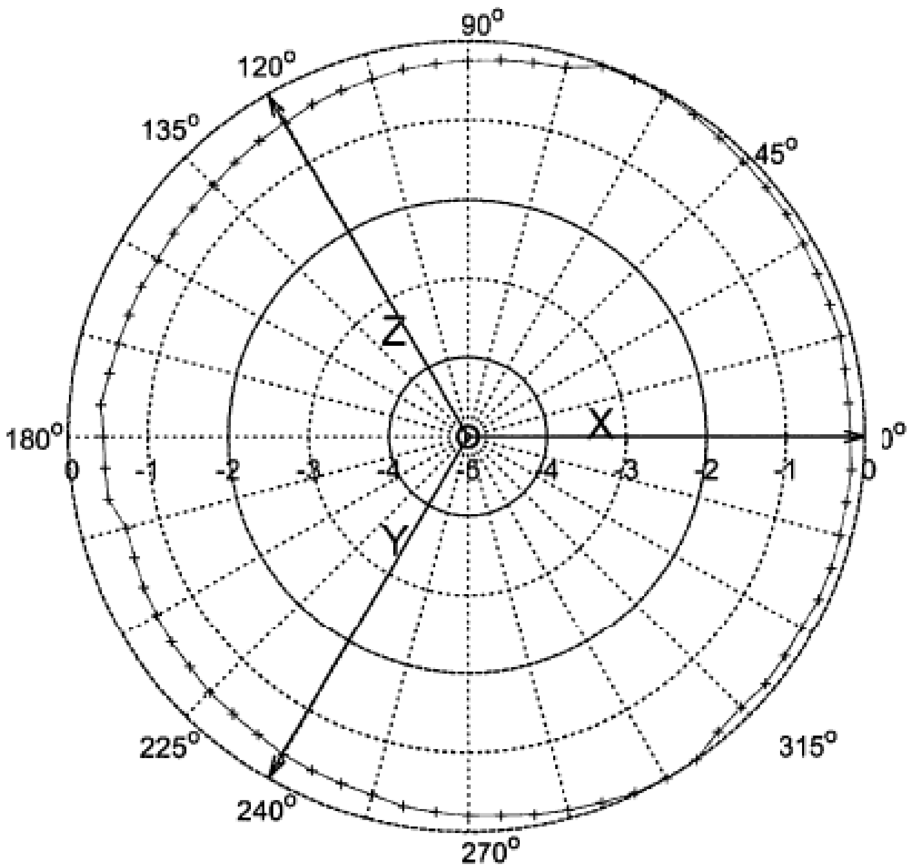

Figure 1: Probe Isotropic Response Chart.

Isotropic response is measured in a 20 V/m field at 400 MHz
*Isotropy is the maximum deviation from the geometric mean as defined by IEEE 1309-2005.

Page 3 of 3

ilac-MRA ACCREDITED Calibration Laboratory Certificate 1207.01

Cert I.D.: 91613

ETS·LINDGREN
An ESCO Technologies Company
1301 Arrow Point Drive
Cedar Park, Texas 78613
(512) 531-6498

ETS·LINDGREN An ESCO Technologies Company
Track# S000025288 Ltd Cal ☐
By GC Date 11-Jun-12
Next Cal Due ______
www.ets-lindgren.com

Certificate of Calibration Conformance

Page 1 of 2

The instrument identified below has been individually calibrated in compliance with the following standard(s):

IEEE 1309 - 2005, Institute of Electrical and Electronics Engineers, Standard for Calibration of Electromagnetic Field Sensors and *Probes*, Excluding Antennas from 9 kHz to 40 GHz

Environment: Laboratory MTE is maintained in a temperature controlled environment with ambient conditions from 18 to 28 C, relative humidity less than 90%. The instrument under test has been calibrated in a suitable environment using an EMCO TEM Cell 5101C, GTEM! 5305 and an RF Shielded EMC Chamber which is conducive to maintaining accurate and reliable measurement quality.

Manufacturer:	ETS-Lindgren	**Operating Range:**	5-300MHz / 30mA/m-10A/m
Model Number:	H200	**Instrument Type:**	Isotropic Magnetic Field Probe (2)
Serial Number/ ID:	*00084225*	**Date Code:**	
Tracking Number:	**S 000025288**	**Alternate ID:**	
Date Completed:	11-Jun-12	**Customer:**	AGILENT/MOTOROLA (FL)
Test Type:	Standard Field, Field Strength		

Calibration Uncertainty: Direct Field Method 1.15dB
k=2, (95% Confidence Level)

Test Remarks: Probe tested with HI-2200 s/n 00086887.

Calibration Traceability: All Measuring and Test Equipment (M/TE) identified below are traceable to the SI units through the National Institute for Standards and Technology (NIST) or other recognized National Metrology Institute. Calibration Laboratory and Quality System controls are compliant with ISO/IEC 17025-2005 and ANSI/NCSL Z540-1-1994.

Standards and Equipment Used:
Make / Model / Name / S/N / Recall Date

HP	8648C	Sig Gen	3836A04299	01-Feb-13
Hewlett Packard	E4419B	Power Meter	US39250717	01-Feb-13

Condition of Instrument Upon Receipt:
In Tolerance to Internal Quality Standards

On Release:
In Tolerance to Internal Quality Standards

Calibration Completed By
George Cisneros, Calibration Technian

Attested and Issued on 11-Jun-12
Terry D. O'Neill, Calibration Manager

This document provides traceability of measurements to recognized national standards using controlled processes at the ETS-Lindgren Calibration Laboratory. Uncertainties listed are derived from the methods described by NIST Tech Note 1297. This certificate and report may not be reproduced, except in full, without the written approval of ETS-Lindgren Calibration Laboratory in accordance with ISO/IEC 17025-2005 and ANSI/NCSL Z540-1-1994. QAF 1127 (03/11)

CALIBRATION REPORT

Magnetic Field Sensor

Model	*S/N*
H200	00084225
HI-2200	86887

Date: 11 Jun 2012

As received, the instrument was found: X Within Tolerance
Out of Tolerance
(New Instrument)

Frequency Response

Frequency Response		*Nominal Field*	*Cal Factor**	*Deviation*
	MHz	*A/m*	(Happlied/Hindicated)	*dB*
1	10	0.08	1.04	-0.32
2	15	0.08	1.00	0.00
3	30	0.08	1.00	0.00
4	50	0.08	0.98	0.18
5	75	0.08	0.96	0.34
6	100	0.08	0.93	0.61
7	150	0.08	0.86	1.28
8	175	0.08	0.84	1.53
9	200	0.08	0.82	1.97
10	250	0.08	0.72	3.28
11	300	0.08	0.60	4.56

* Corrected magnetic field values (A/m) can be obtained by multiplying the Cal Factor with the indicated H field readings.

Linearity

Maximum linearity deviation is 0.03 dB
(measurements taken from 30 mA/m to 9 A/m at 27.12 MHz)

Test Conditions

Calibration performed at ambient room temperature: 23 ±3°C

Page 2 of 2

Appendix C - Photos of Assessed Antennas

DVR 700 antenna: HAF4016A

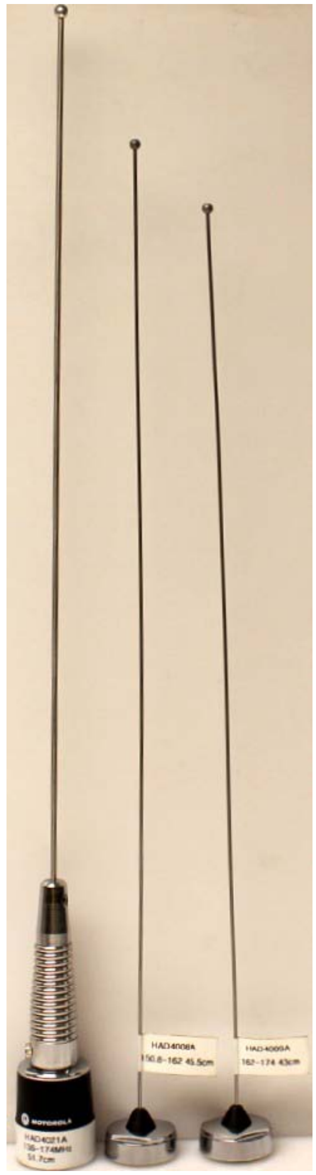

Companion Mobile antennas (left to right):
HAD4021A, HAD4008A, HAD4009A

Appendix D – MPE Measurement Results

DVR (700MHz 5W) - MPE measurement data for Bystander

D.U.T. Info.							Probe Info.			MPE Measurement													
Ant Loc.	**Ant. Model/ Desc.**	**Ant. Gain (dBi)**	**Tx Freq (MHz)**	**Max Pwr (W)**	**Initial Pwr (W)**	**Test Mode**	**E/H Field**	**Probe Cal. Factor**	**Test Pos.**	**20 cm**	**40 cm**	**60 cm**	**80 cm**	**100 cm**	**120 cm**	**140 cm**	**160 cm**	**180 cm**	**200 cm**	**DUT Max. TX Factor**	**Avg. over Body (mW cm^2)**	**Calc. P.D. (mW/cm^2)**	**Max Calc. P.D. (mW/cm^2)**
Trunk	HAF4016A (764-870MHz)	2.15	764.000	5.0	5.0	CW	E	1.03	BS1	0.000	0.000	0.001	0.001	0.002	0.002	0.003	0.003	0.003	0.003	1.0	0.002	0.002	0.00
Trunk	HAF4016A (764-870MHz)	2.15	770.000	5.0	5.0	CW	E	1.03	BS1	0.000	0.000	0.000	0.000	0.001	0.001	0.001	0.002	0.002	0.002	1.0	0.001	0.001	0.00
Trunk	HAF4016A (764-870MHz)	2.15	775.000	5.0	5.0	CW	E	1.04	BS1	0.000	0.000	0.000	0.001	0.001	0.001	0.001	0.001	0.002	0.002	1.0	0.001	0.001	0.00
Trunk	HAF4016A (764-870MHz)	2.15	794.000	5.0	5.0	CW	E	1.04	BS1	0.000	0.000	0.000	0.000	0.001	0.001	0.001	0.002	0.002	0.002	1.0	0.001	0.001	0.00
Trunk	HAF4016A (764-870MHz)	2.15	800.000	5.0	5.0	CW	E	1.04	BS1	0.000	0.000	0.000	0.000	0.001	0.001	0.001	0.001	0.002	0.002	1.0	0.001	0.001	0.00
Trunk	HAF4016A (764-870MHz)	2.15	806.000	5.0	5.0	CW	E	1.04	BS1	0.000	0.000	0.001	0.001	0.001	0.001	0.002	0.002	0.003	0.003	1.0	0.001	0.001	0.00
Trunk	HAF4016A (764-870MHz)	2.15	764.000	5.0	5.0	CW	E	1.03	BS2	0.000	0.000	0.000	0.001	0.002	0.003	0.007	0.009	0.010	0.010	1.0	0.004	0.004	0.00
Trunk	HAF4016A (764-870MHz)	2.15	770.000	5.0	5.0	CW	E	1.03	BS2	0.000	0.000	0.000	0.001	0.002	0.003	0.004	0.007	0.007	0.008	1.0	0.003	0.003	0.00
Trunk	HAF4016A (764-870MHz)	2.15	775.000	5.0	5.0	CW	E	1.04	BS2	0.000	0.001	0.001	0.001	0.002	0.004	0.005	0.008	0.008	0.007	1.0	0.004	0.004	0.00
Trunk	HAF4016A (764-870MHz)	2.15	794.000	5.0	5.0	CW	E	1.04	BS2	0.001	0.001	0.001	0.002	0.002	0.003	0.006	0.008	0.008	0.007	1.0	0.004	0.004	0.00
Trunk	HAF4016A (764-870MHz)	2.15	800.000	5.0	5.0	CW	E	1.04	BS2	0.001	0.001	0.001	0.002	0.002	0.005	0.007	0.008	0.009	0.009	1.0	0.005	0.005	0.00
Trunk	HAF4016A (764-870MHz)	2.15	806.000	5.0	5.0	CW	E	1.04	BS2	0.001	0.002	0.002	0.003	0.004	0.007	0.011	0.011	0.013	0.013	1.0	0.007	0.007	0.01
Trunk	HAF4016A (764-870MHz)	2.15	764.000	5.0	5.0	CW	E	1.03	BS3	0.001	0.001	0.002	0.003	0.006	0.008	0.013	0.017	0.018	0.016	1.0	0.009	0.009	0.01
Trunk	HAF4016A (764-870MHz)	2.15	770.000	5.0	5.0	CW	E	1.03	BS3	0.001	0.001	0.001	0.002	0.004	0.006	0.008	0.011	0.013	0.011	1.0	0.006	0.006	0.01
Trunk	HAF4016A (764-870MHz)	2.15	775.000	5.0	5.0	CW	E	1.04	BS3	0.001	0.001	0.001	0.002	0.004	0.006	0.010	0.011	0.014	0.013	1.0	0.006	0.007	0.01

MPE calculations are defined in section 13.0.

DVR (700MHz 5W) - MPE measurement data for Bystander

D.U.T. Info.							Probe Info.			MPE Measurement													
Ant Loc.	Ant. Model/ Desc.	Ant. Gain (dBi)	Tx Freq (MHz)	Max Pwr (W)	Initial Pwr (W)	Test Mode	E/H Field	Probe Cal. Factor	Test Pos.	20 cm	40 cm	60 cm	80 cm	100 cm	120 cm	140 cm	160 cm	180 cm	200 cm	DUT Max. TX Factor	Avg. over Body (mW cm^2)	Calc. P.D. (mW/cm^2)	Max Calc. P.D. (mW/cm^2)
Trunk	HAF4016A (764-870MHz)	2.15	794.000	5.0	5.0	CW	E	1.04	BS3	0.000	0.001	0.001	0.002	0.004	0.006	0.008	0.011	0.011	0.009	1.0	0.005	0.006	0.01
Trunk	HAF4016A (764-870MHz)	2.15	800.000	5.0	5.0	CW	E	1.04	BS3	0.001	0.001	0.001	0.002	0.003	0.006	0.009	0.012	0.013	0.010	1.0	0.006	0.006	0.01
Trunk	HAF4016A (764-870MHz)	2.15	806.000	5.0	5.0	CW	E	1.04	BS3	0.001	0.001	0.002	0.003	0.004	0.008	0.013	0.017	0.020	0.016	1.0	0.009	0.009	0.01
Trunk	HAF4016A (764-870MHz)	2.15	764.000	5.0	5.0	CW	E	1.03	BS4	0.001	0.002	0.003	0.006	0.008	0.011	0.014	0.014	0.011	0.009	1.0	0.008	0.008	0.01
Trunk	HAF4016A (764-870MHz)	2.15	770.000	5.0	5.0	CW	E	1.03	BS4	0.001	0.001	0.003	0.005	0.006	0.009	0.011	0.010	0.008	0.006	1.0	0.006	0.006	0.01
Trunk	HAF4016A (764-870MHz)	2.15	775.000	5.0	5.0	CW	E	1.04	BS4	0.001	0.001	0.003	0.005	0.007	0.010	0.012	0.012	0.010	0.007	1.0	0.007	0.007	0.01
Trunk	HAF4016A (764-870MHz)	2.15	794.000	5.0	5.0	CW	E	1.04	BS4	0.000	0.001	0.002	0.004	0.005	0.007	0.009	0.008	0.007	0.006	1.0	0.005	0.005	0.01
Trunk	HAF4016A (764-870MHz)	2.15	800.000	5.0	5.0	CW	E	1.04	BS4	0.000	0.001	0.002	0.004	0.005	0.007	0.008	0.008	0.008	0.007	1.0	0.005	0.005	0.01
Trunk	HAF4016A (764-870MHz)	2.15	806.000	5.0	5.0	CW	E	1.04	BS4	0.001	0.002	0.004	0.006	0.007	0.010	0.012	0.012	0.011	0.010	1.0	0.008	0.008	0.01
Trunk	HAF4016A (764-870MHz)	2.15	764.000	5.0	5.0	CW	E	1.03	BS5	0.003	0.005	0.007	0.010	0.014	0.020	0.026	0.026	0.023	0.017	1.0	0.015	0.016	0.02
Trunk	HAF4016A (764-870MHz)	2.15	770.000	5.0	5.0	CW	E	1.03	BS5	0.003	0.004	0.006	0.008	0.012	0.019	0.024	0.025	0.019	0.013	1.0	0.013	0.014	0.01
Trunk	HAF4016A (764-870MHz)	2.15	775.000	5.0	5.0	CW	E	1.04	BS5	0.003	0.005	0.007	0.009	0.014	0.022	0.028	0.029	0.022	0.014	1.0	0.015	0.016	0.02
Trunk	HAF4016A (764-870MHz)	2.15	794.000	5.0	5.0	CW	E	1.04	BS5	0.002	0.003	0.004	0.005	0.009	0.015	0.020	0.023	0.021	0.014	1.0	0.012	0.012	0.01
Trunk	HAF4016A (764-870MHz)	2.15	800.000	5.0	5.0	CW	E	1.04	BS5	0.002	0.003	0.004	0.006	0.010	0.015	0.022	0.024	0.023	0.016	1.0	0.013	0.013	0.01
Trunk	HAF4016A (764-870MHz)	2.15	806.000	5.0	5.0	CW	E	1.04	BS5	0.003	0.004	0.004	0.008	0.014	0.020	0.028	0.032	0.031	0.026	1.0	0.017	0.018	0.02

MPE calculations are defined in section 13.0.

DVR (700MHz 5W) - MPE measurement data for Passenger

D.U.T. Info.							Probe Info.			MPE Measurement						
Ant Loc.	**Ant. Model/ Desc.**	**Ant. Gain (dBi)**	**Tx Freq (MHz)**	**Max Pwr (W)**	**Initial Pwr (W)**	**Test Mode**	**E/H Field**	**Probe Cal. Factor**	**Test Pos.**	**Head**	**Chest**	**Lower Trunk**	**DUT Max. TX Factor**	**Avg. over Body (mW/cm^2)**	**Calc. P.D. (mW/cm^2)**	**Max Calc. P.D. (mW/cm^2)**
Trunk	HAF4016A (764-870MHz)	2.15	764.000	5.0	5.0	CW	E	1.03	PB	0.042	0.027	0.017	1.0	0.029	0.030	0.03
Trunk	HAF4016A (764-870MHz)	2.15	770.000	5.0	5.0	CW	E	1.03	PB	0.037	0.019	0.013	1.0	0.023	0.024	0.02
Trunk	HAF4016A (764-870MHz)	2.15	775.000	5.0	5.0	CW	E	1.04	PB	0.053	0.032	0.022	1.0	0.036	0.037	0.04
Trunk	HAF4016A (764-870MHz)	2.15	794.000	5.0	5.0	CW	E	1.04	PB	0.036	0.014	0.021	1.0	0.024	0.025	0.02
Trunk	HAF4016A (764-870MHz)	2.15	800.000	5.0	5.0	CW	E	1.04	PB	0.030	0.018	0.021	1.0	0.023	0.024	0.02
Trunk	HAF4016A (764-870MHz)	2.15	806.000	5.0	5.0	CW	E	1.04	PB	0.059	0.033	0.034	1.0	0.042	0.044	0.04
Trunk	HAF4016A (764-870MHz)	2.15	764.000	5.0	5.0	CW	E	1.03	PF	0.018	0.011	0.012	1.0	0.014	0.014	0.01
Trunk	HAF4016A (764-870MHz)	2.15	770.000	5.0	5.0	CW	E	1.03	PF	0.016	0.010	0.010	1.0	0.012	0.012	0.01
Trunk	HAF4016A (764-870MHz)	2.15	775.000	5.0	5.0	CW	E	1.04	PF	0.018	0.012	0.014	1.0	0.015	0.015	0.02
Trunk	HAF4016A (764-870MHz)	2.15	794.000	5.0	5.0	CW	E	1.04	PF	0.024	0.020	0.011	1.0	0.018	0.019	0.02
Trunk	HAF4016A (764-870MHz)	2.15	800.000	5.0	5.0	CW	E	1.04	PF	0.020	0.022	0.008	1.0	0.017	0.017	0.02
Trunk	HAF4016A (764-870MHz)	2.15	806.000	5.0	5.0	CW	E	1.04	PF	0.030	0.024	0.010	1.0	0.021	0.022	0.02

MPE calculations are defined in section 13.0.

Companion Mobile (VHF 100W) - MPE measurement data for Bystander

D.U.T. Info.							Probe Info.			MPE measurement													
Ant Loc.	**Ant. Model/ Desc.**	**Ant. Gain (dBi)**	**Tx Freq (MHz)**	**Max Pwr (W)**	**Initial Pwr (W)**	**Test Mode**	**E/H Field**	**Probe Cal. Factor**	**Test Pos.**	**20 cm**	**40 cm**	**60 cm**	**80 cm**	**100 cm**	**120 cm**	**140 cm**	**160 cm**	**180 cm**	**200 cm**	**DUT Max. TX Factor**	**Avg. over Body (mW/ cm^2)**	**Calc. P.D. (mW/ cm^2)**	**Max Calc. P.D. (mW/ cm^2)**
Roof	HAD4008A (150.8-162MHz)	2.15	150.800	120	116	CW	E	1	BS1	0.064	0.116	0.136	0.137	0.141	0.171	0.216	0.248	0.239	0.203	0.5	0.167	0.084	0.09
Roof	HAD4008A (150.8-162MHz)	2.15	156.400	120	117	CW	E	1	BS1	0.068	0.101	0.115	0.123	0.14	0.19	0.246	0.281	0.269	0.232	0.5	0.177	0.088	0.09
Roof	HAD4008A (150.8-162MHz)	2.15	162.000	120	117	CW	E	1	BS1	0.066	0.095	0.109	0.121	0.161	0.234	0.292	0.305	0.28	0.239	0.5	0.190	0.095	0.10
Roof	HAD4009A (162-174MHz)	2.15	162.000	120	117	CW	E	1	BS1	0.049	0.081	0.09	0.101	0.135	0.188	0.239	0.258	0.246	0.21	0.5	0.160	0.080	0.08
Roof	HAD4009A (162-174MHz)	2.15	167.700	120	117	CW	E	1	BS1	0.082	0.122	0.146	0.169	0.222	0.289	0.327	0.33	0.286	0.238	0.5	0.221	0.111	0.11
Roof	HAD4009A (162-174MHz)	2.15	173.400	120	118	CW	E	1	BS1	0.117	0.176	0.218	0.251	0.301	0.359	0.386	0.363	0.305	0.235	0.5	0.271	0.136	0.14
Roof	HAD4021A (136-174MHz)	2.15	136.000	120	116	CW	E	0.99	BS1	0.076	0.136	0.167	0.158	0.144	0.124	0.133	0.14	0.149	0.141	0.5	0.137	0.068	0.07
Roof	HAD4021A (136-174MHz)	2.15	140.900	120	116	CW	E	1	BS1	0.062	0.111	0.132	0.113	0.087	0.081	0.101	0.122	0.127	0.113	0.5	0.105	0.052	0.05
Roof	HAD4021A (136-174MHz)	2.15	145.900	120	116	CW	E	1	BS1	0.05	0.088	0.102	0.112	0.081	0.098	0.134	0.161	0.164	0.146	0.5	0.114	0.057	0.06
Roof	HAD4021A (136-174MHz)	2.15	150.800	120	116	CW	E	1	BS1	0.068	0.11	0.128	0.116	0.116	0.152	0.197	0.233	0.23	0.198	0.5	0.155	0.077	0.08
Roof	HAD4021A (136-174MHz)	2.15	158.300	120	116	CW	E	1	BS1	0.062	0.097	0.11	0.107	0.132	0.184	0.239	0.268	0.252	0.214	0.5	0.167	0.083	0.09
Roof	HAD4021A (136-174MHz)	2.15	165.900	120	118	CW	E	1	BS1	0.059	0.089	0.106	0.118	0.159	0.217	0.265	0.262	0.238	0.202	0.5	0.172	0.086	0.09
Roof	HAD4021A (136-174MHz)	2.15	173.400	120	118	CW	E	1	BS1	0.09	0.143	0.183	0.207	0.254	0.3	0.318	0.297	0.242	0.184	0.5	0.222	0.111	0.11

MPE calculations are defined in section 13.0.

Companion Mobile (VHF 100W) - MPE measurement data for Bystander

D.U.T. Info.							Probe Info.			MPE measurement													
Ant Loc.	**Ant. Model/ Desc.**	**Ant. Gain (dBi)**	**Tx Freq (MHz)**	**Max Pwr (W)**	**Initial Pwr (W)**	**Test Mode**	**E/H Field**	**Probe Cal. Factor**	**Test Pos.**	**20 cm**	**40 cm**	**60 cm**	**80 cm**	**100 cm**	**120 cm**	**140 cm**	**160 cm**	**180 cm**	**200 cm**	**DUT Max. TX Factor**	**Avg. over Body (mW/ cm^2)**	**Calc. P.D. (mW/ cm^2)**	**Max Calc. P.D. (mW/ cm^2)**
Roof	HAD4008A (150.8-162MHz)	2.15	150.800	120	116	CW	E	1	BS2	0.108	0.183	0.239	0.251	0.242	0.238	0.252	0.265	0.246	0.226	0.5	0.225	0.113	0.12
Roof	HAD4008A (150.8-162MHz)	2.15	156.400	120	117	CW	E	1	BS2	0.12	0.212	0.287	0.301	0.27	0.264	0.268	0.263	0.247	0.215	0.5	0.245	0.122	0.13
Roof	HAD4008A (150.8-162MHz)	2.15	162.000	120	117	CW	E	1	BS2	0.129	0.235	0.316	0.336	0.322	0.304	0.298	0.285	0.253	0.216	0.5	0.269	0.135	0.14
Roof	HAD4009A (162-174MHz)	2.15	162.000	120	117	CW	E	1	BS2	0.104	0.205	0.278	0.297	0.288	0.276	0.267	0.254	0.228	0.195	0.5	0.239	0.120	0.12
Roof	HAD4009A (162-174MHz)	2.15	167.700	120	117	CW	E	1	BS2	0.183	0.317	0.424	0.438	0.412	0.378	0.349	0.324	0.281	0.249	0.5	0.336	0.168	0.17
Roof	HAD4009A (162-174MHz)	2.15	173.400	120	118	CW	E	1	BS2	0.214	0.378	0.479	0.47	0.419	0.382	0.359	0.326	0.271	0.211	0.5	0.351	0.175	0.18
Roof	HAD4021A (136-174MHz)	2.15	136.000	120	116	CW	E	0.99	BS2	0.093	0.174	0.232	0.244	0.219	0.202	0.184	0.173	0.163	0.149	0.5	0.183	0.091	0.09
Roof	HAD4021A (136-174MHz)	2.15	140.900	120	116	CW	E	1	BS2	0.076	0.137	0.18	0.189	0.177	0.162	0.151	0.15	0.146	0.136	0.5	0.150	0.075	0.08
Roof	HAD4021A (136-174MHz)	2.15	145.900	120	116	CW	E	1	BS2	0.104	0.175	0.222	0.233	0.226	0.209	0.205	0.203	0.192	0.178	0.5	0.195	0.097	0.10
Roof	HAD4021A (136-174MHz)	2.15	150.800	120	116	CW	E	1	BS2	0.111	0.179	0.231	0.242	0.229	0.23	0.237	0.239	0.226	0.207	0.5	0.213	0.107	0.11
Roof	HAD4021A (136-174MHz)	2.15	158.300	120	116	CW	E	1	BS2	0.11	0.195	0.261	0.264	0.25	0.241	0.247	0.244	0.226	0.198	0.5	0.224	0.112	0.12
Roof	HAD4021A (136-174MHz)	2.15	165.900	120	118	CW	E	1	BS2	0.139	0.244	0.329	0.345	0.317	0.295	0.267	0.247	0.214	0.0192	0.5	0.242	0.121	0.12
Roof	HAD4021A (136-174MHz)	2.15	173.400	120	118	CW	E	1	BS2	0.198	0.326	0.403	0.373	0.319	0.287	0.267	0.24	0.202	0.165	0.5	0.278	0.139	0.14

MPE calculations are defined in section 13.0.

Companion Mobile (VHF 100W) - MPE measurement data for Bystander

D.U.T. Info.							Probe Info.			MPE measurement													
Ant Loc.	Ant. Model/ Desc.	Ant. Gain (dBi)	Tx Freq (MHz)	Max Pwr (W)	Initial Pwr (W)	Test Mode	E/H Field	Probe Cal. Factor	Test Pos.	20 cm	40 cm	60 cm	80 cm	100 cm	120 cm	140 cm	160 cm	180 cm	200 cm	DUT Max. TX Factor	Avg. over Body (mW/ cm^2)	Calc. P.D. (mW/ cm^2)	Max Calc. P.D. (mW/ cm^2)
Roof	HAD4008A (150.8-162MHz)	2.15	150.800	120	116	CW	E	1	BS3	0.118	0.178	0.213	0.248	0.244	0.215	0.193	0.18	0.162	0.142	0.5	0.189	0.095	0.10
Roof	HAD4008A (150.8-162MHz)	2.15	156.400	120	117	CW	E	1	BS3	0.119	0.184	0.27	0.291	0.285	0.252	0.223	0.2	0.182	0.172	0.5	0.218	0.109	0.11
Roof	HAD4008A (150.8-162MHz)	2.15	162.000	120	117	CW	E	1	BS3	0.119	0.193	0.264	0.329	0.319	0.274	0.247	0.221	0.209	0.177	0.5	0.235	0.118	0.12
Roof	HAD4009A (162-174MHz)	2.15	162.000	120	117	CW	E	1	BS3	0.114	0.191	0.267	0.298	0.273	0.259	0.228	0.21	0.188	0.164	0.5	0.219	0.110	0.11
Roof	HAD4009A (162-174MHz)	2.15	167.700	120	117	CW	E	1	BS3	0.137	0.217	0.297	0.349	0.336	0.286	0.235	0.208	0.196	0.168	0.5	0.243	0.121	0.12
Roof	HAD4009A (162-174MHz)	2.15	173.400	120	118	CW	E	1	BS3	0.156	0.232	0.3	0.356	0.303	0.249	0.208	0.187	0.157	0.112	0.5	0.226	0.113	0.11
Roof	HAD4021A (136-174MHz)	2.15	136.000	120	116	CW	E	0.99	BS3	0.078	0.119	0.156	0.189	0.202	0.193	0.168	0.155	0.133	0.112	0.5	0.151	0.075	0.08
Roof	HAD4021A (136-174MHz)	2.15	140.900	120	116	CW	E	1	BS3	0.097	0.128	0.154	0.163	0.158	0.147	0.134	0.115	0.101	0.092	0.5	0.129	0.064	0.07
Roof	HAD4021A (136-174MHz)	2.15	145.900	120	116	CW	E	1	BS3	0.123	0.159	0.19	0.222	0.202	0.193	0.176	0.157	0.141	0.114	0.5	0.168	0.084	0.09
Roof	HAD4021A (136-174MHz)	2.15	150.800	120	116	CW	E	1	BS3	0.118	0.18	0.221	0.24	0.236	0.212	0.191	0.17	0.158	0.145	0.5	0.187	0.094	0.10
Roof	HAD4021A (136-174MHz)	2.15	158.300	120	116	CW	E	1	BS3	0.129	0.191	0.245	0.276	0.264	0.232	0.213	0.202	0.184	0.157	0.5	0.209	0.105	0.11
Roof	HAD4021A (136-174MHz)	2.15	165.900	120	118	CW	E	1	BS3	0.129	0.173	0.214	0.241	0.224	0.208	0.176	0.169	0.162	0.129	0.5	0.183	0.091	0.09
Roof	HAD4021A (136-174MHz)	2.15	173.400	120	118	CW	E	1	BS3	0.123	0.181	0.219	0.234	0.216	0.198	0.159	0.132	0.112	0.082	0.5	0.166	0.083	0.08

MPE calculations are defined in section 13.0.

Companion Mobile (VHF 100W) - MPE measurement data for Bystander

D.U.T. Info.							Probe Info.			MPE measurement													
Ant Loc.	**Ant. Model/ Desc.**	**Ant. Gain (dBi)**	**Tx Freq (MHz)**	**Max Pwr (W)**	**Initial Pwr (W)**	**Test Mode**	**E/H Field**	**Probe Cal. Factor**	**Test Pos.**	**20 cm**	**40 cm**	**60 cm**	**80 cm**	**100 cm**	**120 cm**	**140 cm**	**160 cm**	**180 cm**	**200 cm**	**DUT Max. TX Factor**	**Avg. over Body (mW/ cm^2)**	**Calc. P.D. (mW/ cm^2)**	**Max Calc. P.D. (mW/ cm^2)**
Roof	HAD4008A (150.8-162MHz)	2.15	150.800	120	116	CW	E	1	BS4	0.086	0.163	0.218	0.232	0.213	0.184	0.151	0.133	0.121	0.102	0.5	0.160	0.080	0.08
Roof	HAD4008A (150.8-162MHz)	2.15	156.400	120	117	CW	E	1	BS4	0.078	0.148	0.197	0.202	0.18	0.148	0.121	0.102	0.08	0.062	0.5	0.132	0.066	0.07
Roof	HAD4008A (150.8-162MHz)	2.15	162.000	120	117	CW	E	1	BS4	0.088	0.157	0.204	0.205	0.179	0.152	0.129	0.113	0.097	0.082	0.5	0.141	0.070	0.07
Roof	HAD4009A (162-174MHz)	2.15	162.000	120	117	CW	E	1	BS4	0.08	0.145	0.181	0.182	0.16	0.133	0.116	0.1	0.087	0.075	0.5	0.126	0.063	0.06
Roof	HAD4009A (162-174MHz)	2.15	167.700	120	117	CW	E	1	BS4	0.071	0.134	0.171	0.17	0.143	0.118	0.105	0.104	0.098	0.084	0.5	0.120	0.060	0.06
Roof	HAD4009A (162-174MHz)	2.15	173.400	120	118	CW	E	1	BS4	0.082	0.149	0.192	0.189	0.164	0.137	0.12	0.11	0.105	0.099	0.5	0.135	0.067	0.07
Roof	HAD4021A (136-174MHz)	2.15	136.000	120	116	CW	E	0.99	BS4	0.068	0.121	0.169	0.193	0.191	0.177	0.158	0.143	0.128	0.116	0.5	0.146	0.073	0.08
Roof	HAD4021A (136-174MHz)	2.15	140.900	120	116	CW	E	1	BS4	0.06	0.108	0.147	0.16	0.153	0.139	0.129	0.117	0.106	0.096	0.5	0.122	0.061	0.06
Roof	HAD4021A (136-174MHz)	2.15	145.900	120	116	CW	E	1	BS4	0.068	0.131	0.174	0.188	0.178	0.154	0.134	0.119	0.108	0.097	0.5	0.135	0.068	0.07
Roof	HAD4021A (136-174MHz)	2.15	150.800	120	116	CW	E	1	BS4	0.081	0.156	0.207	0.221	0.202	0.174	0.144	0.124	0.113	0.098	0.5	0.152	0.076	0.08
Roof	HAD4021A (136-174MHz)	2.15	158.300	120	116	CW	E	1	BS4	0.065	0.123	0.157	0.16	0.142	0.114	0.093	0.077	0.064	0.056	0.5	0.105	0.053	0.05
Roof	HAD4021A (136-174MHz)	2.15	165.900	120	118	CW	E	1	BS4	0.059	0.113	0.143	0.142	0.122	0.103	0.083	0.072	0.065	0.062	0.5	0.096	0.048	0.05
Roof	HAD4021A (136-174MHz)	2.15	173.400	120	118	CW	E	1	BS4	0.064	0.12	0.152	0.154	0.136	0.115	0.1	0.088	0.086	0.084	0.5	0.110	0.055	0.06

MPE calculations are defined in section 13.0.

Companion Mobile (VHF 100W) - MPE measurement data for Bystander

D.U.T. Info.							Probe Info.			MPE measurement													
Ant Loc.	**Ant. Model/ Desc.**	**Ant. Gain (dBi)**	**Tx Freq (MHz)**	**Max Pwr (W)**	**Initial Pwr (W)**	**Test Mode**	**E/H Field**	**Probe Cal. Factor**	**Test Pos.**	**20 cm**	**40 cm**	**60 cm**	**80 cm**	**100 cm**	**120 cm**	**140 cm**	**160 cm**	**180 cm**	**200 cm**	**DUT Max. TX Factor**	**Avg. over Body (mW/ cm^2)**	**Calc. P.D. (mW/ cm^2)**	**Max Calc. P.D. (mW/ cm^2)**
Roof	HAD4008A (150.8-162MHz)	2.15	150.800	120	116	CW	E	1	BS5	0.035	0.066	0.082	0.084	0.075	0.063	0.058	0.056	0.056	0.057	0.5	0.063	0.032	0.03
Roof	HAD4008A (150.8-162MHz)	2.15	156.400	120	117	CW	E	1	BS5	0.051	0.077	0.093	0.086	0.071	0.06	0.058	0.056	0.055	0.058	0.5	0.067	0.033	0.03
Roof	HAD4008A (150.8-162MHz)	2.15	162.000	120	117	CW	E	1	BS5	0.042	0.065	0.076	0.073	0.06	0.053	0.05	0.053	0.057	0.062	0.5	0.059	0.030	0.03
Roof	HAD4009A (162-174MHz)	2.15	162.000	120	117	CW	E	1	BS5	0.038	0.057	0.068	0.063	0.054	0.046	0.045	0.048	0.051	0.054	0.5	0.052	0.026	0.03
Roof	HAD4009A (162-174MHz)	2.15	167.700	120	117	CW	E	1	BS5	0.037	0.063	0.075	0.065	0.049	0.038	0.039	0.043	0.049	0.05	0.5	0.051	0.025	0.03
Roof	HAD4009A (162-174MHz)	2.15	173.400	120	118	CW	E	1	BS5	0.04	0.065	0.073	0.062	0.048	0.043	0.048	0.057	0.064	0.066	0.5	0.057	0.028	0.03
Roof	HAD4021A (136-174MHz)	2.15	136.000	120	116	CW	E	0.99	BS5	0.037	0.066	0.088	0.096	0.093	0.083	0.076	0.072	0.072	0.068	0.5	0.075	0.037	0.04
Roof	HAD4021A (136-174MHz)	2.15	140.900	120	116	CW	E	1	BS5	0.04	0.068	0.088	0.09	0.083	0.075	0.071	0.07	0.07	0.067	0.5	0.072	0.036	0.04
Roof	HAD4021A (136-174MHz)	2.15	145.900	120	116	CW	E	1	BS5	0.04	0.071	0.092	0.096	0.085	0.074	0.066	0.063	0.061	0.06	0.5	0.071	0.035	0.04
Roof	HAD4021A (136-174MHz)	2.15	150.800	120	116	CW	E	1	BS5	0.033	0.061	0.078	0.077	0.068	0.058	0.052	0.051	0.053	0.054	0.5	0.059	0.029	0.03
Roof	HAD4021A (136-174MHz)	2.15	158.300	120	116	CW	E	1	BS5	0.038	0.059	0.068	0.063	0.051	0.043	0.042	0.042	0.045	0.047	0.5	0.050	0.025	0.03
Roof	HAD4021A (136-174MHz)	2.15	165.900	120	118	CW	E	1	BS5	0.032	0.054	0.065	0.058	0.048	0.042	0.043	0.046	0.049	0.05	0.5	0.049	0.024	0.02
Roof	HAD4021A (136-174MHz)	2.15	173.400	120	118	CW	E	1	BS5	0.028	0.045	0.05	0.042	0.035	0.033	0.039	0.046	0.051	0.056	0.5	0.043	0.021	0.02

MPE calculations are defined in section 13.0.

Companion Mobile (VHF 100W) - MPE measurement data for Bystander

D.U.T. Info.							Probe Info.			MPE measurement													
Ant Loc.	Ant. Model/ Desc.	Ant. Gain (dBi)	Tx Freq (MHz)	Max Pwr (W)	Initial Pwr (W)	Test Mode	E/H Field	Probe Cal. Factor	Test Pos.	20 cm	40 cm	60 cm	80 cm	100 cm	120 cm	140 cm	160 cm	180 cm	200 cm	DUT Max. TX Factor	Avg. over Body (mW/ cm^2)	Calc. P.D. (mW/ cm^2)	Max Calc. P.D. (mW/ cm^2)
Roof	HAD4008A (150.8-162MHz)	2.15	150.800	120	116	CW	H	0.86	BS1	0.046	0.049	0.064	0.08	0.093	0.098	0.097	0.089	0.08	0.071	0.5	0.077	0.082	0.08
Roof	HAD4008A (150.8-162MHz)	2.15	156.400	120	117	CW	H	0.85	BS1	0.051	0.058	0.071	0.086	0.097	0.1	0.097	0.089	0.08	0.071	0.5	0.080	0.087	0.09
Roof	HAD4008A (150.8-162MHz)	2.15	162.000	120	117	CW	H	0.85	BS1	0.059	0.062	0.075	0.088	0.097	0.099	0.094	0.086	0.079	0.072	0.5	0.081	0.090	0.09
Roof	HAD4009A (162-174MHz)	2.15	162.000	120	117	CW	H	0.85	BS1	0.055	0.057	0.07	0.082	0.09	0.091	0.087	0.08	0.074	0.067	0.5	0.075	0.077	0.08
Roof	HAD4009A (162-174MHz)	2.15	167.700	120	117	CW	H	0.85	BS1	0.067	0.072	0.085	0.097	0.104	0.105	0.102	0.095	0.087	0.082	0.5	0.090	0.109	0.11
Roof	HAD4009A (162-174MHz)	2.15	173.400	120	118	CW	H	0.84	BS1	0.077	0.081	0.095	0.11	0.119	0.121	0.115	0.107	0.096	0.087	0.5	0.101	0.135	0.14
Roof	HAD4021A (136-174MHz)	2.15	136.000	120	116	CW	H	0.88	BS1	0.051	0.05	0.053	0.068	0.08	0.087	0.087	0.081	0.072	0.061	0.5	0.069	0.069	0.07
Roof	HAD4021A (136-174MHz)	2.15	140.900	120	116	CW	H	0.87	BS1	0.047	0.044	0.052	0.065	0.077	0.082	0.081	0.075	0.066	0.055	0.5	0.064	0.059	0.06
Roof	HAD4021A (136-174MHz)	2.15	145.900	120	116	CW	H	0.87	BS1	0.044	0.05	0.052	0.067	0.079	0.085	0.085	0.08	0.073	0.063	0.5	0.068	0.066	0.07
Roof	HAD4021A (136-174MHz)	2.15	150.800	120	116	CW	H	0.86	BS1	0.05	0.052	0.062	0.08	0.089	0.092	0.092	0.089	0.079	0.068	0.5	0.075	0.079	0.08
Roof	HAD4021A (136-174MHz)	2.15	158.300	120	116	CW	H	0.85	BS1	0.054	0.058	0.071	0.086	0.096	0.099	0.094	0.086	0.076	0.066	0.5	0.079	0.084	0.09
Roof	HAD4021A (136-174MHz)	2.15	165.900	120	118	CW	H	0.85	BS1	0.058	0.062	0.073	0.086	0.093	0.095	0.092	0.085	0.078	0.073	0.5	0.080	0.086	0.09
Roof	HAD4021A (136-174MHz)	2.15	173.400	120	118	CW	H	0.84	BS1	0.069	0.073	0.087	0.101	0.11	0.11	0.104	0.094	0.084	0.073	0.5	0.091	0.109	0.11

MPE calculations are defined in section 13.0.

Companion Mobile (VHF 100W) - MPE measurement data for Bystander

D.U.T. Info.							Probe Info.			MPE measurement													
Ant Loc.	**Ant. Model/ Desc.**	**Ant. Gain (dBi)**	**Tx Freq (MHz)**	**Max Pwr (W)**	**Initial Pwr (W)**	**Test Mode**	**E/H Field**	**Probe Cal. Factor**	**Test Pos.**	**20 cm**	**40 cm**	**60 cm**	**80 cm**	**100 cm**	**120 cm**	**140 cm**	**160 cm**	**180 cm**	**200 cm**	**DUT Max. TX Factor**	**Avg. over Body (mW/ cm^2)**	**Calc. P.D. (mW/ cm^2)**	**Max Calc. P.D. (mW/ cm^2)**
Roof	HAD4008A (150.8-162MHz)	2.15	150.800	120	116	CW	H	0.86	BS2	0.062	0.064	0.072	0.087	0.098	0.109	0.105	0.1	0.09	0.082	0.5	0.087	0.105	0.11
Roof	HAD4008A (150.8-162MHz)	2.15	156.400	120	117	CW	H	0.85	BS2	0.069	0.072	0.086	0.101	0.111	0.114	0.109	0.1	0.088	0.078	0.5	0.093	0.117	0.12
Roof	HAD4008A (150.8-162MHz)	2.15	162.000	120	117	CW	H	0.85	BS2	0.069	0.076	0.092	0.108	0.118	0.119	0.113	0.104	0.093	0.083	0.5	0.098	0.129	0.13
Roof	HAD4009A (162-174MHz)	2.15	162.000	120	117	CW	H	0.85	BS2	0.065	0.073	0.087	0.102	0.112	0.114	0.108	0.099	0.088	0.079	0.5	0.093	0.117	0.12
Roof	HAD4009A (162-174MHz)	2.15	167.700	120	117	CW	H	0.85	BS2	0.085	0.088	0.104	0.122	0.132	0.134	0.127	0.116	0.101	0.091	0.5	0.110	0.165	0.17
Roof	HAD4009A (162-174MHz)	2.15	173.400	120	118	CW	H	0.84	BS2	0.092	0.095	0.112	0.129	0.138	0.135	0.123	0.108	0.093	0.08	0.5	0.111	0.162	0.17
Roof	HAD4021A (136-174MHz)	2.15	136.000	120	116	CW	H	0.88	BS2	0.067	0.056	0.061	0.07	0.081	0.09	0.091	0.088	0.081	0.079	0.5	0.076	0.085	0.09
Roof	HAD4021A (136-174MHz)	2.15	140.900	120	116	CW	H	0.87	BS2	0.06	0.054	0.056	0.067	0.077	0.085	0.084	0.08	0.073	0.066	0.5	0.070	0.070	0.07
Roof	HAD4021A (136-174MHz)	2.15	145.900	120	116	CW	H	0.87	BS2	0.066	0.062	0.068	0.08	0.091	0.097	0.096	0.091	0.083	0.074	0.5	0.081	0.093	0.10
Roof	HAD4021A (136-174MHz)	2.15	150.800	120	116	CW	H	0.86	BS2	0.067	0.061	0.071	0.084	0.095	0.101	0.1	0.096	0.086	0.078	0.5	0.084	0.098	0.10
Roof	HAD4021A (136-174MHz)	2.15	158.300	120	116	CW	H	0.85	BS2	0.07	0.072	0.085	0.1	0.109	0.11	0.104	0.094	0.083	0.073	0.5	0.090	0.110	0.11
Roof	HAD4021A (136-174MHz)	2.15	165.900	120	118	CW	H	0.85	BS2	0.078	0.08	0.092	0.106	0.115	0.116	0.11	0.1	0.089	0.079	0.5	0.097	0.127	0.13
Roof	HAD4021A (136-174MHz)	2.15	173.400	120	118	CW	H	0.84	BS2	0.084	0.088	0.103	0.116	0.122	0.119	0.108	0.093	0.079	0.067	0.5	0.098	0.127	0.13

MPE calculations are defined in section 13.0.

Companion Mobile (VHF 100W) - MPE measurement data for Bystander

D.U.T. Info.							Probe Info.			MPE measurement													
Ant Loc.	Ant. Model/ Desc.	Ant. Gain (dBi)	Tx Freq (MHz)	Max Pwr (W)	Initial Pwr (W)	Test Mode	E/H Field	Probe Cal. Factor	Test Pos.	20 cm	40 cm	60 cm	80 cm	100 cm	120 cm	140 cm	160 cm	180 cm	200 cm	DUT Max. TX Factor	Avg. over Body (mW/ cm^2)	Calc. P.D. (mW/ cm^2)	Max Calc. P.D. (mW/ cm^2)
Roof	HAD4008A (150.8-162MHz)	2.15	150.800	120	116	CW	H	0.86	BS3	0.066	0.07	0.077	0.084	0.088	0.089	0.086	0.081	0.075	0.071	0.5	0.079	0.086	0.09
Roof	HAD4008A (150.8-162MHz)	2.15	156.400	120	117	CW	H	0.85	BS3	0.073	0.068	0.078	0.088	0.095	0.096	0.094	0.089	0.084	0.082	0.5	0.085	0.098	0.10
Roof	HAD4008A (150.8-162MHz)	2.15	162.000	120	117	CW	H	0.85	BS3	0.059	0.078	0.089	0.099	0.104	0.106	0.1	0.093	0.085	0.079	0.5	0.089	0.108	0.11
Roof	HAD4009A (162-174MHz)	2.15	162.000	120	117	CW	H	0.85	BS3	0.063	0.075	0.086	0.096	0.103	0.102	0.097	0.09	0.081	0.072	0.5	0.087	0.102	0.10
Roof	HAD4009A (162-174MHz)	2.15	167.700	120	117	CW	H	0.85	BS3	0.06	0.068	0.082	0.098	0.107	0.112	0.11	0.1	0.09	0.081	0.5	0.091	0.112	0.12
Roof	HAD4009A (162-174MHz)	2.15	173.400	120	118	CW	H	0.84	BS3	0.065	0.071	0.088	0.102	0.111	0.113	0.107	0.102	0.089	0.079	0.5	0.093	0.114	0.12
Roof	HAD4021A (136-174MHz)	2.15	136.000	120	116	CW	H	0.88	BS3	0.05	0.059	0.065	0.072	0.077	0.078	0.077	0.075	0.07	0.068	0.5	0.069	0.070	0.07
Roof	HAD4021A (136-174MHz)	2.15	140.900	120	116	CW	H	0.87	BS3	0.046	0.052	0.057	0.063	0.067	0.069	0.068	0.067	0.064	0.063	0.5	0.062	0.054	0.06
Roof	HAD4021A (136-174MHz)	2.15	145.900	120	116	CW	H	0.87	BS3	0.051	0.056	0.065	0.073	0.077	0.079	0.077	0.074	0.071	0.069	0.5	0.069	0.068	0.07
Roof	HAD4021A (136-174MHz)	2.15	150.800	120	116	CW	H	0.86	BS3	0.056	0.059	0.069	0.079	0.083	0.084	0.081	0.078	0.077	0.072	0.5	0.074	0.076	0.08
Roof	HAD4021A (136-174MHz)	2.15	158.300	120	116	CW	H	0.85	BS3	0.061	0.065	0.072	0.081	0.09	0.093	0.091	0.09	0.083	0.077	0.5	0.080	0.088	0.09
Roof	HAD4021A (136-174MHz)	2.15	165.900	120	118	CW	H	0.85	BS3	0.055	0.061	0.073	0.085	0.092	0.093	0.091	0.084	0.075	0.066	0.5	0.078	0.082	0.08
Roof	HAD4021A (136-174MHz)	2.15	173.400	120	118	CW	H	0.84	BS3	0.051	0.065	0.078	0.088	0.097	0.099	0.095	0.088	0.079	0.069	0.5	0.081	0.087	0.09

MPE calculations are defined in section 13.0.

Companion Mobile (VHF 100W) - MPE measurement data for Bystander

D.U.T. Info.							**Probe Info.**			**MPE measurement**													
Ant Loc.	**Ant. Model/ Desc.**	**Ant. Gain (dBi)**	**Tx Freq (MHz)**	**Max Pwr (W)**	**Initial Pwr (W)**	**Test Mode**	**E/H Field**	**Probe Cal. Factor**	**Test Pos.**	**20 cm**	**40 cm**	**60 cm**	**80 cm**	**100 cm**	**120 cm**	**140 cm**	**160 cm**	**180 cm**	**200 cm**	**DUT Max. TX Factor**	**Avg. over Body (mW/ cm^2)**	**Calc. P.D. (mW/ cm^2)**	**Max Calc. P.D. (mW/ cm^2)**
Roof	HAD4008A (150.8-162MHz)	2.15	150.800	120	116	CW	H	0.86	BS4	0.058	0.065	0.076	0.084	0.089	0.089	0.085	0.079	0.071	0.064	0.5	0.076	0.081	0.08
Roof	HAD4008A (150.8-162MHz)	2.15	156.400	120	117	CW	H	0.85	BS4	0.055	0.063	0.074	0.081	0.084	0.082	0.077	0.07	0.063	0.055	0.5	0.070	0.067	0.07
Roof	HAD4008A (150.8-162MHz)	2.15	162.000	120	117	CW	H	0.85	BS4	0.06	0.068	0.079	0.086	0.089	0.087	0.083	0.077	0.071	0.065	0.5	0.077	0.080	0.08
Roof	HAD4009A (162-174MHz)	2.15	162.000	120	117	CW	H	0.85	BS4	0.057	0.065	0.075	0.081	0.084	0.082	0.078	0.073	0.067	0.06	0.5	0.072	0.071	0.07
Roof	HAD4009A (162-174MHz)	2.15	167.700	120	117	CW	H	0.85	BS4	0.054	0.064	0.074	0.08	0.081	0.079	0.075	0.069	0.064	0.059	0.5	0.070	0.067	0.07
Roof	HAD4009A (162-174MHz)	2.15	173.400	120	118	CW	H	0.84	BS4	0.056	0.065	0.077	0.085	0.089	0.088	0.084	0.078	0.072	0.066	0.5	0.076	0.077	0.08
Roof	HAD4021A (136-174MHz)	2.15	136.000	120	116	CW	H	0.88	BS4	0.047	0.051	0.059	0.069	0.077	0.081	0.083	0.081	0.077	0.07	0.5	0.070	0.071	0.07
Roof	HAD4021A (136-174MHz)	2.15	140.900	120	116	CW	H	0.87	BS4	0.045	0.05	0.058	0.066	0.073	0.075	0.075	0.073	0.068	0.062	0.5	0.065	0.059	0.06
Roof	HAD4021A (136-174MHz)	2.15	145.900	120	116	CW	H	0.87	BS4	0.051	0.056	0.066	0.075	0.081	0.082	0.081	0.076	0.071	0.064	0.5	0.070	0.071	0.07
Roof	HAD4021A (136-174MHz)	2.15	150.800	120	116	CW	H	0.86	BS4	0.056	0.063	0.073	0.082	0.086	0.086	0.083	0.076	0.069	0.061	0.5	0.074	0.075	0.08
Roof	HAD4021A (136-174MHz)	2.15	158.300	120	116	CW	H	0.85	BS4	0.051	0.059	0.069	0.075	0.077	0.074	0.07	0.064	0.058	0.052	0.5	0.065	0.057	0.06
Roof	HAD4021A (136-174MHz)	2.15	165.900	120	118	CW	H	0.85	BS4	0.051	0.059	0.069	0.074	0.075	0.072	0.067	0.062	0.057	0.051	0.5	0.064	0.055	0.06
Roof	HAD4021A (136-174MHz)	2.15	173.400	120	118	CW	H	0.84	BS4	0.05	0.057	0.067	0.075	0.078	0.078	0.075	0.07	0.064	0.058	0.5	0.067	0.060	0.06

MPE calculations are defined in section 13.0.

Companion Mobile (VHF 100W) - MPE measurement data for Bystander

D.U.T. Info.							Probe Info.			MPE measurement													
Ant Loc.	**Ant. Model/ Desc.**	**Ant. Gain (dBi)**	**Tx Freq (MHz)**	**Max Pwr (W)**	**Initial Pwr (W)**	**Test Mode**	**E/H Field**	**Probe Cal. Factor**	**Test Pos.**	**20 cm**	**40 cm**	**60 cm**	**80 cm**	**100 cm**	**120 cm**	**140 cm**	**160 cm**	**180 cm**	**200 cm**	**DUT Max. TX Factor**	**Avg. over Body (mW/ cm^2)**	**Calc. P.D. (mW/ cm^2)**	**Max Calc. P.D. (mW/ cm^2)**
Roof	HAD4008A (150.8-162MHz)	2.15	150.800	120	116	CW	H	0.86	BS5	0.04	0.043	0.049	0.054	0.058	0.061	0.061	0.058	0.054	0.051	0.5	0.053	0.039	0.04
Roof	HAD4008A (150.8-162MHz)	2.15	156.400	120	117	CW	H	0.85	BS5	0.046	0.047	0.05	0.055	0.058	0.06	0.06	0.056	0.053	0.049	0.5	0.053	0.039	0.04
Roof	HAD4008A (150.8-162MHz)	2.15	162.000	120	117	CW	H	0.85	BS5	0.042	0.04	0.042	0.047	0.052	0.055	0.056	0.055	0.052	0.049	0.5	0.049	0.033	0.03
Roof	HAD4009A (162-174MHz)	2.15	162.000	120	117	CW	H	0.85	BS5	0.04	0.038	0.04	0.045	0.049	0.052	0.054	0.052	0.05	0.047	0.5	0.047	0.030	0.03
Roof	HAD4009A (162-174MHz)	2.15	167.700	120	117	CW	H	0.85	BS5	0.04	0.037	0.041	0.048	0.053	0.057	0.058	0.056	0.053	0.049	0.5	0.049	0.033	0.03
Roof	HAD4009A (162-174MHz)	2.15	173.400	120	118	CW	H	0.84	BS5	0.042	0.041	0.044	0.048	0.052	0.055	0.057	0.056	0.056	0.053	0.5	0.050	0.034	0.03
Roof	HAD4021A (136-174MHz)	2.15	136.000	120	116	CW	H	0.88	BS5	0.04	0.042	0.047	0.054	0.059	0.063	0.065	0.064	0.061	0.056	0.5	0.055	0.044	0.05
Roof	HAD4021A (136-174MHz)	2.15	140.900	120	116	CW	H	0.87	BS5	0.044	0.046	0.049	0.054	0.058	0.062	0.064	0.063	0.061	0.057	0.5	0.056	0.044	0.05
Roof	HAD4021A (136-174MHz)	2.15	145.900	120	116	CW	H	0.87	BS5	0.044	0.047	0.052	0.057	0.06	0.062	0.062	0.06	0.056	0.052	0.5	0.055	0.043	0.04
Roof	HAD4021A (136-174MHz)	2.15	150.800	120	116	CW	H	0.86	BS5	0.04	0.043	0.05	0.055	0.059	0.061	0.06	0.057	0.053	0.05	0.5	0.053	0.039	0.04
Roof	HAD4021A (136-174MHz)	2.15	158.300	120	116	CW	H	0.85	BS5	0.042	0.042	0.044	0.048	0.05	0.05	0.05	0.048	0.046	0.043	0.5	0.046	0.029	0.03
Roof	HAD4021A (136-174MHz)	2.15	165.900	120	118	CW	H	0.85	BS5	0.036	0.035	0.038	0.044	0.049	0.052	0.052	0.051	0.048	0.044	0.5	0.045	0.027	0.03
Roof	HAD4021A (136-174MHz)	2.15	173.400	120	118	CW	H	0.84	BS5	0.037	0.036	0.039	0.043	0.047	0.049	0.05	0.054	0.052	0.049	0.5	0.046	0.028	0.03

MPE calculations are defined in section 13.0.

Companion Mobile (VHF 100W) - MPE measurement data for Passenger

D.U.T. Info.							Probe Info.			MPE measurement						
Ant Loc.	**Ant. Model/ Desc.**	**Ant. Gain (dBi)**	**Tx Freq (MHz)**	**Max Pwr (W)**	**Initial Pwr (W)**	**Test Mode**	**E/H Field**	**Probe Cal. Factor**	**Test Pos.**	**Head**	**Chest**	**Lower Trunk**	**DUT Max. TX Factor**	**Avg. over Body (mW/ cm^2)**	**Calc. P.D. (mW/ cm^2)**	**Max Calc. P.D. (mW/ cm^2)**
Roof	HAD4008A (150.8-162MHz)	2.15	150.800	120	116	CW	E	1	PB	0.257	0.154	0.116	0.5	0.176	0.088	0.09
Roof	HAD4008A (150.8-162MHz)	2.15	156.400	120	117	CW	E	1	PB	0.057	0.052	0.044	0.5	0.051	0.026	0.03
Roof	HAD4008A (150.8-162MHz)	2.15	162.000	120	117	CW	E	1	PB	0.271	0.228	0.163	0.5	0.221	0.110	0.11
Roof	HAD4009A (162-174MHz)	2.15	162.000	120	117	CW	E	1	PB	0.275	0.271	0.174	0.5	0.240	0.120	0.12
Roof	HAD4009A (162-174MHz)	2.15	167.700	120	117	CW	E	1	PB	0.173	0.204	0.236	0.5	0.204	0.102	0.10
Roof	HAD4009A (162-174MHz)	2.15	173.400	120	118	CW	E	1	PB	0.128	0.07	0.115	0.5	0.104	0.052	0.05
Roof	HAD4021A (136-174MHz)	2.15	136.000	120	116	CW	E	1	PB	0.232	0.285	0.225	0.5	0.247	0.124	0.13
Roof	HAD4021A (136-174MHz)	2.15	140.900	120	116	CW	E	1	PB	0.111	0.207	0.244	0.5	0.187	0.094	0.10
Roof	HAD4021A (136-174MHz)	2.15	145.900	120	116	CW	E	1	PB	0.087	0.114	0.227	0.5	0.143	0.071	0.07
Roof	HAD4021A (136-174MHz)	2.15	150.800	120	116	CW	E	1	PB	0.231	0.13	0.106	0.5	0.156	0.078	0.08
Roof	HAD4021A (136-174MHz)	2.15	158.300	120	116	CW	E	1	PB	0.097	0.076	0.054	0.5	0.076	0.038	0.04
Roof	HAD4021A (136-174MHz)	2.15	165.900	120	118	CW	E	1	PB	0.156	0.178	0.177	0.5	0.170	0.085	0.09
Roof	HAD4021A (136-174MHz)	2.15	173.400	120	118	CW	E	1	PB	0.094	0.049	0.085	0.5	0.076	0.038	0.04

MPE calculations are defined in section 13.0.

Companion Mobile (VHF 100W) - MPE measurement data for Passenger

D.U.T. Info.							Probe Info.			MPE measurement						
Ant Loc.	**Ant. Model/ Desc.**	**Ant. Gain (dBi)**	**Tx Freq (MHz)**	**Max Pwr (W)**	**Initial Pwr (W)**	**Test Mode**	**E/H Field**	**Probe Cal. Factor**	**Test Pos.**	**Head**	**Chest**	**Lower Trunk**	**DUT Max. TX Factor**	**Avg. over Body (mW/ cm^2)**	**Calc. P.D. (mW/ cm^2)**	**Max Calc. P.D. (mW/ cm^2)**
Roof	HAD4008A (150.8-162MHz)	2.15	150.800	120	116	CW	E	1	PF	0.408	0.687	0.489	0.5	0.528	0.264	0.27
Roof	HAD4008A (150.8-162MHz)	2.15	156.400	120	117	CW	E	1	PF	0.282	0.319	0.273	0.5	0.291	0.146	0.15
Roof	HAD4008A (150.8-162MHz)	2.15	162.000	120	117	CW	E	1	PF	0.235	0.244	0.206	0.5	0.228	0.114	0.12
Roof	HAD4009A (162-174MHz)	2.15	162.000	120	117	CW	E	1	PF	0.261	0.151	0.187	0.5	0.200	0.100	0.10
Roof	HAD4009A (162-174MHz)	2.15	167.700	120	117	CW	E	1	PF	0.305	0.226	0.173	0.5	0.235	0.117	0.12
Roof	HAD4009A (162-174MHz)	2.15	173.400	120	118	CW	E	1	PF	0.308	0.249	0.16	0.5	0.239	0.120	0.12
Roof	HAD4021A (136-174MHz)	2.15	136.000	120	116	CW	E	1	PF	0.126	0.194	0.199	0.5	0.173	0.087	0.09
Roof	HAD4021A (136-174MHz)	2.15	140.900	120	116	CW	E	1	PF	0.227	0.33	0.424	0.5	0.327	0.164	0.17
Roof	HAD4021A (136-174MHz)	2.15	145.900	120	116	CW	E	1	PF	0.44	0.634	0.442	0.5	0.505	0.253	0.26
Roof	HAD4021A (136-174MHz)	2.15	150.800	120	116	CW	E	1	PF	0.38	0.702	0.525	0.5	0.536	0.268	0.28
Roof	HAD4021A (136-174MHz)	2.15	158.300	120	116	CW	E	1	PF	0.118	0.192	0.23	0.5	0.180	0.090	0.09
Roof	HAD4021A (136-174MHz)	2.15	165.900	120	118	CW	E	1	PF	0.207	0.177	0.15	0.5	0.178	0.089	0.09
Roof	HAD4021A (136-174MHz)	2.15	173.400	120	118	CW	E	1	PF	0.194	0.209	0.128	0.5	0.177	0.089	0.09

MPE calculations are defined in section 13.0.

Companion Mobile (VHF 100W) - MPE measurement data for Passenger

D.U.T. Info.							Probe Info.			MPE measurement						
Ant Loc.	Ant. Model/ Desc.	Ant. Gain (dBi)	Tx Freq (MHz)	Max Pwr (W)	Initial Pwr (W)	Test Mode	E/H Field	Probe Cal. Factor	Test Pos.	Head	Chest	Lower Trunk	DUT Max. TX Factor	Avg. over Body (mW/ cm^2)	Calc. P.D. (mW/ cm^2)	Max Calc. P.D. (mW/ cm^2)
Roof	HAD4008A (150.8-162MHz)	2.15	150.800	120	116	CW	H	0.86	PB	0.074	0.063	0.066	0.5	0.068	0.064	0.07
Roof	HAD4008A (150.8-162MHz)	2.15	156.400	120	117	CW	H	0.85	PB	0.051	0.046	0.047	0.5	0.048	0.031	0.03
Roof	HAD4008A (150.8-162MHz)	2.15	162.000	120	117	CW	H	0.85	PB	0.074	0.046	0.032	0.5	0.051	0.035	0.04
Roof	HAD4009A (162-174MHz)	2.15	162.000	120	117	CW	H	0.85	PB	0.071	0.046	0.032	0.5	0.050	0.034	0.03
Roof	HAD4009A (162-174MHz)	2.15	167.700	120	117	CW	H	0.85	PB	0.097	0.082	0.052	0.5	0.077	0.081	0.08
Roof	HAD4009A (162-174MHz)	2.15	173.400	120	118	CW	H	0.84	PB	0.07	0.068	0.049	0.5	0.062	0.052	0.05
Roof	HAD4021A (136-174MHz)	2.15	136.000	120	116	CW	H	0.88	PB	0.085	0.077	0.073	0.5	0.078	0.090	0.09
Roof	HAD4021A (136-174MHz)	2.15	140.900	120	116	CW	H	0.87	PB	0.072	0.074	0.078	0.5	0.075	0.080	0.08
Roof	HAD4021A (136-174MHz)	2.15	145.900	120	116	CW	H	0.87	PB	0.082	0.077	0.09	0.5	0.083	0.098	0.10
Roof	HAD4021A (136-174MHz)	2.15	150.800	120	116	CW	H	0.86	PB	0.073	0.061	0.065	0.5	0.066	0.061	0.06
Roof	HAD4021A (136-174MHz)	2.15	158.300	120	116	CW	H	0.85	PB	0.047	0.032	0.03	0.5	0.036	0.018	0.02
Roof	HAD4021A (136-174MHz)	2.15	165.900	120	118	CW	H	0.85	PB	0.082	0.063	0.035	0.5	0.060	0.049	0.05
Roof	HAD4021A (136-174MHz)	2.15	173.400	120	118	CW	H	0.84	PB	0.06	0.061	0.043	0.5	0.055	0.040	0.04

MPE calculations are defined in section 13.0.

Companion Mobile (VHF 100W) - MPE measurement data for Passenger

D.U.T. Info.							Probe Info.			MPE measurement						
Ant Loc.	**Ant. Model/ Desc.**	**Ant. Gain (dBi)**	**Tx Freq (MHz)**	**Max Pwr (W)**	**Initial Pwr (W)**	**Test Mode**	**E/H Field**	**Probe Cal. Factor**	**Test Pos.**	**Head**	**Chest**	**Lower Trunk**	**DUT Max. TX Factor**	**Avg. over Body (mW/ cm^2)**	**Calc. P.D. (mW/ cm^2)**	**Max Calc. P.D. (mW/ cm^2)**
Roof	HAD4008A (150.8-162MHz)	2.15	150.800	120	116	CW	H	0.86	PF	0.131	0.145	0.095	0.5	0.124	0.213	0.22
Roof	HAD4008A (150.8-162MHz)	2.15	156.400	120	117	CW	H	0.85	PF	0.091	0.102	0.075	0.5	0.089	0.109	0.11
Roof	HAD4008A (150.8-162MHz)	2.15	162.000	120	117	CW	H	0.85	PF	0.076	0.067	0.053	0.5	0.065	0.058	0.06
Roof	HAD4009A (162-174MHz)	2.15	162.000	120	117	CW	H	0.85	PF	0.08	0.055	0.051	0.5	0.062	0.052	0.05
Roof	HAD4009A (162-174MHz)	2.15	167.700	120	117	CW	H	0.85	PF	0.066	0.073	0.053	0.5	0.064	0.056	0.06
Roof	HAD4009A (162-174MHz)	2.15	173.400	120	118	CW	H	0.84	PF	0.085	0.078	0.062	0.5	0.075	0.075	0.08
Roof	HAD4021A (136-174MHz)	2.15	136.000	120	116	CW	H	0.88	PF	0.082	0.091	0.081	0.5	0.085	0.105	0.11
Roof	HAD4021A (136-174MHz)	2.15	140.900	120	116	CW	H	0.87	PF	0.086	0.112	0.102	0.5	0.100	0.143	0.15
Roof	HAD4021A (136-174MHz)	2.15	145.900	120	116	CW	H	0.87	PF	0.128	0.16	0.131	0.5	0.140	0.278	0.29
Roof	HAD4021A (136-174MHz)	2.15	150.800	120	116	CW	H	0.86	PF	0.120	0.136	0.098	0.5	0.118	0.194	0.20
Roof	HAD4021A (136-174MHz)	2.15	158.300	120	116	CW	H	0.85	PF	0.082	0.08	0.064	0.5	0.075	0.077	0.08
Roof	HAD4021A (136-174MHz)	2.15	165.900	120	118	CW	H	0.85	PF	0.075	0.067	0.053	0.5	0.065	0.058	0.06
Roof	HAD4021A (136-174MHz)	2.15	173.400	120	118	CW	H	0.84	PF	0.08	0.074	0.047	0.5	0.067	0.060	0.06

MPE calculations are defined in section 13.0.

Appendix E - SAR Simulation Report

MOTOROLA SOLUTIONS

COMPUTATIONAL EME COMPLIANCE ASSESSMENT OF THE DIGITAL VEHICULAR REPEATER (DVR 700), MODEL # DQPMDVR7000P, AND APX7500 MODEL # M30TXS9PW1AN MOBILE RADIO.

March 11, 2013

William Elliott, Giorgi Bit-Babik, Ph.D., and Antonio Faraone, Ph.D.
Motorola Solutions EME Research Lab, Plantation, Florida

Introduction

This report summarizes the computational [numerical modeling] analysis performed to document compliance of the DVR 700, 5 watt model # DQPMDVR7000P interfaced with, and transmitting simultaneously with companion VHF Mobile Radio models M30TXS9PW1AN with maximum transmit power up to 120 watts and vehicle-mounted antennas with the Federal Communications Commission (FCC) guidelines for human exposure to radio frequency (RF) emissions. The DVR radio operates in the 764-806 MHz frequency band while the companion VHF mobile radios operate in the 136-174 MHz band.

This computational analysis supplements the measurements conducted to evaluate the compliance of the exposure from this mobile radio with respect to applicable *maximum permissible exposure* (MPE) limits. All test conditions (9 in total) that did not conform with applicable MPE limits were analyzed to determine whether those conditions complied with the *specific absorption rate* (SAR) limits for general public exposure (1.6 W/kg averaged over 1 gram of tissue and 0.08 W/kg averaged over the whole body) set forth in FCC guidelines, which are based on the IEEE C95.1-1999 standard [1]. The same test conditions were also analyzed to determine compliance with the SAR limits set forth in the ICNIRP [3] guidelines and IEEE Std. C95.1-2005 standard [4] (2.0 W/kg averaged over 10 gram of tissue and 0.08 W/kg averaged over the whole body). In total 9 independent simulations have been performed. Six simulations are addressing the driver exposure to the DVR 700 radio with trunk mounted quarter wavelength antennas, and the other three are addressing the driver exposure to the VHF Mobile Radio with roof mounted antenna.

For all simulations a commercial code based on Finite-Difference-Time-Domain (FDTD) methodology was employed to carry out the computational analysis. It is well established and recognized within the scientific community that SAR is the primary dosimetric quantity used to evaluate the human body's absorption of RF energy and that MPEs are in fact derived from SAR. Accordingly, the SAR computations provide a scientifically valid and more relevant estimate of human exposure to RF energy.

Method

The simulation code employed is XFDTD™ v7.2, by Remcom Inc., State College, PA. This computational suite features a heterogeneous full body standing model (High Fidelity Body Mesh), derived from the so-called Visible Human [2], discretized in 3 mm voxels. The dielectric properties of 23 body tissues are automatically assigned by XFDTD™ at any specific frequency. The "seated" man model was obtained from the standing model by modifying the articulation angles at the hips and the knees. Details of the computational method and model are provided in the Appendix to this report.

The car model has been imported into XFDTD™ from the CAD file of a sedan car having dimensions 4.98 m (L) x 1.85 m (W) x 1.18 m (H), and discretized with maximum resolution of 5 mm. The Figure 1 below show both the CAD model and the photo of the actual car This CAD model has been incorporated into the IEC/IEEE 62704-2 draft standard.

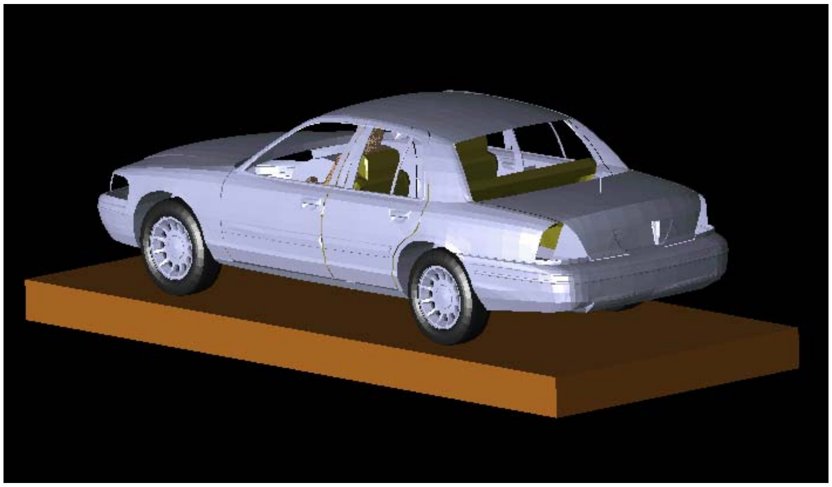

Figure 1: The photo picture of the car used in field measurements and the corresponding CAD model used in simulations

For driver exposure, the antenna position is on the trunk and on the roof that replicate the experimental conditions used in MPE measurements. According to the IEC/IEEE 62704-2 draft standard (February, 2012) for exposure simulations from vehicle mount antennas the lossy dielectric slab with 30 cm thickness, dielectric constant of 8 and conductivity of 0.01 S/m has been introduced in the computational model to properly account for the effect of the ground (pavement) on exposure.

Figure 2 shows some of the XFDTD™ computational models used for driver exposure to roof mounted (a) and trunk mounted (b) antennas

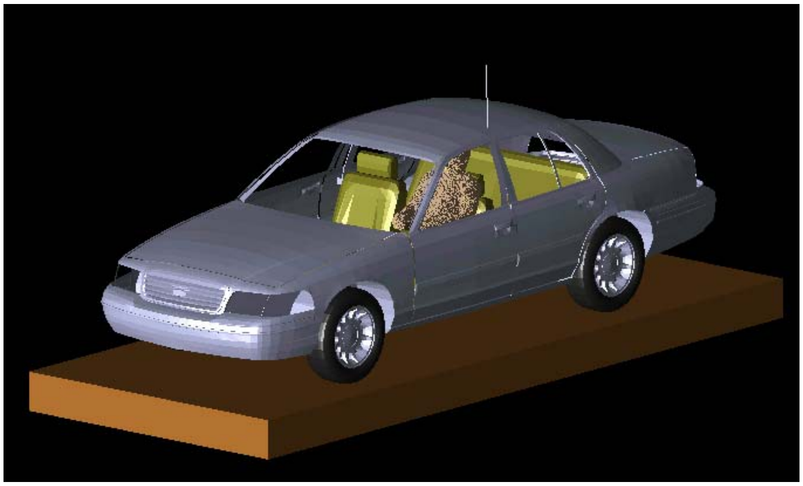
(a)

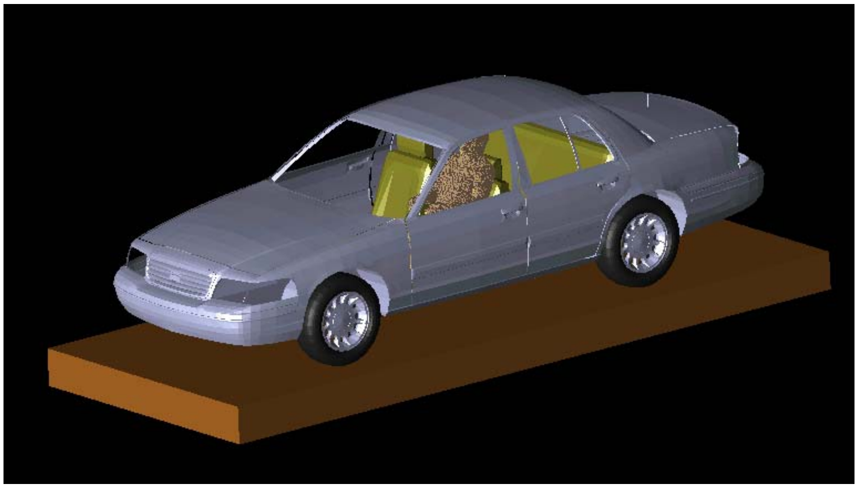
(b)

Figure 2: Driver model exposed to roof mounted (a) and trunk mounted (b) antennas: XFDTD geometry.

The computational code employs a time-harmonic excitation to produce a steady state electromagnetic field in the exposed body. Subsequently, the corresponding SAR distribution is automatically processed in order to determine the whole-body, 1-g, and 10-g average SAR. The maximum average output power from VHF mobile radio antenna is 120 W. Since the ohmic losses in the cable and in the car materials, as well as the mismatch losses at the antenna feed-point, are neglected, and source-based time averaging (50% talk time) is employed, all computational results are normalized to half of it, i.e., 60 W average net output power. The maximum average output power from DVR 700 radio is 5 W and the computational results are normalized to 5 W. The DVR 700 radio operates in a repeater mode and therefore all simulations are normalized to 100% average output power.

Two independent set simulations, one for DVR 700 trunk mount antenna and one for VHF radio roof-mount antenna were performed. Since VHF mobile radio and DVR 700 radio can transmit simultaneously, the maximum peak and whole body average SAR results from each set of data were combined to compute the peak SAR value for the simultaneous exposure from both radios. The obtained combined peak SAR value is an overestimation of the actual exposure because the peak SAR values from the roof- and trunk-mount antennas that contribute to the combined value are not found at the same location in the body.

Results of SAR computations for car passengers

The test conditions for DVR 700 radio requiring SAR computations are summarized in Table I, together with the antenna data, the SAR results, and power density (P.D.) as obtained from the measurements in the corresponding test conditions. The conditions are for antennas mounted on the trunk. The antenna length in Table I includes the 1.8 cm magnetic mount base used in measurements to position the antenna on the vehicle. The same length was used in simulation model. The seated human body model is located in the driver location. The model is surrounded by air, as the seat, which is made out of poorly conductive fabrics, is not included in the computational model. All the transmit frequencies and antenna lengths combinations reported in Table I have been simulated individually.

Table I: Results of the SAR computations for passenger exposure
from DVR 700 trunk-mount antennas

Mount location	Antenna Kit #	Antenna length (cm)	Freq [MHz]	P.D. (mw/cm^2)	Exposure location	SAR [W/kg]		
						1-g	10-g	WB
Trunk	HAF4016A	10.80	764.0000	0.01	Driver	0.059	0.030	0.0014
			770.0000	0.01		0.059	0.030	0.0012
			775.0000 **Fig 3&4**	0.02		0.066	0.033	0.0012
			794.0000	0.02		0.042	0.030	0.0011
			800.0000	0.02		0.047	0.024	0.0012
			806.0000	0.02		0.066	0.036	0.0015

The SAR distribution in the passenger model in the exposure condition that gave highest 1-g SAR is reported in Figure 3 (775.0 MHz, driver exposure condition, HAF4016A antenna).

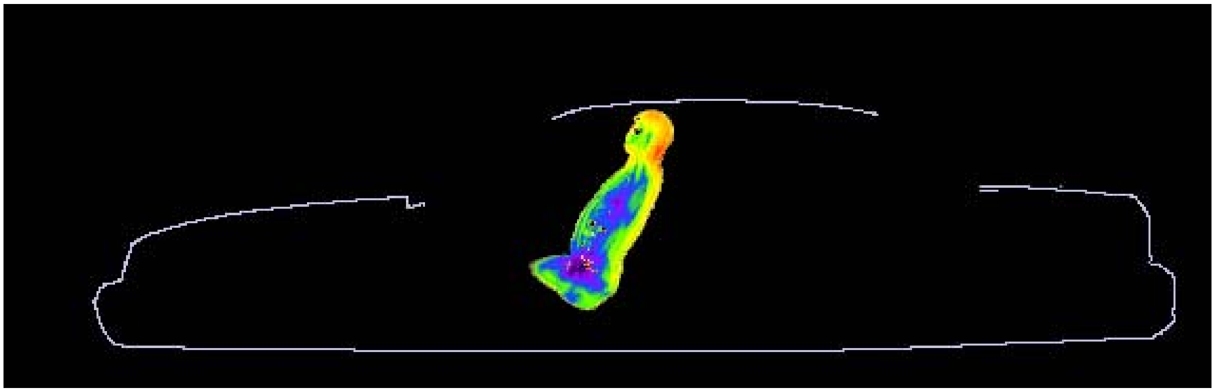

Figure 3. SAR distribution at 775.0 MHz in the driver model produced by the roof-mount HAF4016A antenna. The contour plot is relative to the plane where the peak 1-g average SAR for this exposure condition occurs.

The two pictures below in Figure 4 show the E and H field distributions in the plane of the antenna corresponding to the location in Figure 3.

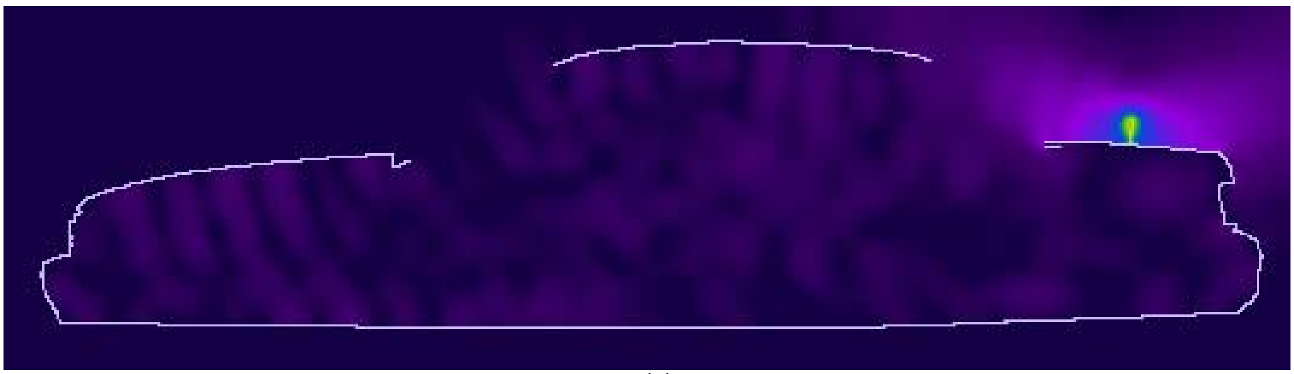

(a)

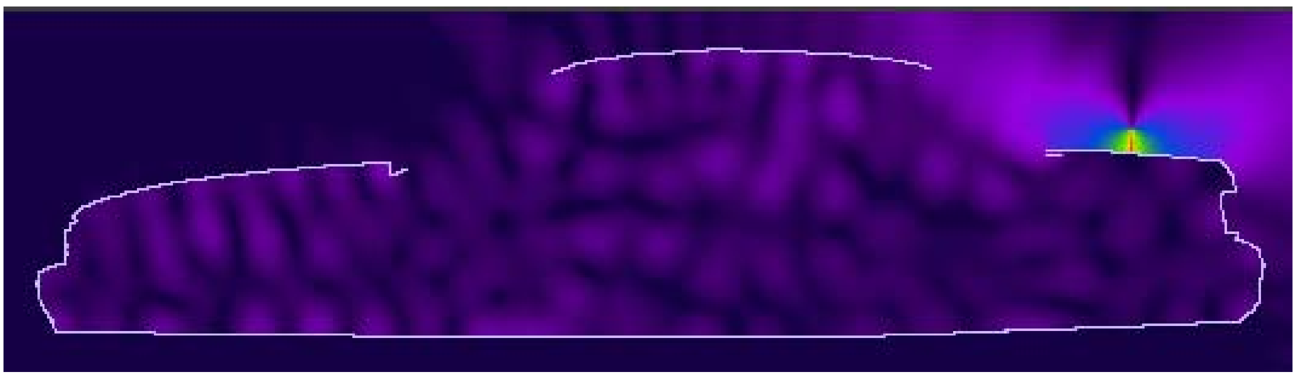

(b)

Figure 4. (a) E-field distribution corresponding to exposure condition of Figure 3, and (b) H-field distribution corresponding to exposure condition of Figure 3.

The highest 1-g SAR in the driver exposure condition with the HAF4016A trunk mounted antenna was produced at 775.0 MHz.

Results of SAR computations with the roof mounted antenna

The test conditions for VHF mobile radio requiring SAR computations are summarized in Table II, together with the antenna data and the SAR results. The conditions are for antenna mounted on the side of the roof. The seated human body model is located in the driver location. The model is surrounded by air, as the seat, which is made out of poorly conductive fabrics, is not included in the computational model. All the transmit frequencies and antenna lengths combinations reported in Table II have been simulated individually.

Table II: Results of the SAR computations for passenger exposure
from VHF mobile radio roof-mount antennas (50% talk time)

Mount location	Antenna Kit #	Antenna length (cm)	Freq [MHz]	P.D. (mw/cm^2)	Exposure location	SAR [W/kg]		
						1-g	10-g	WB
Roof	HAD4008A	47.3	150.8	0.27	Driver	0.321	0.237	0.0131
Roof	HAD4021A	53.5	145.9 **Fig 5&6**	0.29		0.974	0.585	0.0241
			150.8	0.28		0.307	0.223	0.0128

The SAR distribution in the passenger model in the exposure condition that gave highest 1-g SAR is reported in Figure 5 (145.9 MHz, driver exposure condition, HAD4021A antenna).

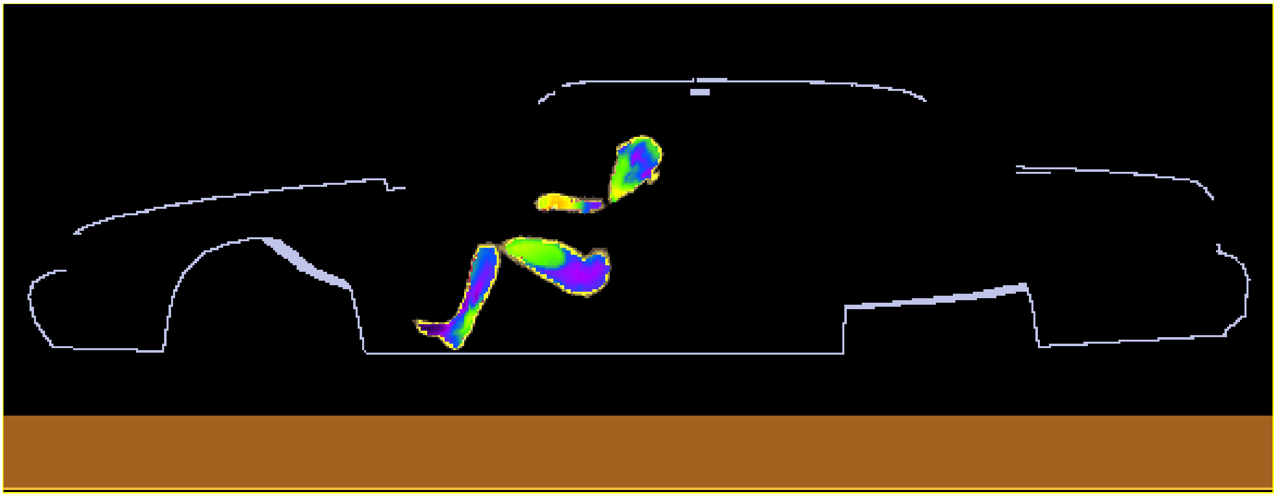

Figure 5. SAR distribution at 145.9 MHz in the driver model produced by the roof-mount HAD4021A antenna. The contour plot is relative to the plane where the peak 1-g average SAR for this exposure condition occurs.

The two pictures below in Figure 6 show the E and H field distributions in the plane of the antenna corresponding to the condition in Figure 3.

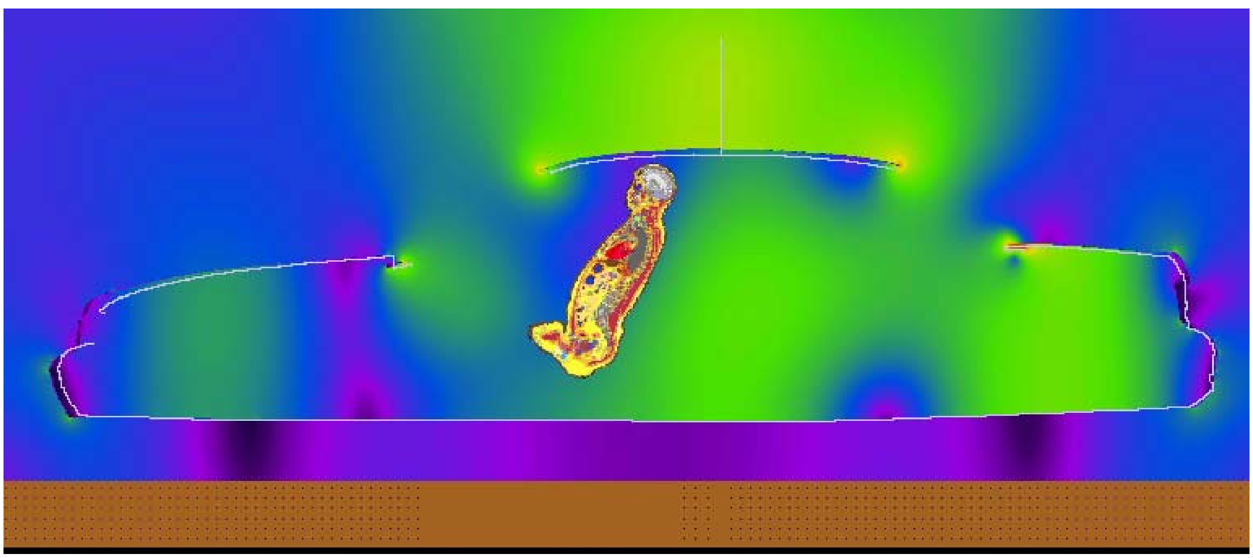

a)

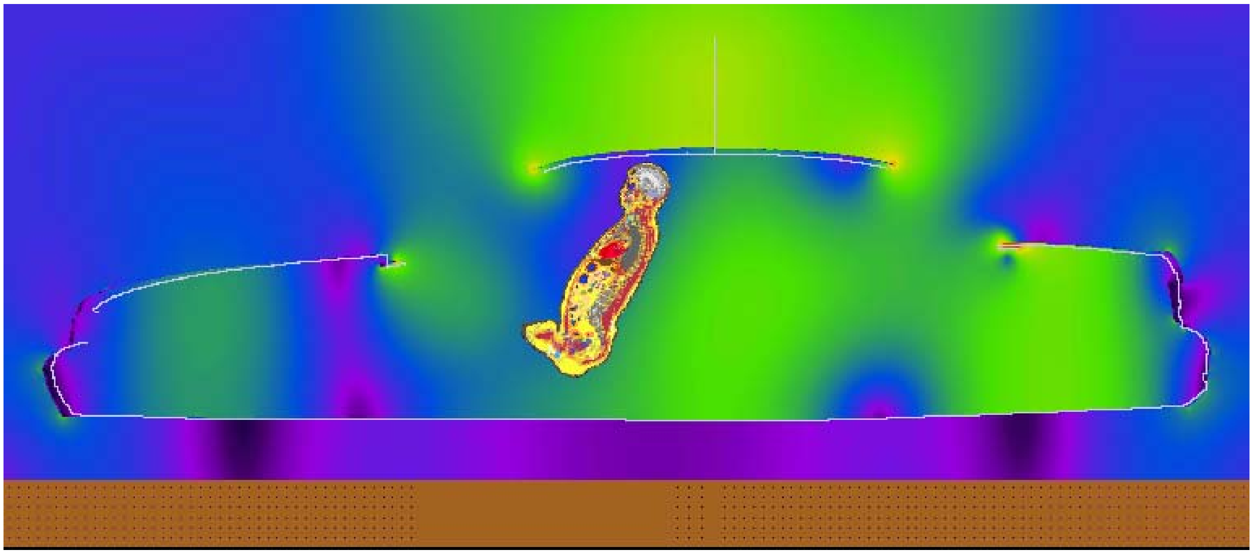

b)

Figure 6. (a) E-field distribution corresponding to exposure condition of Figure 3, and (b) H-field distribution corresponding to exposure condition of Figure 3.

For each location of the passenger on the front seat (driver and right side) the peak SAR values were identified for both DVR 700 and VHF mobile radio exposure and then combined to produce the composite peak SAR value. Table III and Table IV present those values.

Table III: Peak 1-g average SAR for both passenger locations on the front seat and composite 1-g average SAR from simultaneous exposure.

Passenger location	DVR 700 [W/kg]	VHF mobile radio [W/kg]	Total [W/kg]
Driver	0.07	0.97	1.04

Table IV: Peak whole body average SAR for both passenger locations on the front seat and composite whole body average SAR from simultaneous exposure.

Passenger location	DVR 700 [W/kg]	VHF mobile radio [W/kg]	Total [W/kg]
Driver	0.0015	0.0241	0.0256

From Table III and Table IV the maximum combined peak 1-g SAR is 1.04 W/kg, less than the 1.6 W/kg limit, while the maximum combined whole-body average SAR is 0.0256 W/kg, less than the 0.08 W/kg limit. The overall maximum combined peak 10-g SAR is 0.621 W/kg, less than the 2.0 W/kg limit.

Conclusions

Under the test conditions described for evaluating exposure to the RF electromagnetic fields emitted by vehicle-mounted antennas used in conjunction with these mobile radio products, the present analysis shows that the computed maximum SAR values are compliant with the FCC general public SAR limits. All maximum computed SAR values are compliant with the corresponding ICNIRP and IEEE Std. C95.1-2005 SAR limits.

References

[1] IEEE Standard C95.1-1999. *IEEE Standard for Safety Levels with Respect to Human Exposure to RF Electromagnetic Fields*, 3 kHz to 300 GHz.

[2] http://www.nlm.nih.gov/research/visible/visible_human.html

[3] ICNIRP (International Commission on Non-Ionising Radiation Protection). 1998. *Guidelines for limiting exposure to time-varying electric, magnetic and electromagnetic fields (up to 300 GHz)*. Health Phys. 74:494–522.

[4] IEEE. 2005. *IEEE standard for safety levels with respect to human exposure to radio frequency electromagnetic fields, 3 kHz to 300 GHz*, IEEE Std C95.1-2005

APPENDIX: SPECIFIC INFORMATION FOR SAR COMPUTATIONS

This appendix follows the structure outlined in Appendix B.III of the Supplement C to the FCC OET Bulletin 65. Most of the information regarding the code employed to perform the numerical computations has been adapted from the draft IEC/IEEE 62704-1 and 62704-2 standards, and from the XFDTD™ User Manuals. Remcom Inc., owner of XFDTD™, is kindly acknowledged for the help provided.

1) Computational resources

a) A multiprocessor system equipped with two Intel Xeon X5570 quad-core CPUs and four Tesla C1060 GPUs was employed for all simulations.

b) The memory requirement was from 7 GB to 12 GB. Using the above-mentioned system with 8-cores operating concurrently, the typical simulation would run for 6-10 hours and with all four GPUs activated by the XFDTD version 7.2 this time would be from 60-180 min.

2) FDTD algorithm implementation and validation

a) We employed a commercial code (XFDTD™ v7.2, by Remcom Inc.) that implements the Yee's FDTD formulation [1]. The solution domain was discretized according to a rectangular grid with an adaptive 3-10 mm step in all directions. Sub-gridding was not used. Seven-layer PML absorbing boundary conditions are set at the domain boundary to simulate free space radiation processes. The excitation is a lumped voltage generator with 50-ohm source impedance. The code allows selecting *wire objects* without specifying their radius. We used a wire to represent the antenna. The car body is modeled by solid metal. We did not employ the "thin wire" algorithm since within the adaptive grid the minimum resolution of 3 mm was specified and used to model the antenna and the antenna wire radius was never smaller than one-fifth of the voxel dimension. In fact, the XFDTD™ manual specifies that "In most cases, standard PEC material will serve well as a wire. However, in cases where the wire radius is important to the calculation and is less than 1/4 the length of the average cell edge, the thin wire material may be used to accurately simulate the correct wire diameter." The maximum voxel dimension in the plane normal to the antenna in all our simulations was 3 mm, and the antenna radius is always at least 1 mm (1 mm for the short quarter-wave antennas and 1.5 mm for the long gain antennas), so there was no need to specify a "thin wire" material.

Because the field impinges on the bystander or passenger model at a distance of several tens of voxels from the antenna, the details of antenna wire modeling are not expected to have significant impact on the exposure level.

Some antennas have inductive loading coils located in the mid section as shown in the picture below of the HAE 6010A and HAE 4011A antenna examples.

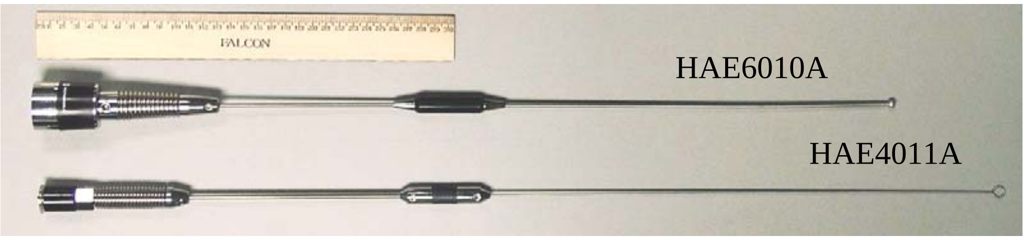

The X-ray of the reactive loads of the HAE4011A and HAE6010A antennas is also presented in the next pictures below. Those elements are significantly shorter than the length of the antenna and are about 1/40 of the wavelength at center operating frequency. They were modeled as lumped reactive elements. The comparison with measurements and validity of such simulation model has been summarized in [9].

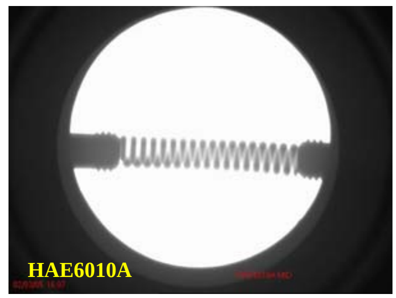

Some antennas, for example HAF4013A and HAF4017A, operating in 7/800 MHz band, may also be different from a simple wire monopoles. In those cases the XFDTD antenna models were validated against high resolution models simulated with alternative simulation tool as described [12] prior of conducting XFDTD exposure simulations.

b) XFDTD™ is one of the most widely employed commercial codes for electromagnetic simulations. It has gone through extensive validation and has proven its accuracy over time in many different applications. One example is provided in [3].

We carried out a validation of the code algorithm by running the canonical test case involving a half-wave wire dipole. The dipole is 0.475 times the free space wavelength at 160 MHz, i.e., 88.5 cm long. The discretization used to model the dipole was 5 mm. Also in this case, the “thin wire” model was not needed. The following picture shows XFDTD™ outputs regarding the antenna feed-point impedance (70.5 – j 6.0 ohm), as well as qualitative distributions of the total E and H fields near the dipole. The radiation pattern is shown as well (one lobe in elevation). As expected, the 3 dB beamwidth is about 78 degrees.

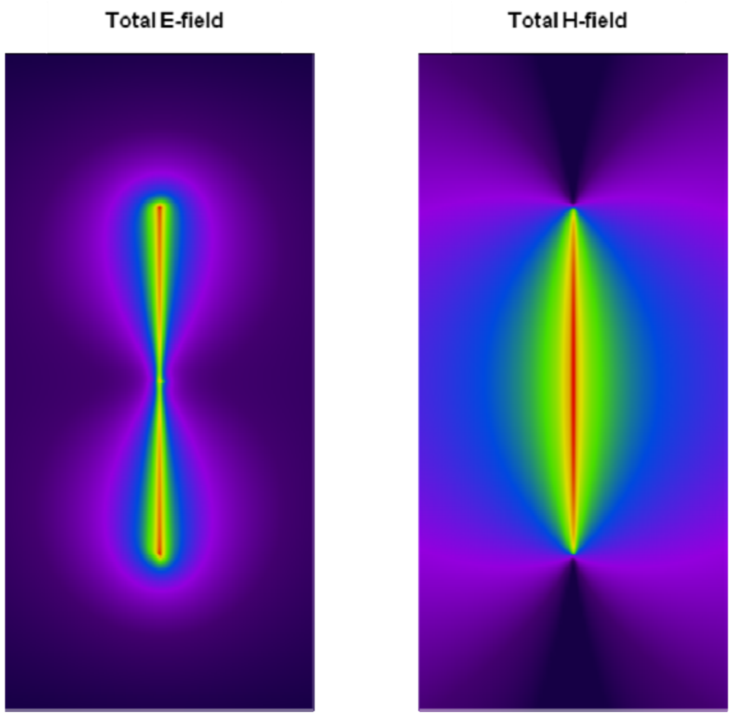

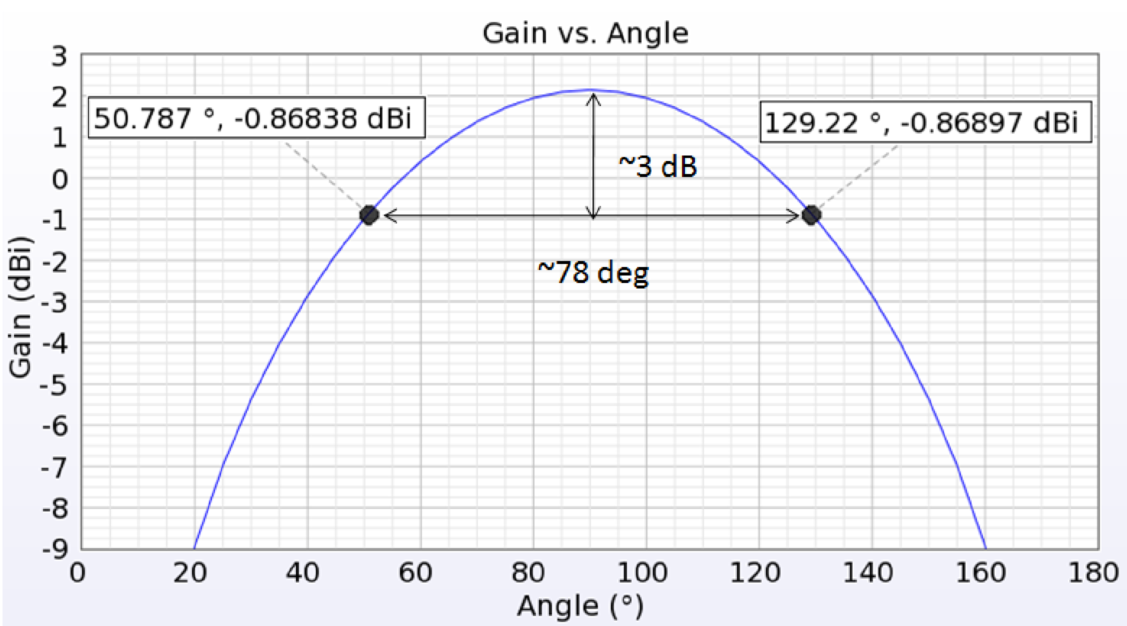

We also compared the XFDTD™ result with the results derived from NEC [4], which is a code based on the method of moments. In this case, we used a dipole with radius 1 mm, length 88.5 cm, and the discretization is 5 mm. The corresponding input impedance at 160 MHz is 69.5-j10.5 ohm. Its frequency dependence is reported in the following figure.

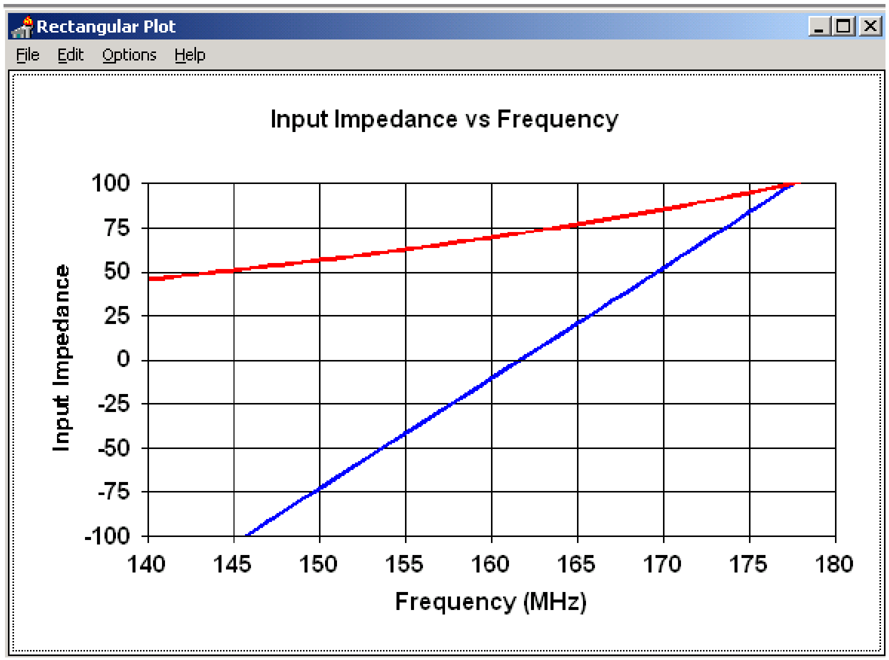

We also carried out similar validation at 400 MHz, i.e., about 35.5 cm long. The following picture shows XFDTD™ outputs regarding the antenna feed-point impedance (75.5 + j 11.9 ohm), as well as qualitative distributions of the total E and H fields near the dipole. The radiation pattern is shown as well (one lobe in elevation). As expected, the 3 dB beamwidth is about 78 degrees in this case as well. The computed results are in good agreement with the known analytical results for the half -wave dipole antenna which could be found in [10].

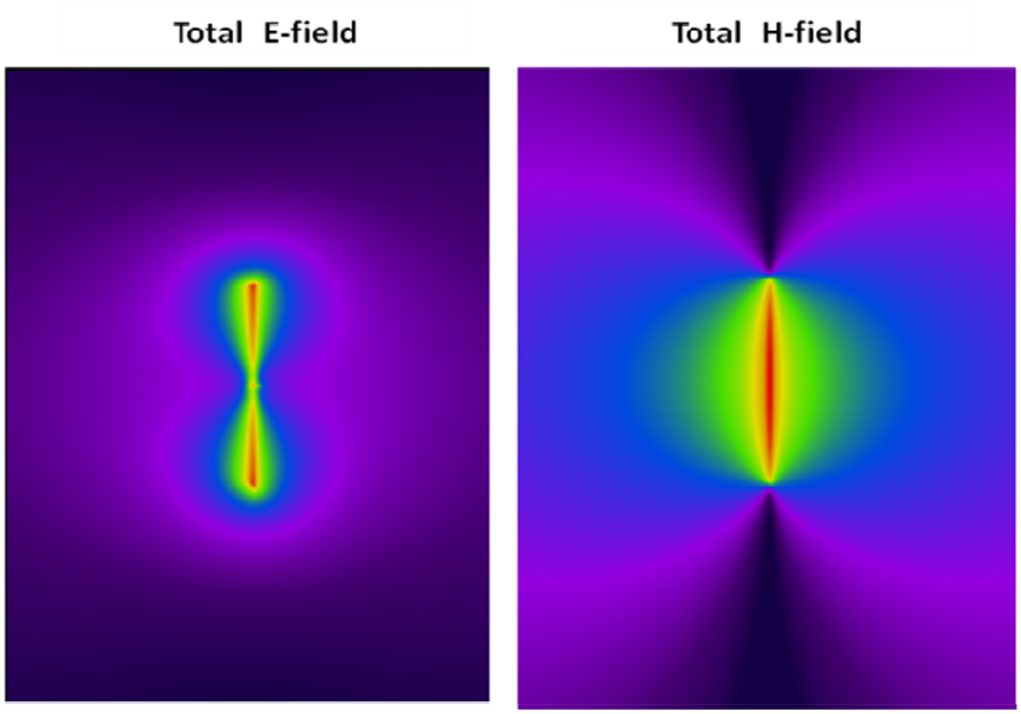

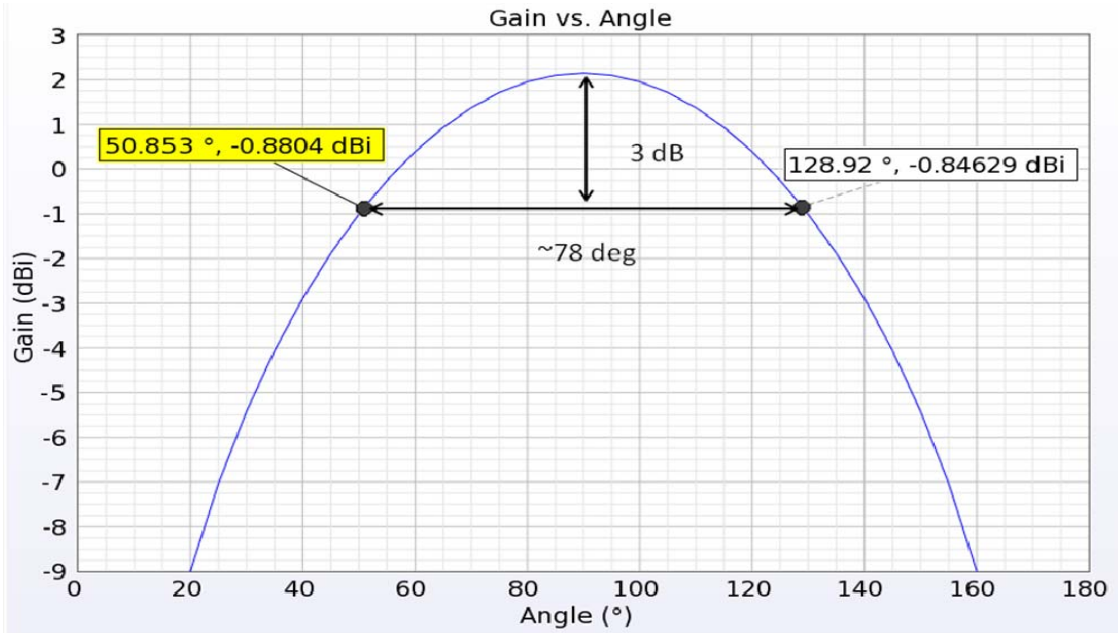

This validation ensures that the input impedance calculation is carried out correctly in XFDTD™, thereby enabling accurate estimates of the radiated power. It further ensures that the wire model employed in XFDTD™, which we used to model the antennas, produces physically meaningful current and fields distributions. Both these aspects ensure that the field quantities are correctly computed both in terms of absolute amplitude and relative distribution.

3) Computational parameters

a) The following table reports the main parameters of the FDTD model employed to perform our computational analysis:

PARAMETER	X	Y	Z
Voxel size	3-10 mm	3-10 mm	1-10 mm
Maximum domain dimensions employed for passenger computations with the trunk-mount antennas	397	910	559
Maximum domain dimensions employed for bystander computations with the trunk-mount antennas	449	791	709
Time step	About 0.7 of the Courant limit (typically 5 *ps*)		
Objects separation from FDTD boundary (mm)	>200	>200	>200
Number of time steps	Enough to reach at least -60 dB convergence		
Excitation	Sinusoidal (not less than 10 periods)		

4) Phantom model implementation and validation

a) The human body models (bystander and/or passenger) employed in our simulations are those defined in the draft IEEE 62704-2 standard. They are originally based on data from the *visible human project* sponsored by the National Library of Medicine (NLM)

(http://www.nlm.nih.gov/research/visible/visible_human.html). The original male data set consists of MRI, CT and anatomical images. Axial MRI images of the head and neck and longitudinal sections of the rest of the body are available at 4 mm intervals. The MRI images have 256 pixel by 256 pixel resolution. Each pixel has 12 bits of gray tone resolution. The CT data consists of axial CT scans of the entire body taken at 1 mm intervals at a resolution of 512 pixels by 512 pixels where each pixel is made up of 12 bits of gray tone. The axial anatomical images are 2048 pixels by 1216 pixels where each pixel is defined by 24 bits of color. The anatomical cross sections are also at 1 mm intervals and coincide with the CT axial images. There are 1871 cross sections. Dr. Michael Smith and Dr. Chris Collins of the Milton S. Hershey Medical Center, Hershey, Pa, created the High Fidelity Body mesh. Details of body model creation are given in the *methods* section in [5].
The final bystander and passenger model was generated for the IEEE 62704-2 standard from the above dataset using the Varipose softwar, Remocm Inc., The body mesh contains 39 tissues materials. Measured values for the tissue parameters for a broad frequency range are included with the mesh data. The correct values are interpolated from the table of measured data and entered into the appropriate mesh variables. The tissue conductivity and permittivity variation *vs.* frequency is included in the XFDTD™ calculation by a multiple-pole approximation to the Cole-Cole approximated tissue parameters reported in [11].

a) The XFDTD™ High Fidelity Body Mesh model correctly represents the anatomical structure and the dielectric properties of body tissues, so it is appropriate for determining the highest exposure expected for normal device operation.

b) One example of the accuracy of XFDTD™ for computing SAR has been provided in [6]. The study reported in [6] is relative to a large-scale benchmark of measurement and computational tools carried out within the IEEE Standards Coordinating Committee 34, Sub-Committee 2.

5) Tissue dielectric parameters

a) The following table reports the dielectric properties computed for the 39 body tissue materials in the employed human body models at 150 MHz.

#	Tissue	ε_r	σ (S/m)	Density (kg/m^3)
1	bile	85.3	1.60	928
2	body fluid	71.3	1.26	1050
3	eye cornea	69.0	1.07	1051
4	fat	12.2	0.07	911
5	lymph	65.7	0.81	1035
6	mucous membrane	59.2	0.56	1102
7	toe, finger, and nails	14.4	0.07	1908
8	nerve spine	42.3	0.36	1075
9	muscle	62.2	0.73	1090
10	heart	80.7	0.79	1081
11	white matter	50.3	0.35	1041
12	stomach	73.3	0.92	1088
13	glands	65.7	0.81	1028
14	blood vessel	54.0	0.49	1102
15	liver	61.7	0.53	1079
16	gall bladder	71.3	1.06	1071
17	spleen	78.8	0.86	1089
18	cerebellum	74.6	0.85	1045
19	cortical bone	14.4	0.07	1908
20	cartilage	51.4	0.50	1100
21	ligaments	50.8	0.50	1142
22	skin	61.5	0.54	1109
23	large intestine	73.8	0.72	1088
24	tooth	14.4	0.07	2180
25	grey_matter	70.1	0.60	1045
26	eye lens	41.7	0.32	1076
27	outer lung	61.9	0.59	1050
28	small intestine	83.4	1.72	1030
29	eye sclera	63.5	0.93	1032
30	inner lung	28.3	0.32	394
31	pancreas	65.7	0.81	1087
32	blood	71.3	1.26	1050
33	cerebro_spinal_fluid	81.2	2.16	1007
34	eye vitreoushumor	69.1	1.51	1005
35	kidneys	85.0	0.88	1066
36	bone marrow	13.2	0.16	1029
37	bladder	21.4	0.30	1086
38	testicles	70.3	0.94	1082
39	cancellous bone	25.5	0.19	1178

The following table reports the dielectric properties computed for the 39 body tissue materials in the employed human body models at 450 MHz.

#	Tissue	ε_r	σ (S/m)	Density (kg/m^3)
1	bile	72.2	1.71	928
2	body fluid	63.7	1.37	1050
3	eye cornea	58.5	1.21	1051
4	fat	11.6	0.08	911
5	lymph	61.2	0.89	1035
6	mucous membrane	49.2	0.69	1102
7	toe, finger, and nails	13.0	0.10	1908
8	nerve spine	34.9	0.46	1075
9	muscle	56.8	0.81	1090
10	heart	65.0	0.99	1081
11	white matter	41.5	0.46	1041
12	stomach	67.1	1.02	1088
13	glands	61.2	0.89	1028
14	blood vessel	46.6	0.57	1102
15	liver	50.4	0.67	1079
16	gall bladder	60.7	1.15	1071
17	spleen	62.1	1.05	1089
18	cerebellum	54.7	1.06	1045
19	cortical bone	13.0	0.10	1908
20	cartilage	45.0	0.60	1100
21	ligaments	47.0	0.57	1142
22	skin	45.8	0.71	1109
23	large intestine	61.7	0.88	1088
24	tooth	13.0	0.10	2180
25	grey_matter	56.6	0.76	1045
26	eye lens	37.2	0.38	1076
27	outer lung	54.0	0.70	1050
28	small intestine	64.9	1.93	1030
29	eye sclera	57.2	1.02	1032
30	inner lung	23.5	0.38	394
31	pancreas	61.2	0.89	1087
32	blood	63.7	1.37	1050
33	cerebro_spinal_fluid	70.5	2.26	1007
34	eye vitreoushumor	69.0	1.54	1005
35	kidneys	65.0	1.13	1066
36	bone marrow	11.8	0.19	1029
37	bladder	19.6	0.33	1086
38	testicles	62.9	1.04	1082
39	cancellous bone	22.2	0.24	1178

b) The tissue types and dielectric parameters used in the SAR computation are appropriate for determining the highest exposure expected for normal device operation, because they are derived from measurements performed on real biological tissues (XFDTD, Reference Manual Version 6.4, Remcom, Inc.).

c) The tabulated list of the dielectric parameters used in phantom models is provided at point 5(a). As regards the device (car plus antenna), we used perfect electric conductors.

6) Transmitter model implementation and validation

a) The essential features that must be modeled correctly for the particular test device model to be valid are:

- Car body. The car model is very similar to the car used for MPE measurements, so as to be able to correlate measured and simulated field values. This car model has been developed for the SAR computational draft standard IEC/IEEE 62704-2.
- Antenna. We used a straight wire, even when the gain antenna has a base coil for tuning. All the coil does is compensating for excess capacitance due to the antenna being slightly longer than half a wavelength. We do not need to do that in the model, as we used normalization with respect to the net radiated power, which is determined by the input resistance only. In this way, we neglect mismatch losses and artificially produce an overestimation of the SAR, thereby introducing a conservative bias in the model. This simulation model was also validated by comparing the computed and measured near-field distributions in the condition with antenna mounted on the reference ground plane and showed good agreement experimental data [9].
- Antenna location. We used the same location, relative to the edge of the car trunk, the backseat, or the roof, used in the MPE measurements. The following pictures show a lateral and a perspective view of the bystander and passenger model.

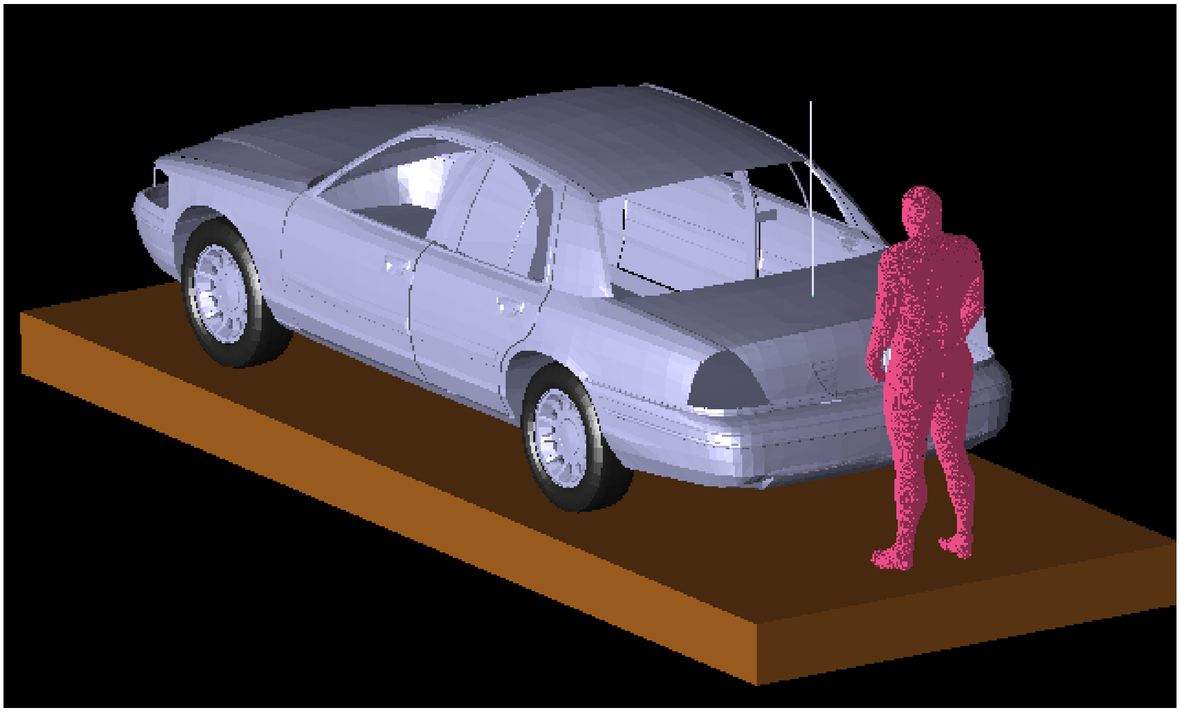

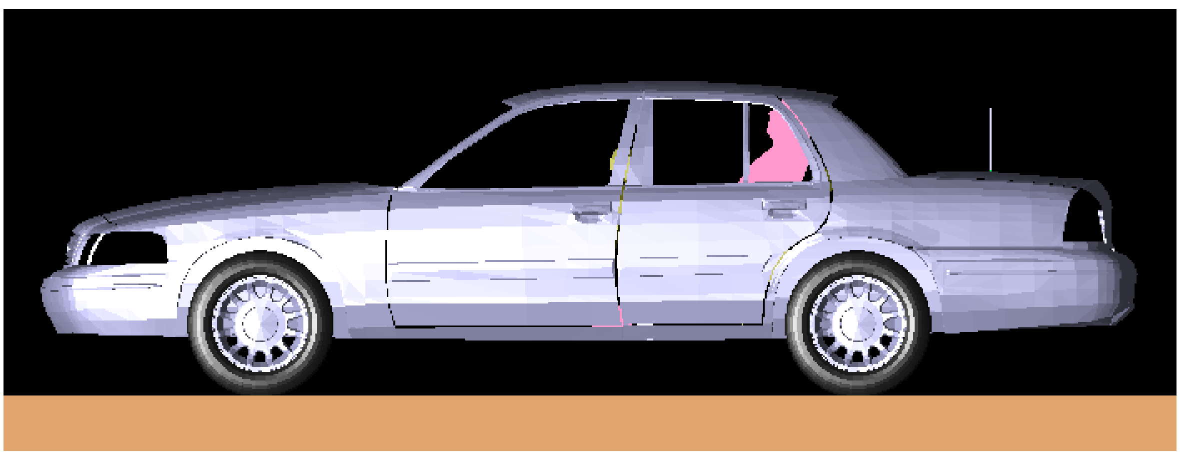

The car model is constituted by perfect electric conductor and does not include wheels in order to reduce its complexity. The passenger model is surrounded by air, as the seat, which is made out of poorly conductive fabrics, is not included in the computational model. The pavement has not been included in the model. The passenger and bystander models were validated for similar antenna and frequency conditions by comparing the MPE measurements at two VHF frequencies (146 MHz and 164 MHz) for antennas used for a VHF mobile radio analyzed previously in 2003 (FCC ID#ABZ99FT3046). The corresponding MPE measurements are reported in the compliance report relative to FCC ID#ABZ99FT3046. The comparison results are presented below, according to following definitions for the equivalent power densities (based on E or H-field):

$$S_E = \frac{|\mathbf{E}|^2}{2\eta}, \quad S_H = \frac{\eta}{2}|\mathbf{H}|^2, \quad \eta = 377\ \Omega$$

<u>Passenger with 43 cm monopole antenna (HAD4009A 164 MHz)</u>

The following figures of the test model show the empty car model, where the red dotted line represents the location of the passenger in the back seat, as it can be observed from the complete model picture above. The comparison has been performed by taking the computed steady-state field values at the red dots locations corresponding to the head, chest, and lower trunk area and comparing them with the corresponding measurements. Such a comparison is carried out at the same average power level (56.5 W) used in the measurements. Steady-state E-field and H-field distributions at a vertical crossing the passenger's head are displayed as well. Finally, a picture of the antenna is shown.

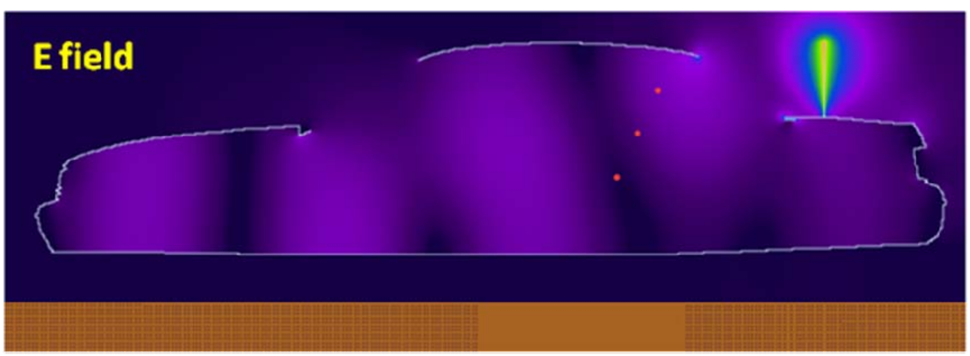

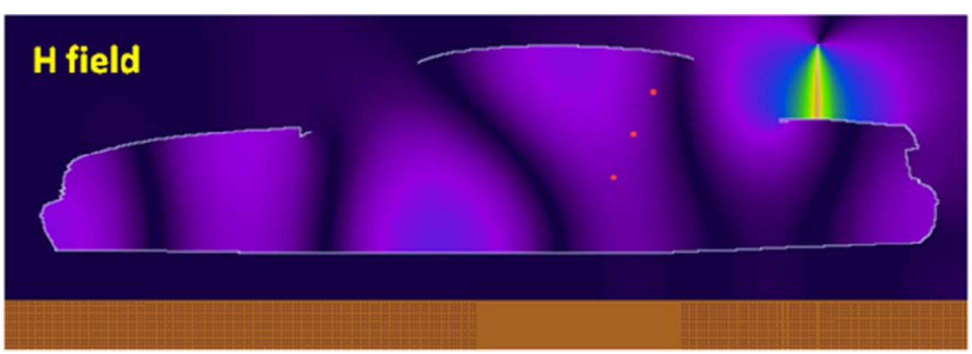

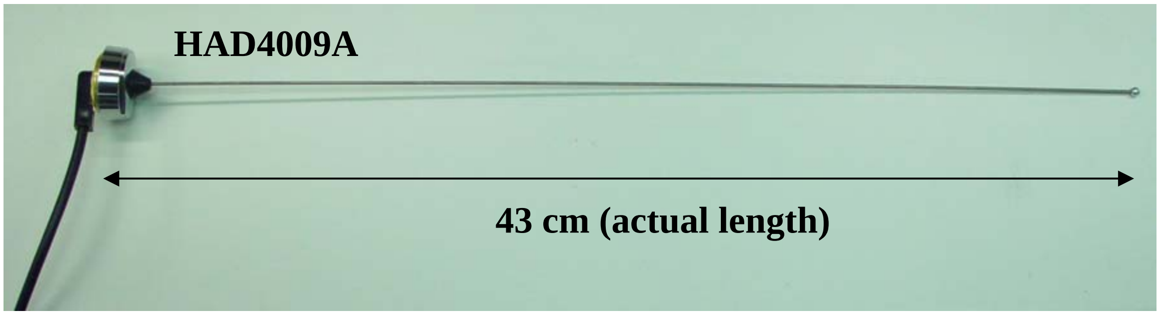

The highest exposure occurs in the middle of the backseat, which is also the case in the measurements. Therefore, the field values were determined on the yellow line centered at the middle of the backseat, approximately at the three locations that are shown by white dots. In actuality, the line is inclined so as to follow the inclination of the passenger's back, as shown previously.

Because the peak exposure occurs in the center of the back seat, that was where we placed the passenger model to perform the SAR evaluations presented in the report. However, it can be observed that the H-field distribution features peaks near the lateral edges of the rear window. That is the reason why we also carried out one SAR computation by placing the passenger laterally in the back seat, in order to determine whether the SAR would be higher in this case.

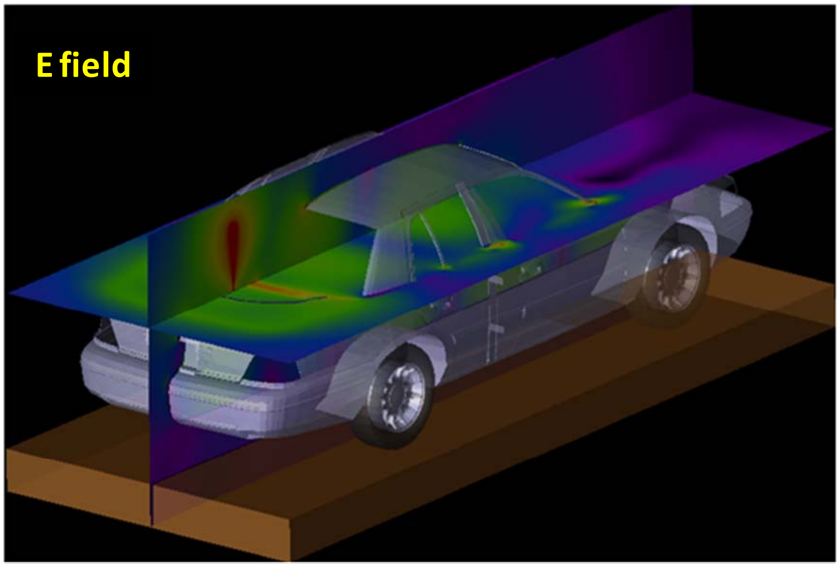

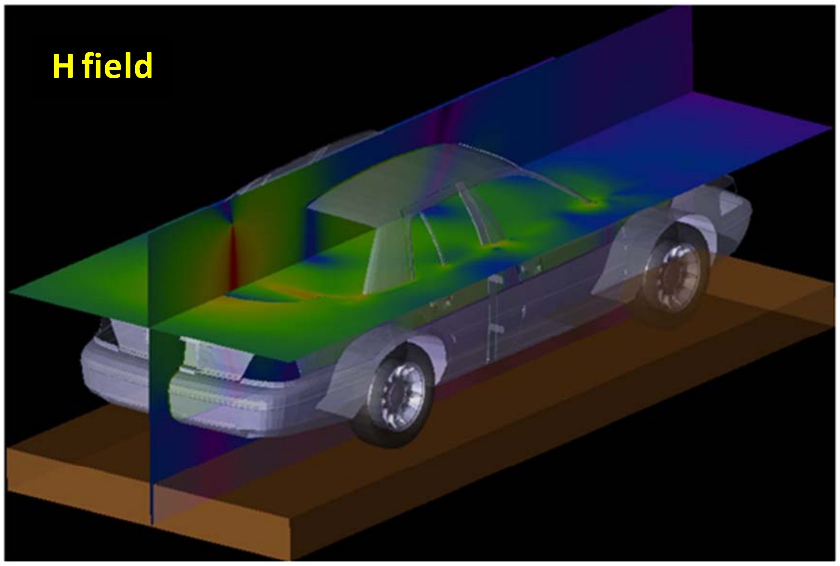

As done in the measurements, the equivalent power density (S) is computed from the E-field, the H-field being much lower. The following table reports the E-field values computed by XFDTD™ at the three locations, and the corresponding power density.

Location	E-field magnitude (V/m)	S (W/m^2)
Head	1.27	2.14E-03
Chest	0.70	6.55E-04
Lower Trunk area	0.20	7.70E-05
	Average S	**9.57E-04**

The input impedance is 24.8-j11.9 ohm, therefore the radiated power (considering the mismatch to the 50 ohm unitary voltage source) is 2.16E-3 W. The scaled-up power density for 56.5 W radiated power is 25.0 W/m^2, corresponding to 2.50 mW/cm^2. Measurements gave an average of 1.29 mW/cm^2, which is a reasonable overestimation considering conservativeness of simulations model. The following table and the graph show a comparison between the simulated power density and the measured one (see also MPE report in FCC ID#ABZ99FT3046, Table 43), normalized to 56.5 W radiated.

Position	SE (meas) mW/cm^2	SE (FDTD) mW/cm^2
Head	2.98	5.59
Chest	0.74	1.71
Lower Trunk	0.14	0.2

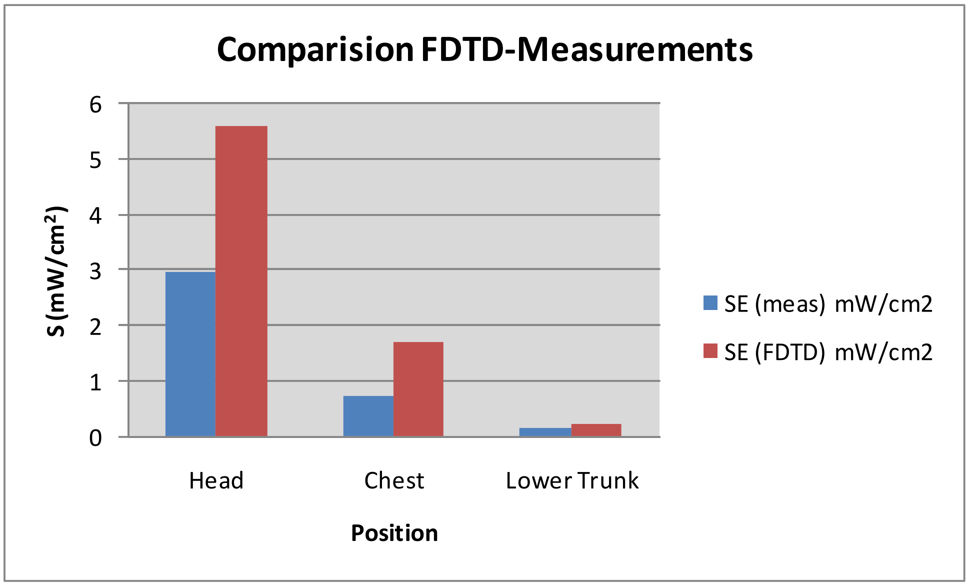

<u>Bystander with 48 cm monopole antenna (HAD4007A 146 MHz)</u>

The following figures show the E-field and H-field distributions across a vertical plane passing for the antenna and cutting the car in half. As done in the measurements, the MPE is computed from both E-field and H-field distributions, along the yellow dotted line at 10 points spaced 20 cm apart from each other up to 2 m in height. These lines and the field evaluation points are approximately indicated in the figures. The E-field and H-field distributions in the vertical plane placed at 60 cm from the antenna, are shown as well. The points where the fields are sampled to determine the equivalent power density (S) are approximately indicated by the white dots. A picture of the antenna is not reported because it is identical to the HAD4009A except for the length.


H field
60 cm
(0 mm, 200 mm, 0 mm)

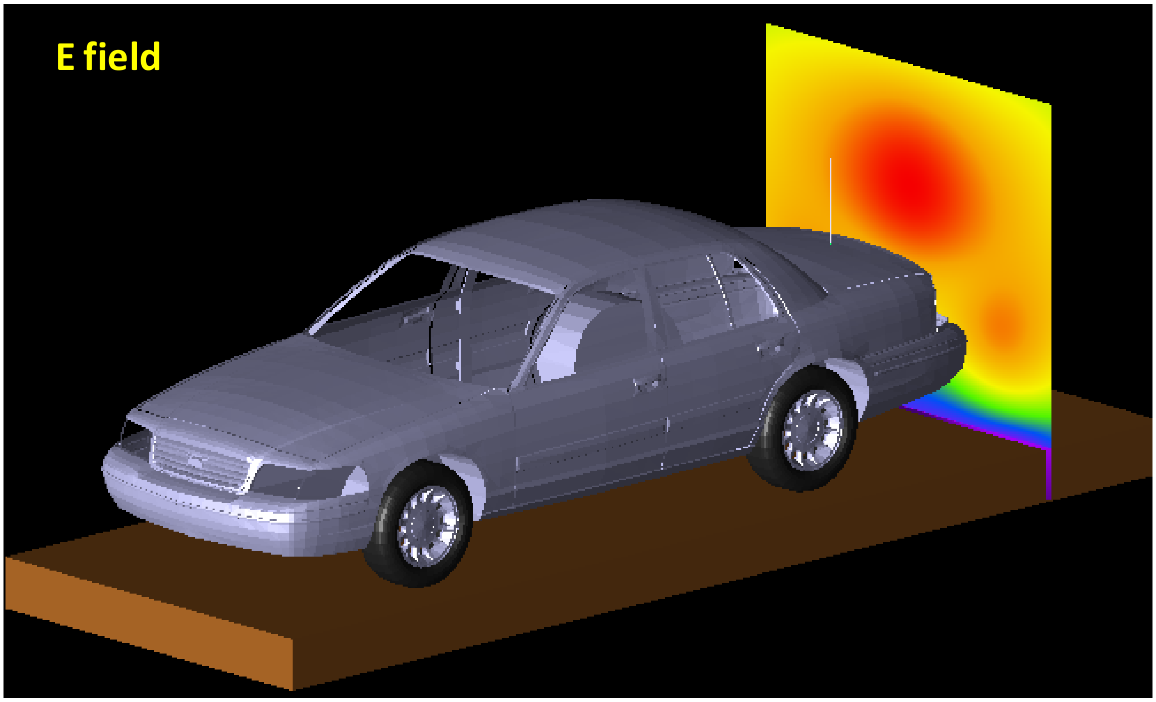
E field

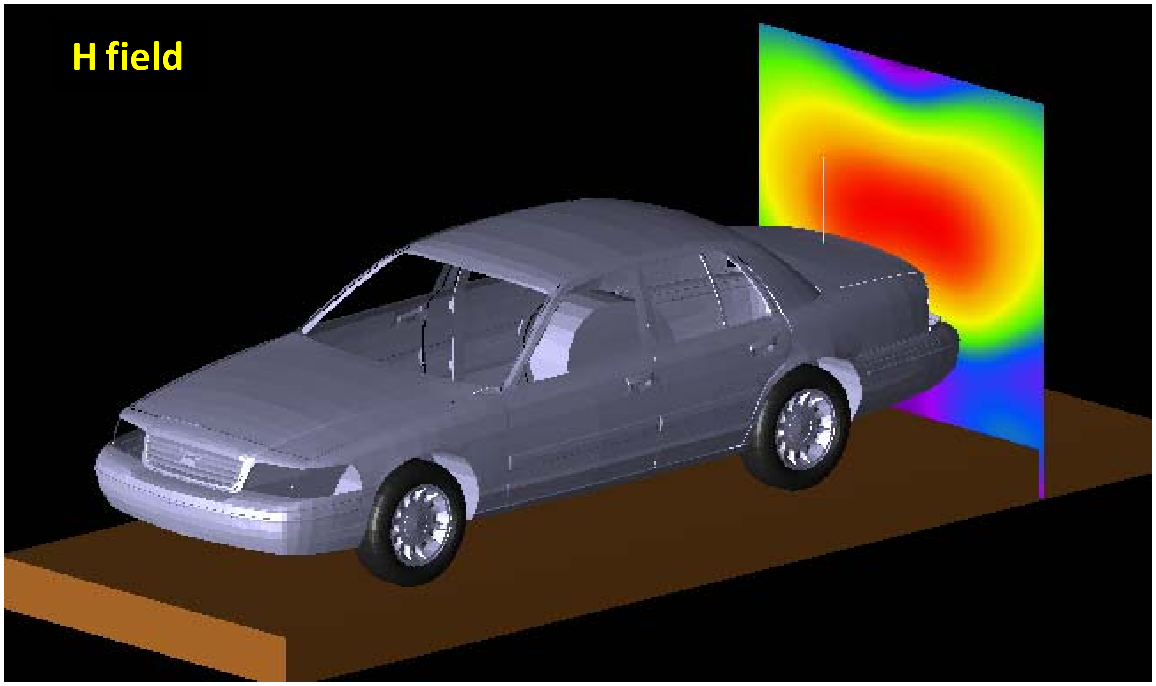

The following table reports the field values computed by XFDTD™ and the corresponding power density values. The average exposure levels are computed as well.

Height (cm)	E (V/m)	S_E (W/m^2)	H (A/m)	S_H (W/m^2)
20	1.84E-01	4.50E-05	5.10E-04	4.89E-05
40	2.71E-01	9.71E-05	6.38E-04	7.68E-05
60	3.58E-01	1.70E-04	1.08E-03	2.20E-04
80	4.42E-01	2.59E-04	1.54E-03	2.20E-04
100	5.85E-01	4.55E-04	1.82E-03	4.48E-04
120	6.86E-01	6.24E-04	1.85E-03	6.23E-04
140	6.82E-01	6.17E-04	1.58E-03	6.42E-04
160	5.93E-01	4.67E-04	1.16E-03	4.72E-04
180	4.63E-01	2.84E-04	7.67E-04	2.52E-04
200	3.41E-01	1.55E-04	4.94E-04	1.11E-04
	Average S_E	**3.17E-04**	**Average S_H**	**3.11E-04**

The input impedance is 33.7-j3.0 ohm, therefore the radiated power (considering the mismatch to the 50 ohm unitary voltage source) is 2.40E-3 W. The scaled-up power density values for 53.2 W radiated power are 7.03 W/m^2 (E), and 6.90 W/m^2 (H), that correspond to 0.70 mW/cm^2 (E), and 0.69 mW/cm^2 (H). Measurements yielded average power density of 0.664 mW/cm^2 (E), and 0.471 mW/cm^2 (H), i.e., which are in good agreement with the simulations. The following table and graph show a comparison between the simulated power density and the measured one, based on E (see MPE report in FCC ID#ABZ99FT3046, Table 1) or H fields (see MPE report in FCC ID#ABZ99FT3046, Table 13), normalized to 53.2 W radiated.

Height (cm)	SE (meas) mW/cm^2	SE (FDTD) mW/cm^2	SH (meas) mW/cm^2	SH (FDTD) mW/cm^2	Avg SE meas mW/cm^2	Avg SE FDTD mW/cm^2	Avg SH meas mW/cm^2	Avg SH FDTD mW/cm^2
20	0.19	0.10	0.2	0.11	0.664	0.703	0.471	0.690
40	0.37	0.22	0.23	0.17				
60	0.55	0.38	0.3	0.49				
80	0.68	0.57	0.56	0.49				
100	1.02	1.01	1.07	0.99				
120	1.15	1.38	1.1	1.38				
140	1.04	1.37	0.56	1.42				
160	0.79	1.03	0.24	1.05				
180	0.5	0.63	0.23	0.56				
200	0.35	0.34	0.22	0.25				

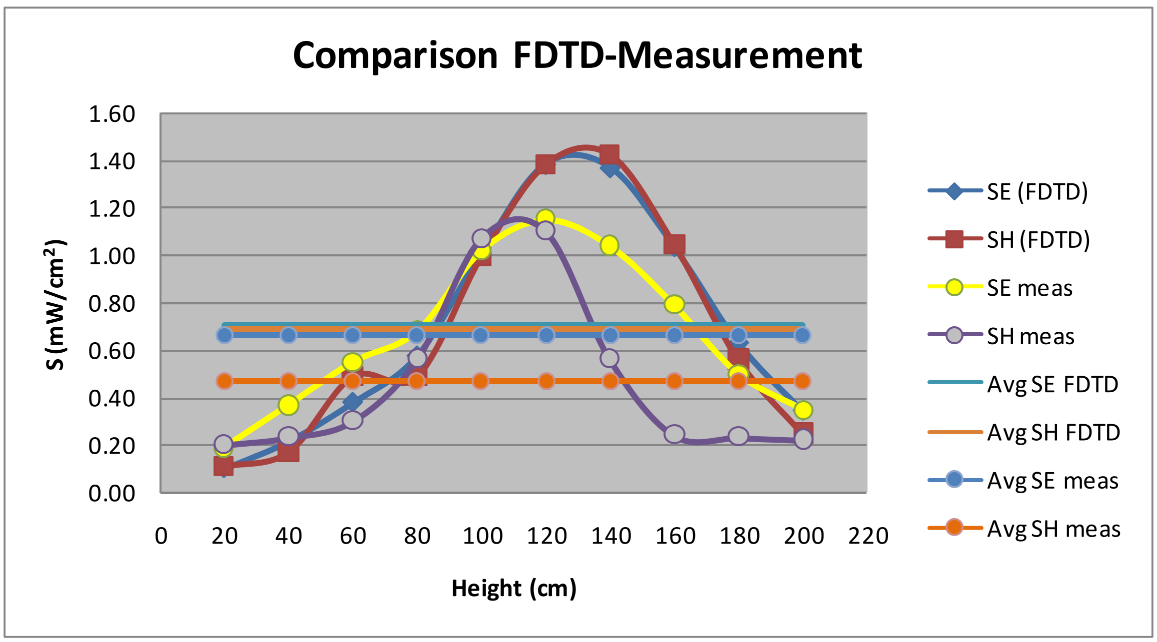

Passenger with 17.5 cm monopole antenna (HAE4002A 421.5 MHz)

The following figure of the test model shows the car model, where the red dots individuate the back seat, as it can be observed from the other figure showing the cross section of the passenger. The comparison has been performed by taking the average of the computed steady-state field values at the six dotted locations, corresponding to the head, chest, and legs along the red dots line, and comparing them with the average of the MPE measurements performed at the head, chest and legs locations. Such a comparison is carried out at the same average power level (22 W, including the 50% duty factor) used in the MPE measurements.

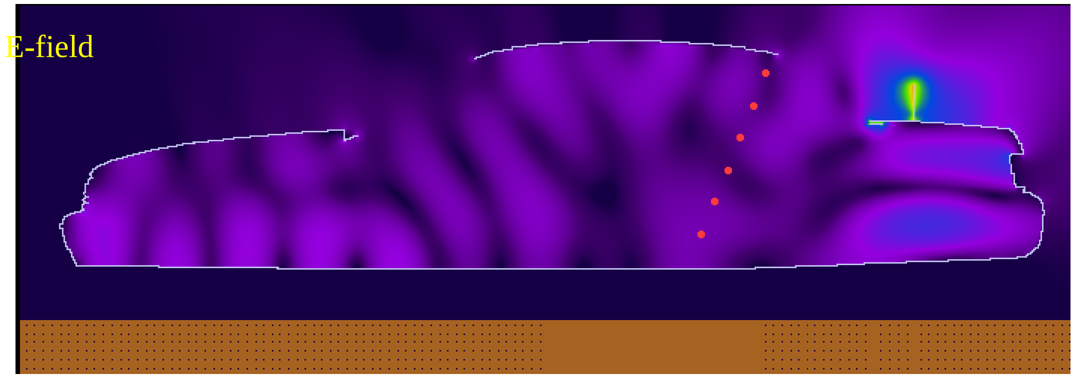

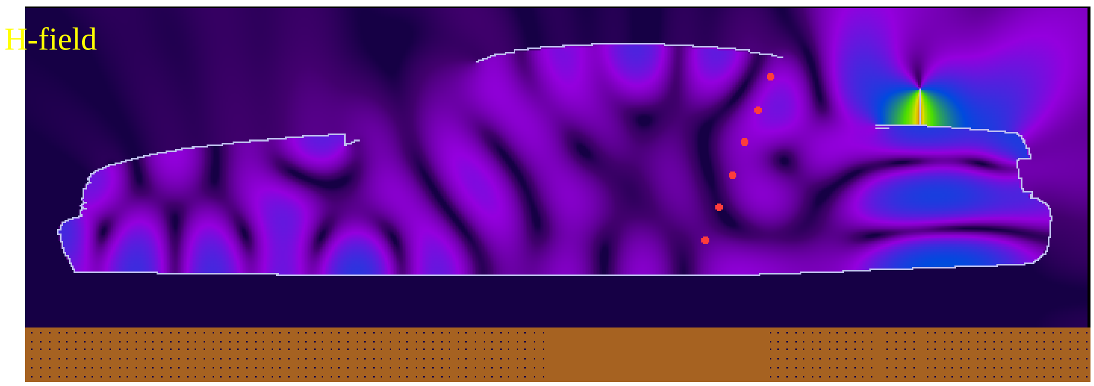

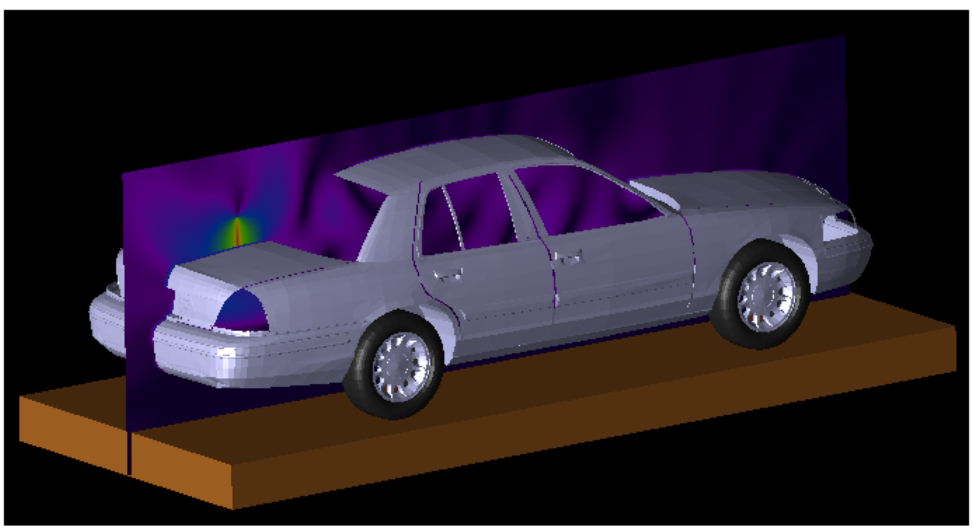

The equivalent power density (S) is computed from the E-field and the H-field separately. The following table reports the E-field values computed by XFDTD™ at the six locations, and the corresponding power density.

Location Number	E-field, V/m	Eq. Power Density 1.0 V source	Scaled Power Dens. 22 W output, mW/cm^2
1	3.11E-01	1.28E-04	1.56E-01
2	4.16E-01	2.29E-04	2.79E-01
3	5.25E-01	3.65E-04	4.45E-01
4	3.86E-01	1.98E-04	2.41E-01
5	3.84E-01	1.96E-04	2.39E-01
6	6.01E-01	4.80E-04	5.85E-01
Equivalent average Power Density			**3.24E-01**

Location Number	H-field, Weber/m2	Eq. Power Density 1.0 V source	Scaled Power Dens. 22 W output, mW/cm^2
1	1.34E-03	3.37E-04	4.11E-01
2	1.08E-03	2.21E-04	2.70E-01
3	5.59E-04	5.89E-05	7.18E-02
4	5.45E-04	5.60E-05	6.82E-02
5	5.45E-04	5.59E-05	6.82E-02
6	5.23E-04	5.16E-05	6.29E-02
Equivalent average Power Density			**1.59E-01**

The radiated power (considering the mismatch to the 50 ohm unitary voltage source) is 1.81E-3 W, therefore a factor equal to 12188 is required to scale up to 22 W radiated. The corresponding scaled-up power densities are reported in the tables above, which show that the simulation overestimates the average power density from the MPE measurements (0.297 mW/cm^2), as derived from the measured E-field reported in the following table:

Position	SE (meas), 22 W output mW/cm^2
Head	0.38
Chest	0.33
Lower Trunk	0.16

The simulations tend to overestimate the average power density levels, which is understandable since there are no ohmic losses and perfect impedance matching is enforced in the computational models. Based on these results, we conclude that the simulation will produce slight exposure overestimates (about 9%).

b) Descriptions and illustrations showing the correspondence between the modeled test device and the actual device, with respect to shape, size, dimensions and near-field radiating characteristics, are found in the main report.

c) Verification that the test device model is equivalent to the actual device for predicting the SAR distributions descends from the fact that the car and antenna size and location in the numerical model correspond to those used in the measurements.

d) The peak SAR is in the neck region for the passenger, which is in line with MPE measurements and predictions.

Passenger with 63.5 cm monopole antenna (HAE6010A 425 MHz)

The following figures show the car model with the field distribution in the horizontal planes where the MPE measurements have been performed. The comparison has been performed by taking the average of the computed steady-state field values at the three locations, corresponding to the head, chest, and lower trunk, and comparing them with the average of the MPE measurements performed at the head, chest and lower trunk locations. Such a comparison is carried out at the same average power level (61.5 W, including the 50% duty factor) used in the MPE measurements.

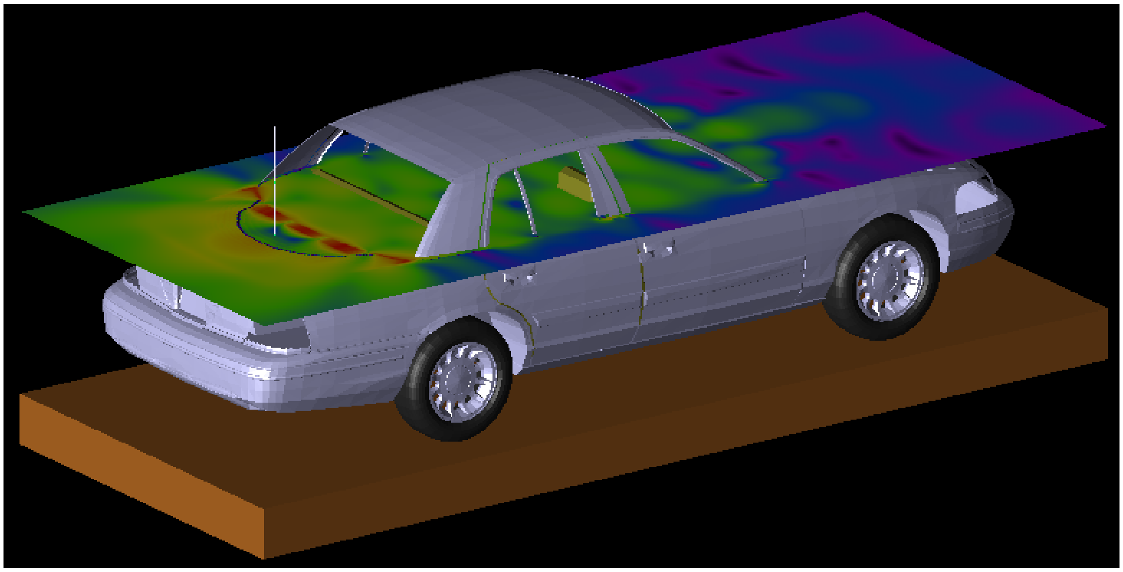

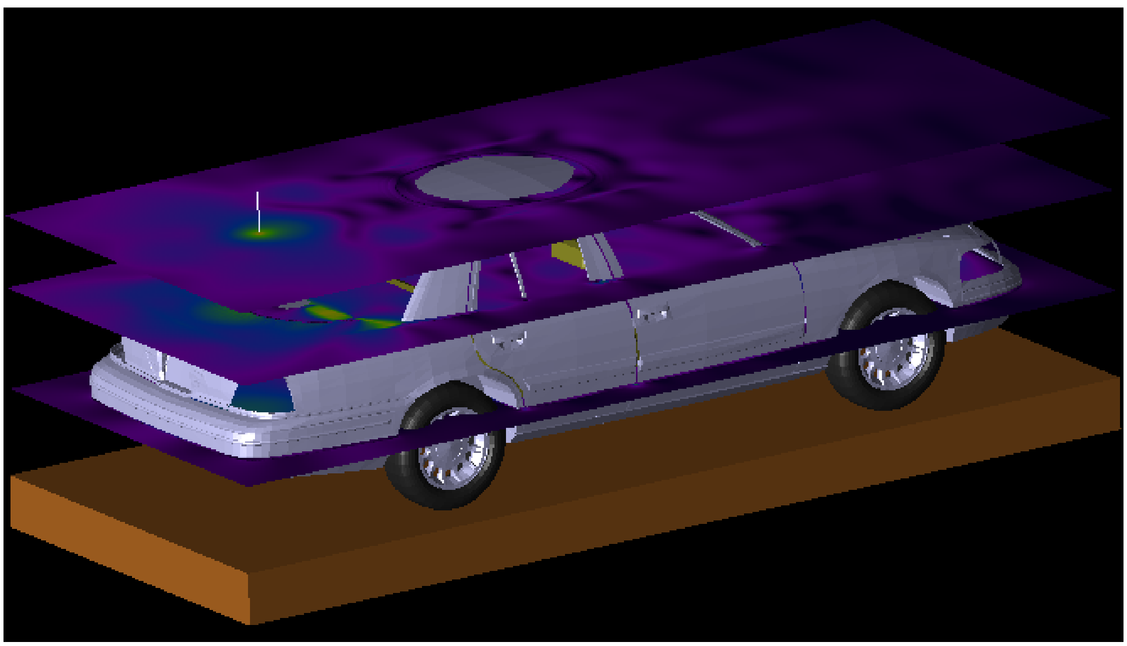

The equivalent power density (S) is computed from the E-field. The following table reports the E-field values computed by XFDTD™ at the three locations, and the corresponding power density.

Location Number	E-field, V/m	Eq. Power Density 1.0 V source	Scaled Power Dens. 61.5 W output, mW/cm^2
1	2.26E-01	6.76E-05	0.74
2	3.60E-01	1.72E-04	1.89
3	1.40E-01	2.59E-05	0.28
Equivalent average Power Density			**0.97**

The corresponding scaled-up power densities are reported in the tables above, which show that the simulation overestimates the average power density from the MPE measurements (0.52 mW/cm^2), as derived from the measured E-field reported in the following table:

Position	SE (meas), 60 W output mW/cm^2
Head	0.72
Chest	0.64
Lower Trunk	0.19

The simulations tend to overestimate the average power density levels, which is understandable since there are no ohmic losses and perfect impedance matching is enforced in the computational models. Based on these results, we conclude that the simulation will produce exposure overestimates (about 88%).

Bystander with 29 cm monopole antenna (HAE6013A 425 MHz)

The following figures show the E-field and H-field distributions across a vertical plane passing for the antenna and cutting the car in half. As done in the measurements, the MPE is computed from both E-field and H-field distributions, along the yellow dotted line at 10 points spaced 20 cm apart from each other up to 2 m in height. These lines and the field evaluation points are approximately indicated in the figures. The E-field and H-field distributions in the vertical plane placed at 90 cm from the antenna, behind the case, are shown as well. The points where the fields are sampled to determine the equivalent power density (S) are approximately indicated by the white dots. A picture of the antenna is not reported because it is identical to the HAE6013A.

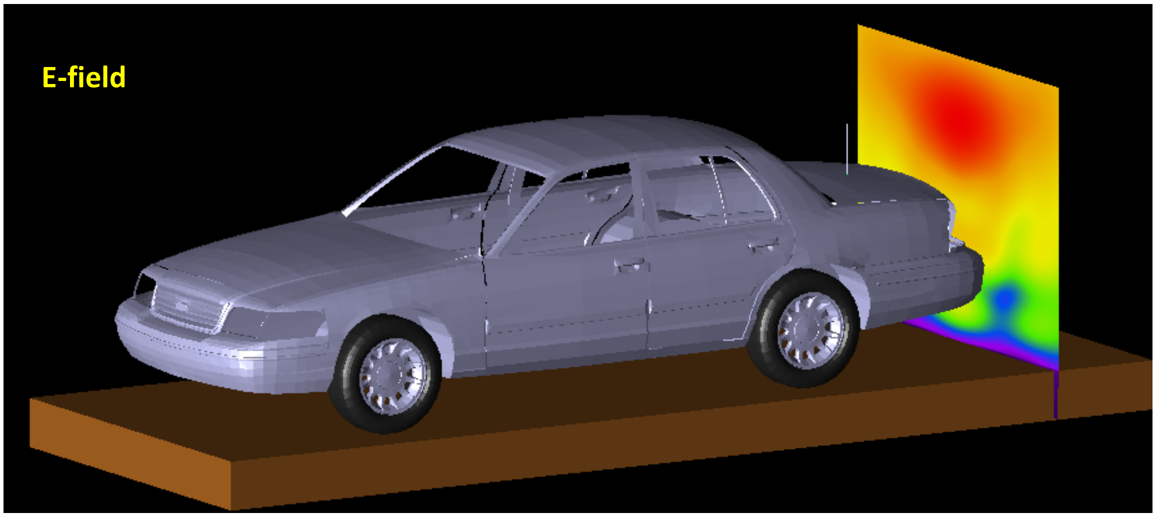

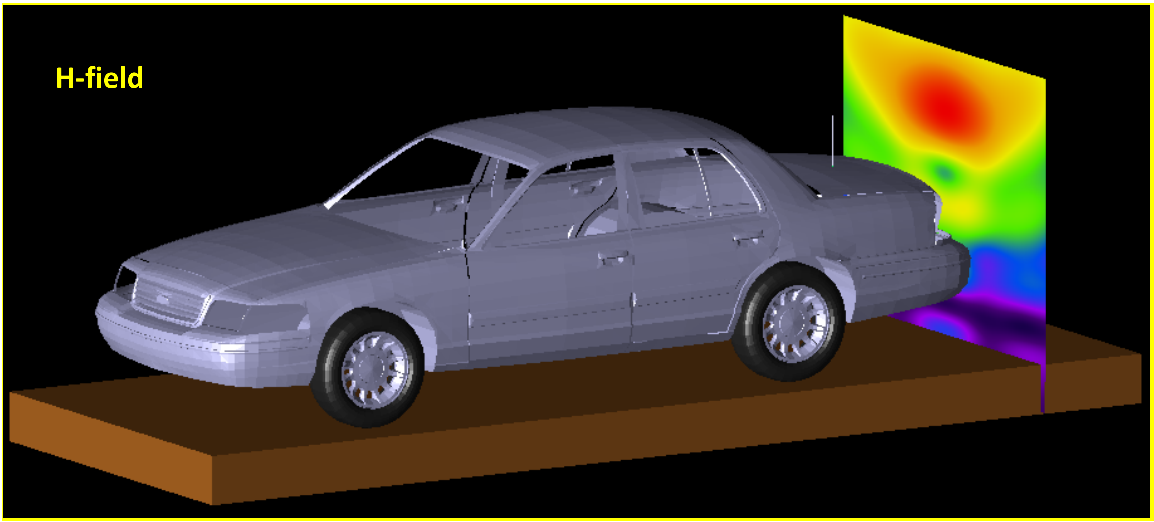

The following table reports the field values computed by XFDTD™ for the 1.0 V source and the corresponding power density values. The average exposure levels are computed as well.

Height (cm)	E (V/m)	S_E (W/m^2)	H (A/m)	S_H (W/m^2)
0	5.67E-02	4.27E-06	3.11E-04	1.83E-05
20	1.40E-01	2.59E-05	1.78E-04	5.96E-06

40	1.24E-01	2.03E-05	4.29E-04	3.47E-05
60	1.69E-01	3.79E-05	3.88E-04	2.84E-05
80	1.52E-01	3.08E-05	4.74E-04	4.24E-05
100	1.87E-01	4.65E-05	3.71E-04	2.59E-05
120	2.56E-01	8.67E-05	6.23E-04	7.31E-05
140	2.71E-01	9.73E-05	7.50E-04	1.06E-04
160	2.60E-01	8.94E-05	7.33E-04	1.01E-04
180	2.00E-01	5.31E-05	5.40E-04	5.50E-05
Average S_E		**4.92E-05**	**Average S_H**	**4.91E-05**

Since the conducted power during the MPE measurement was 123 W the calculated power density was then scaled up for 61.5 W radiated power (taking into account 50% talk time). This model does not include the mismatch loss, loss in the cable and finite conductivity of the car surface and as represents a conservative model for exposure assessment. The scaled-up power density values for 61.5 W radiated power are 6.03 W/m^2 (E), and 6.02 W/m^2 (H), that correspond to 0.603 mW/cm^2 (E), and 0.602 mW/cm^2 (H). Measurements yielded average power density of 0.309 mW/cm^2 (E), which shows that the calculated power density is overestimated. The following graph shows a comparison between the measured power density and the simulated one, based on E or H fields, normalized to 61.5 W radiated power.

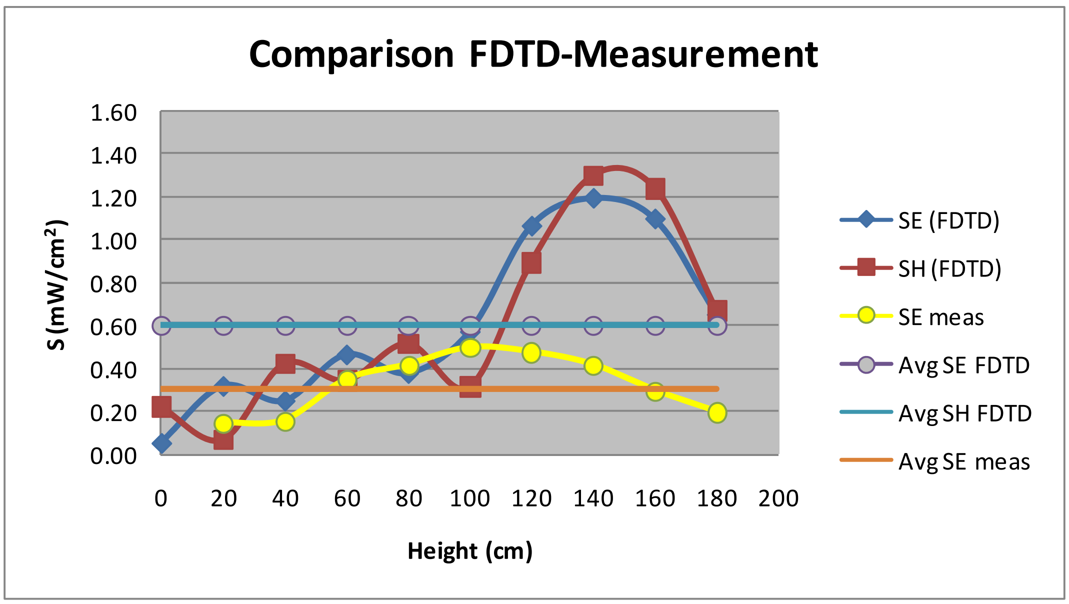

<u>Bystander with 63.5 cm monopole antenna (HAE6010A 425 MHz)</u>

The following figures show the E-field and H-field distributions across a vertical plane passing for the antenna and cutting the car in half. As done in the measurements, the MPE is computed from both E-field and H-field distributions, along the yellow dotted line at 10 points spaced 20 cm apart from each other up to 2 m in height. These lines and the field evaluation points are approximately indicated in the figures. The E-field and H-field distributions in the vertical plane placed at 90 cm from the antenna, behind the case, are shown as well. The points where the fields are sampled to determine the equivalent power density (S) are approximately indicated by the white dots. A picture of the antenna is not reported because it is identical to the HAE6010A.

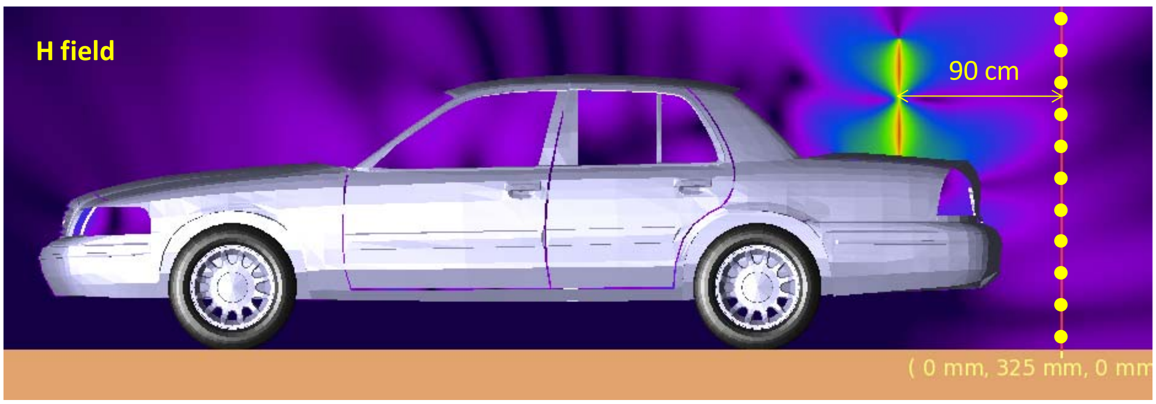

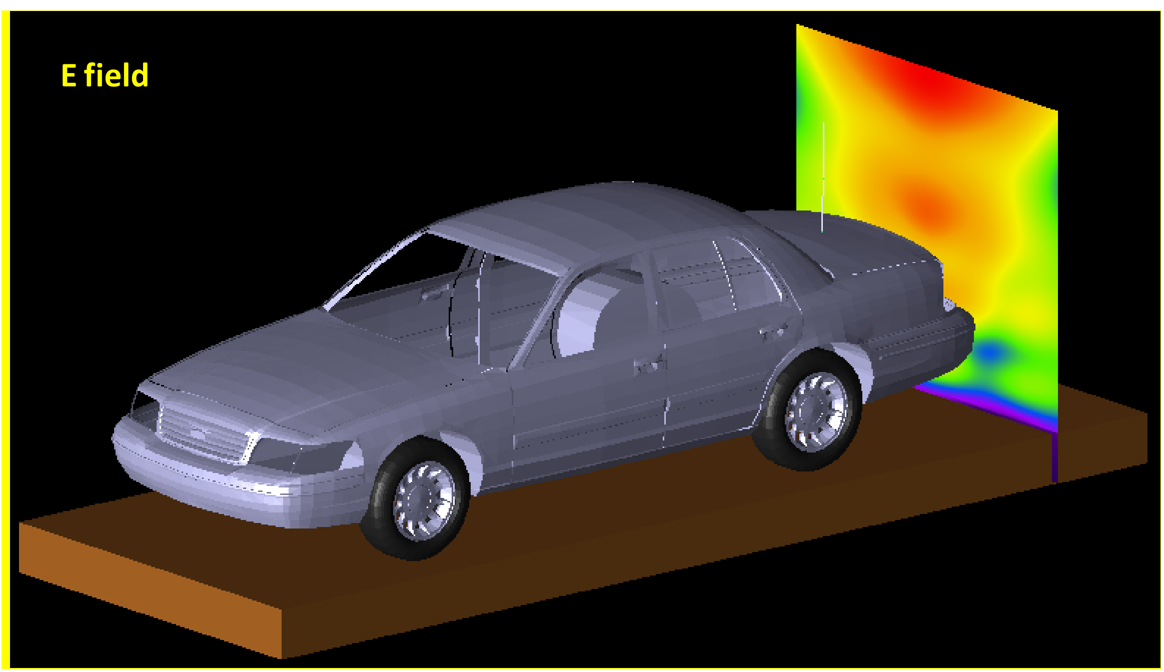

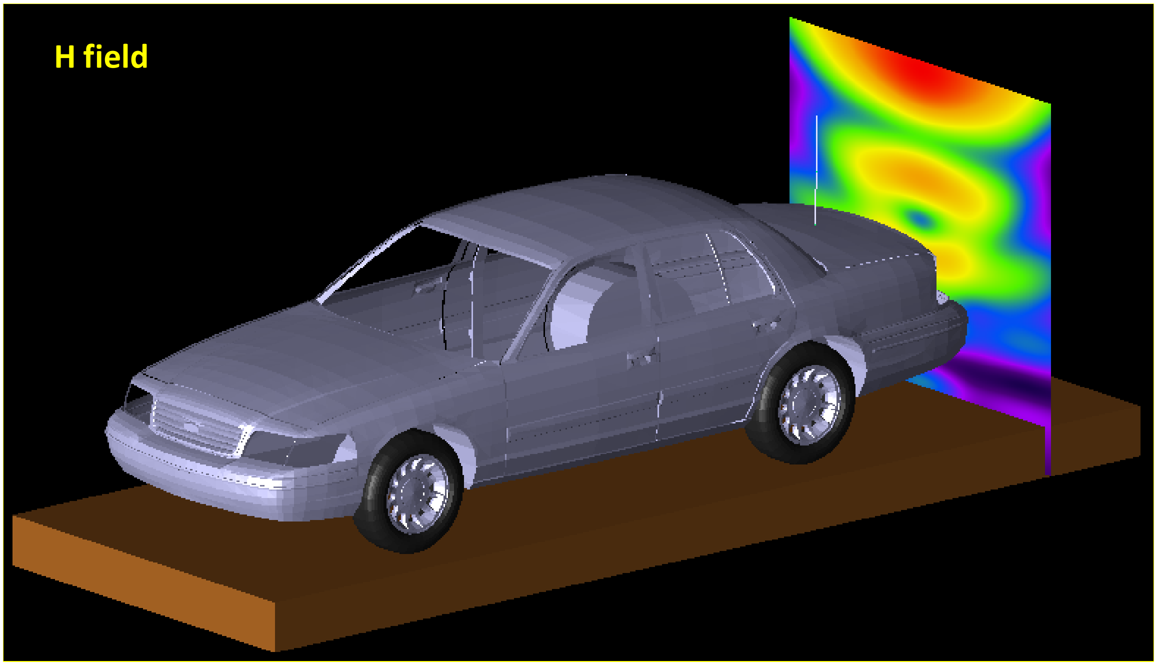

The following table reports the field values computed by XFDTD™ and the corresponding power density values. The average exposure levels are computed as well.

Height (cm)	E (V/m)	S_E (W/m^2)	H (A/m)	S_H (W/m^2)
0	7.55E-02	7.56E-06	4.13E-04	3.21E-05
20	1.79E-01	4.27E-05	2.37E-04	1.06E-05
40	1.56E-01	3.21E-05	5.49E-04	5.69E-05
60	2.12E-01	5.96E-05	4.84E-04	5.69E-05
80	1.78E-01	4.22E-05	5.65E-04	4.42E-05
100	2.07E-01	5.66E-05	3.43E-04	6.03E-05
120	1.99E-01	5.25E-05	5.34E-04	2.21E-05
140	1.70E-01	3.85E-05	4.20E-04	5.37E-05
160	2.18E-01	6.32E-05	5.10E-04	3.33E-05
180	1.80E-01	4.30E-05	8.15E-04	4.90E-05
Average S_E		**4.38E-05**	**Average S_H**	**4.19E-05**

Since the conducted power during the MPE measurement was 123 W the calculated power density was then scaled up for 61.5 W radiated power (taking into account 50% talk time). This model does not include the mismatch loss, loss in the cable and finite conductivity of the car surface and as represents a conservative model for exposure assessment. The scaled-up power density values for 61.5 W radiated power are 4.26 W/m^2 (E), and 4.07 W/m^2 (H), that correspond to 0.426 mW/cm^2 (E), and 0.407 mW/cm^2 (H). Measurements yielded average power density of 0.204 mW/cm^2 (E), which shows that the calculated power density is overestimated. The following graph shows a comparison between the measured power density and the simulated one, based on E or H fields, normalized to 61.5 W radiated power.

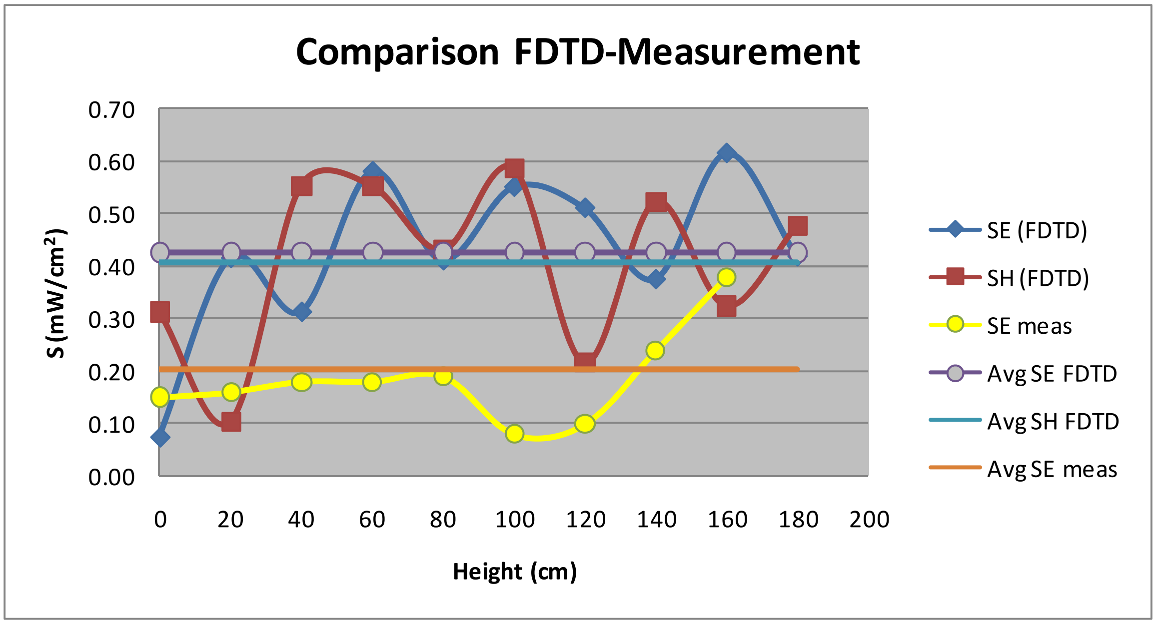
Comparison FDTD-Measurement
S (mW/cm²)
0.70
0.60
0.50
0.40
0.30
0.20
0.10
0.00
0
20
40
60
80
100
120
140
160
180
200
Height (cm)
SE (FDTD)
SH (FDTD)
SE meas
Avg SE FDTD
Avg SH FDTD
Avg SE meas

7) Test device positioning

a) A description of the device test positions used in the SAR computations is provided in the SAR report.

b) Illustrations showing the separation distances between the test device and the phantom for the tested configurations are provided in the SAR report.

8) Steady state termination procedures

a) The criteria used to determine that sinusoidal steady-state conditions have been reached throughout the computational domain for terminating the computations are based on the monitoring of field points to make sure they converge. The simulation projects were set to automatically track the field values throughout computational domain by means of XFDTD simulation control feature which ensures that "*convergence is reached when near-zone data shows a constant amplitude sine wave – when all transients have died down and the only variation left is sinusoidal. In this case "convergence" is tested on the average electric field in the space for its deviation from a pure sine wave. XFDTD automatically places points throughout the space for this purpose*." [XFDTD Reference Manual, version. 6.4 and version 7.2]. This convergence threshold was set to -50 dB.

In addition for at least one passenger and one bystander exposure condition, we placed one "field sensor" near the antenna, others between the body and the domain boundary at different locations, and one inside the head of the model. In all simulations, isotropic E-field sensors were placed at opposite sides of the computational domain. We used isotropic E and H field "sensors", meaning that all three components of the fields are monitored at these points. The following figures show an example of the time waveforms at the field point sensors in two points of the computational domain. We selected points close to antenna as well as furthest one. The highest field levels are observed for the higher index point, as it is closer to the antenna. In all cases, the field reaches the steady-state condition.

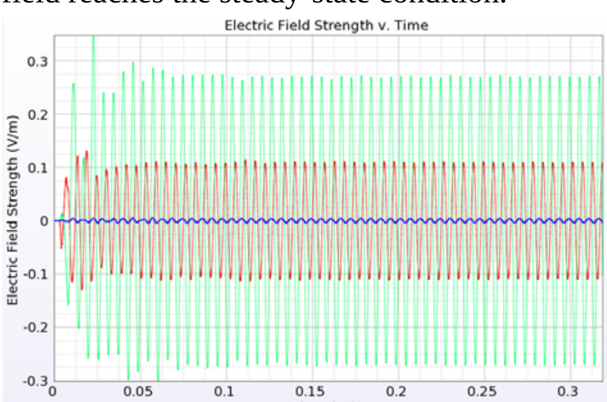

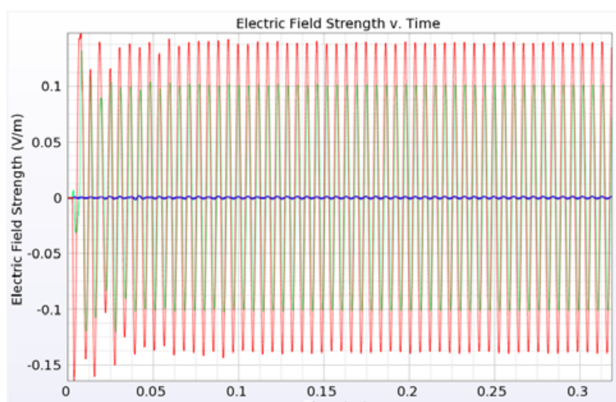

c) The XFDTD™ algorithm determines the field phasors by using the so-called "two-equations two-unknowns" method. Details of the algorithm are explained in [7].

9) Computing peak SAR from field components

a) The SAR for an individual voxel is computed according to the draft IEEE 62704-1 standard. In particular, the three components of the electric field are computed in the center of each voxel and then the SAR is computed as below:

$$SAR = \sigma_{voxel} \frac{|E_x|^2 + |E_y|^2 + |E_z|^2}{2\rho_{voxel}},$$

where σ_{voxel} and ρ_{voxel} are the conductivity and the mass density of the voxel.

10) One-gram and ten-gram averaged SAR procedures

a) XFDTD™ computes the Specific Absorption Rate (SAR) in each complete cell containing lossy dielectric material and with a non-zero material density. Using the SAR values computed for each voxel of the model the averaging calculation employs the method and specifications defined in the draft IEEE 62704-1 standard to generate one-gram and ten-gram average SAR.

11) Total computational uncertainty – We derived an estimate for the uncertainty of FDTD methods in evaluating SAR by referring to [6]. In Fig. 7 in [6] it is shown that the deviation between SAR estimates using the XFDTD™ code and those measured with a compliance system are typically within 10% when the probe is away from the phantom surface so that boundary effects are negligible. In that example, the simulated SAR always exceeds the measured SAR.

As discussed in 6(a), a conservative bias has been introduced in the model so as to reduce concerns regarding the computational uncertainty related to the car modeling, antenna modeling, and phantom modeling. The results of the comparison between measurements and simulations presented in 6(a) suggest that the present model produces an overestimate of the exposure between 4% and 36%. Such a conservative bias should eliminate the need for including uncertainty considerations in the SAR assessment.

12) Test results for determining SAR compliance

a) Illustrations showing the SAR distribution of dominant peak locations produced by the test transmitter, with respect to the phantom and test device, are provided in the SAR report.

b) The input impedance and the total power radiated under the impedance match conditions that occur at the test frequency are provided by XFDTD™. XFDTD™ computes the input impedance by following the method outlined in [8], which consists in performing the integration of the steady-state magnetic field around the feed point edge to compute the steady-state feed point current (*I*), which is then used to divide the feed-gap steady-state voltage (*V*). The net average radiated power is computed as

$$P_{XFDTD} = \frac{1}{2}\mathrm{Re}\left\{VI^*\right\}$$

Both the input impedance and the net average radiated power are provided by XFDTD™ at the end of each individual simulation.

We normalize the SAR to such a power, thereby obtaining SAR per radiated Watt (*normalized SAR*) values for the whole body and the 1-g SAR. Finally, we multiply such normalized SAR values times the max power rating of the device under test. In this way, we obtain the exposure metrics for 100% talk-time, i.e., without applying source-based time averaging.

c) For mobile radios, 50% source-based time averaging is applied by multiplying the SAR values determined at point 12(b) times a 0.5 factor.

REFERENCES

[1] K. S. Yee, "Numerical Solution of Initial Boundary Value Problems Involving Maxwell's Equations in Isotropic Media," *IEEE Transactions on Antennas and Propagation*, vol. 14, no. 3, 302-307, March 1966.

[2] Z. P. Liao, H. L. Wong, G. P. Yang, and Y. F. Yuan, "A transmitting boundary for transient wave analysis," Scientia Sinica, vol. 28, no. 10, pp 1063-1076, Oct. 1984.

[3] Validation exercise: Mie sphere. Remcom Inc. (enclosed PDF)

Remcom.pdf

[4] NEC-Win PRO ™ v 1.1, Nittany Scientific, Inc., Riverton, UT.

[5] C. M. Collins and M. B. Smith, "Calculations of B1 distribution, SNR, and SAR for a surface coil against an anatomically-accurate human body model," *Magn. Reson. Med.*, 45:692-699, 2001. (enclosed TIF)

Collins & Smith.pdf

[6] Martin Siegbahn and Christer Törnevik, "Measurements and FDTD Computations of the IEEE SCC 34 Spherical Bowl and Dipole Antenna," Report to the IEEE Standards Coordinating Committee 34, Sub-Committee 2, 1998. (enclosed PDF)

Ericsson.pdf

[7] C. M. Furse and O. P. Gandhi, "Calculation of electric fields and currents induced in a millimeter-resolution human model at 60 Hz using the FDTD method with a novel time-to-frequency-domain conversion**,"** Antennas and Propagation Society International Symposium, 1996. (enclosed PDF)

Furse & Gandhi.pdf

[8] *The Finite Difference Time Domain Method for Electromagnetics*, Chapter 14.2, by K. S. Kunz and R. J. Luebbers, CRC Press, Boca Raton, Florida, 1993.

[9] *Validation of Mobile Antenna Modeling by Comparison with Near-field Measurements,*" Report to the IEEE Standards Coordinating Committee 34, Sub-Committee 2, 2006. (enclosed PDF)

IEEE1528_2_vld.pdf

[10] *Antenna Theory: analysis and design*, Chapter 4, by C. A. Balanis, 2nd ed. John Wiley & Sons, Inc.

[11] S. Gabriel, R. W. Lau, and C. Gabriel. 1996. The dielectric properties of biological tissues: III. Parametric models for the frequency spectrum of tissues. Phys. Med. Biol. 41:2271–2293.

[12] "Validation of the HAF4013A and HAF4017A antenna Models", Internal report, G. Bit-Babik, 2012

HAF4013A_and_HAF 4017A models.pdf

COMPUTATIONAL EME COMPLIANCE ASSESSMENT OF THE DIGITAL VEHICULAR REPEATER (DVR 700), MODEL # DQPMDVR7000P, AND APX7500 MODEL # M30TXS9PW1AN MOBILE RADIO.

March 11, 2013

William Elliott, Giorgi Bit-Babik, Ph.D., and Antonio Faraone, Ph.D.
Motorola Solutions EME Research Lab, Plantation, Florida

Introduction

This report summarizes the computational [numerical modeling] analysis performed to document compliance of the DVR 700, 5 watt model # DQPMDVR7000P interfaced with, and transmitting simultaneously with companion VHF Mobile Radio models M30TXS9PW1AN with maximum transmit power up to 120 watts and vehicle-mounted antennas with the Federal Communications Commission (FCC) guidelines for human exposure to radio frequency (RF) emissions. The DVR radio operates in the 764-806 MHz frequency band while the companion VHF mobile radios operate in the 136-174 MHz band.

This computational analysis supplements the measurements conducted to evaluate the compliance of the exposure from this mobile radio with respect to applicable *maximum permissible exposure* (MPE) limits. All test conditions (9 in total) that did not conform with applicable MPE limits were analyzed to determine whether those conditions complied with the *specific absorption rate* (SAR) limits for general public exposure (1.6 W/kg averaged over 1 gram of tissue and 0.08 W/kg averaged over the whole body) set forth in FCC guidelines, which are based on the IEEE C95.1-1999 standard [1]. The same test conditions were also analyzed to determine compliance with the SAR limits set forth in the ICNIRP [3] guidelines and IEEE Std. C95.1-2005 standard [4] (2.0 W/kg averaged over 10 gram of tissue and 0.08 W/kg averaged over the whole body). In total 9 independent simulations have been performed. Six simulations are addressing the driver exposure to the DVR 700 radio with trunk mounted quarter wavelength antennas, and the other three are addressing the driver exposure to the VHF Mobile Radio with roof mounted antenna.

For all simulations a commercial code based on Finite-Difference-Time-Domain (FDTD) methodology was employed to carry out the computational analysis. It is well established and recognized within the scientific community that SAR is the primary dosimetric quantity used to evaluate the human body's absorption of RF energy and that MPEs are in fact derived from SAR. Accordingly, the SAR computations provide a scientifically valid and more relevant estimate of human exposure to RF energy.

Method

The simulation code employed is XFDTD™ v7.2, by Remcom Inc., State College, PA. This computational suite features a heterogeneous full body standing model (High Fidelity Body Mesh), derived from the so-called Visible Human [2], discretized in 3 mm voxels. The dielectric properties of 23 body tissues are automatically assigned by XFDTD™ at any specific frequency. The "seated" man model was obtained from the standing model by modifying the articulation angles at the hips and the knees. Details of the computational method and model are provided in the Appendix to this report.

The car model has been imported into XFDTD™ from the CAD file of a sedan car having dimensions 4.98 m (L) x 1.85 m (W) x 1.18 m (H), and discretized with maximum resolution of 5 mm. The Figure 1 below show both the CAD model and the photo of the actual car This CAD model has been incorporated into the IEC/IEEE 62704-2 draft standard.

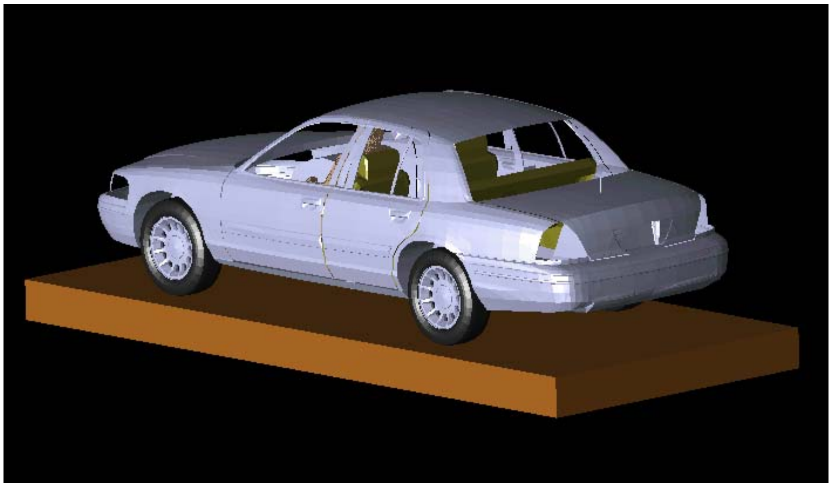

Figure 1: The photo picture of the car used in field measurements and the corresponding CAD model used in simulations

For driver exposure, the antenna position is on the trunk and on the roof that replicate the experimental conditions used in MPE measurements. According to the IEC/IEEE 62704-2 draft standard (February, 2012) for exposure simulations from vehicle mount antennas the lossy dielectric slab with 30 cm thickness, dielectric constant of 8 and conductivity of 0.01 S/m has been introduced in the computational model to properly account for the effect of the ground (pavement) on exposure.

Figure 2 shows some of the XFDTD™ computational models used for driver exposure to roof mounted (a) and trunk mounted (b) antennas

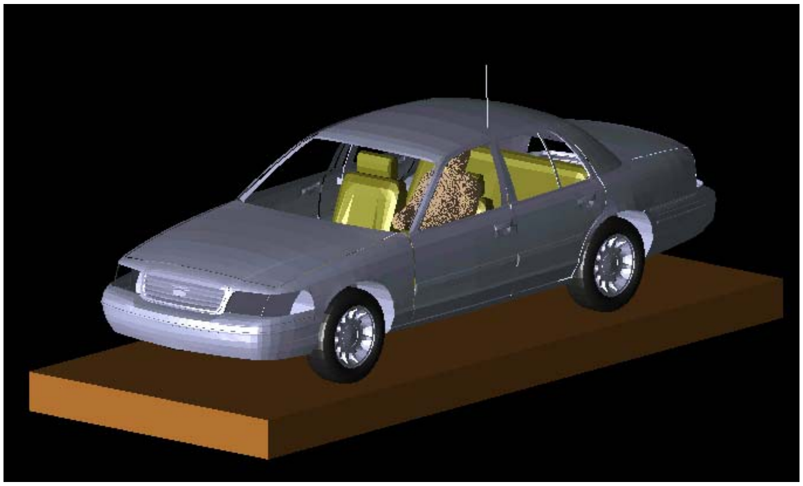

(a)

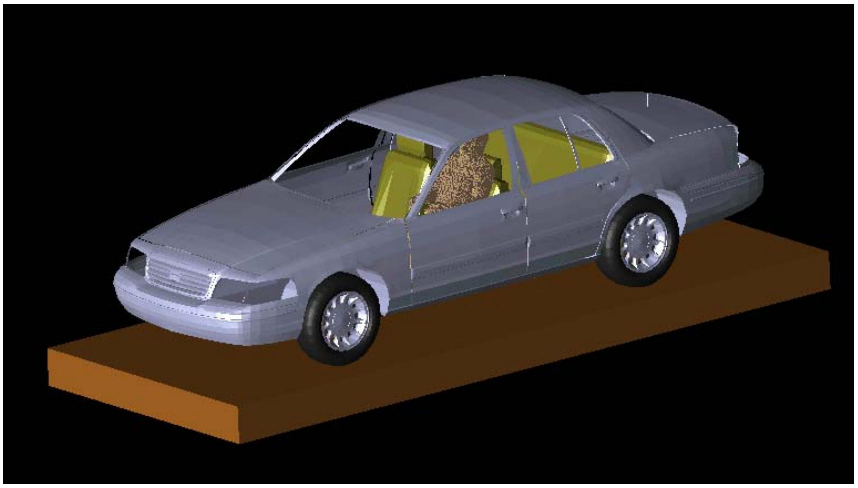
(b)

Figure 2: Driver model exposed to roof mounted (a) and trunk mounted (b) antennas: XFDTD geometry.

The computational code employs a time-harmonic excitation to produce a steady state electromagnetic field in the exposed body. Subsequently, the corresponding SAR distribution is automatically processed in order to determine the whole-body, 1-g, and 10-g average SAR. The maximum average output power from VHF mobile radio antenna is 120 W. Since the ohmic losses in the cable and in the car materials, as well as the mismatch losses at the antenna feed-point, are neglected, and source-based time averaging (50% talk time) is employed, all computational results are normalized to half of it, i.e., 60 W average net output power. The maximum average output power from DVR 700 radio is 5 W and the computational results are normalized to 5 W. The DVR 700 radio operates in a repeater mode and therefore all simulations are normalized to 100% average output power.

Two independent set simulations, one for DVR 700 trunk mount antenna and one for VHF radio roof-mount antenna were performed. Since VHF mobile radio and DVR 700 radio can transmit simultaneously, the maximum peak and whole body average SAR results from each set of data were combined to compute the peak SAR value for the simultaneous exposure from both radios. The obtained combined peak SAR value is an overestimation of the actual exposure because the peak SAR values from the roof- and trunk-mount antennas that contribute to the combined value are not found at the same location in the body.

Results of SAR computations for car passengers

The test conditions for DVR 700 radio requiring SAR computations are summarized in Table I, together with the antenna data, the SAR results, and power density (P.D.) as obtained from the measurements in the corresponding test conditions. The conditions are for antennas mounted on the trunk. The antenna length in Table I includes the 1.8 cm magnetic mount base used in measurements to position the antenna on the vehicle. The same length was used in simulation model. The seated human body model is located in the driver location. The model is surrounded by air, as the seat, which is made out of poorly conductive fabrics, is not included in the computational model. All the transmit frequencies and antenna lengths combinations reported in Table I have been simulated individually.

Table I: Results of the SAR computations for passenger exposure
from DVR 700 trunk-mount antennas

Mount location	Antenna Kit #	Antenna length (cm)	Freq [MHz]	P.D. (mw/cm^2)	Exposure location	SAR [W/kg]		
						1-g	10-g	WB
Trunk	HAF4016A	10.80	764.0000	0.01	Driver	0.059	0.030	0.0014
			770.0000	0.01		0.059	0.030	0.0012
			775.0000 **Fig 3&4**	0.02		0.066	0.033	0.0012
			794.0000	0.02		0.042	0.030	0.0011
			800.0000	0.02		0.047	0.024	0.0012
			806.0000	0.02		0.066	0.036	0.0015

The SAR distribution in the passenger model in the exposure condition that gave highest 1-g SAR is reported in Figure 3 (775.0 MHz, driver exposure condition, HAF4016A antenna).

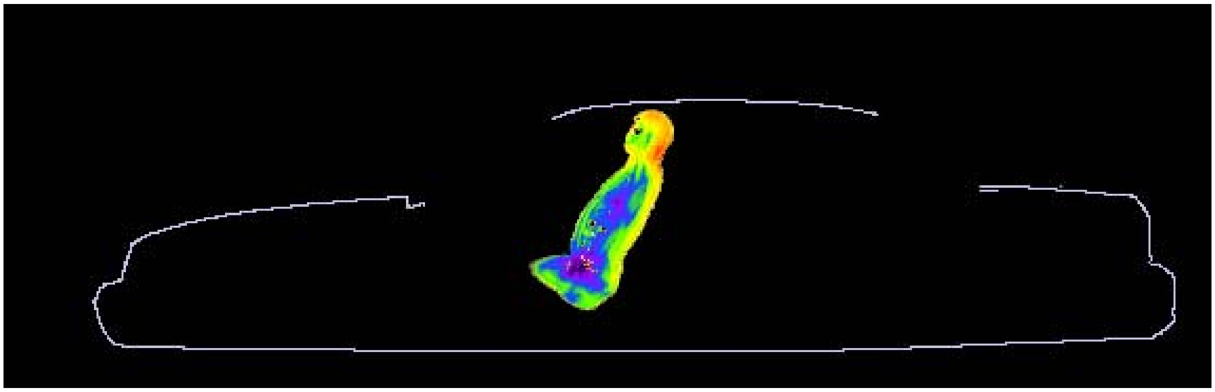

Figure 3. SAR distribution at 775.0 MHz in the driver model produced by the roof-mount HAF4016A antenna. The contour plot is relative to the plane where the peak 1-g average SAR for this exposure condition occurs.

The two pictures below in Figure 4 show the E and H field distributions in the plane of the antenna corresponding to the location in Figure 3.

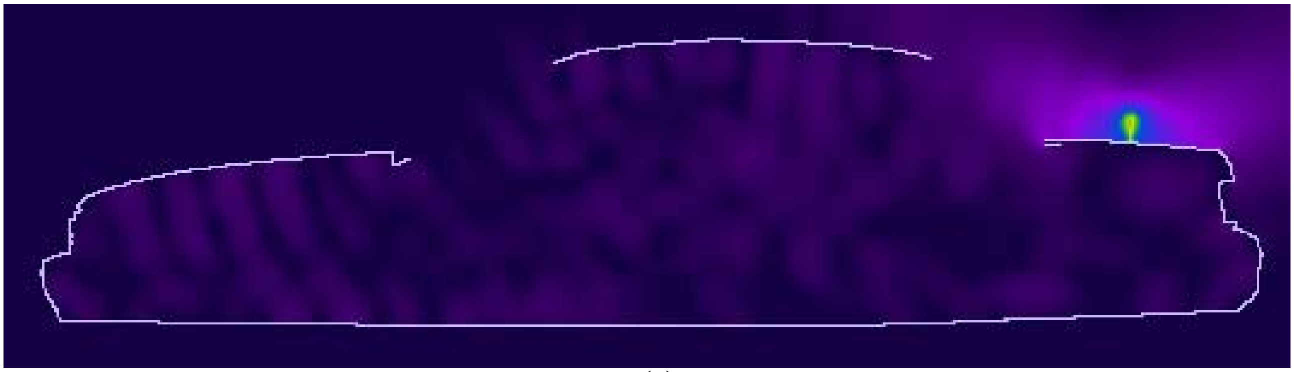

(a)

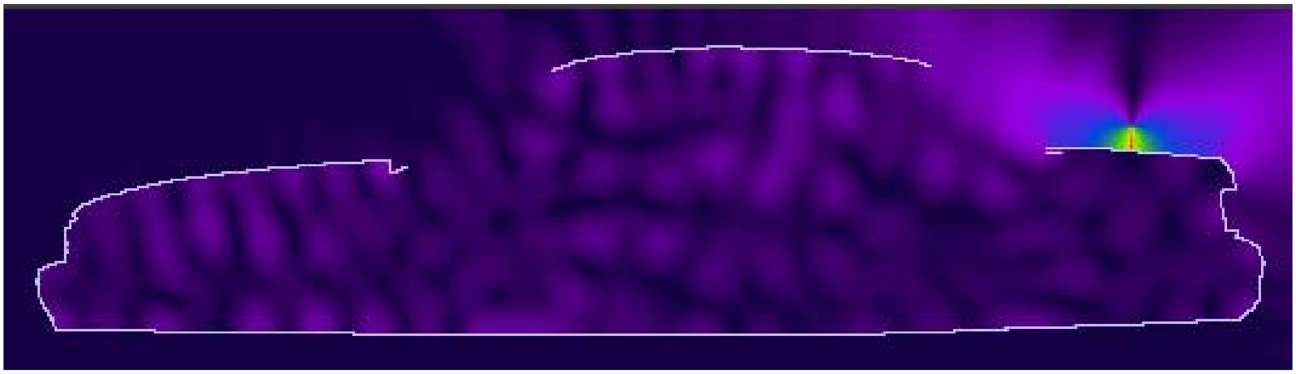

(b)

Figure 4. (a) E-field distribution corresponding to exposure condition of Figure 3, and (b) H-field distribution corresponding to exposure condition of Figure 3.

The highest 1-g SAR in the driver exposure condition with the HAF4016A trunk mounted antenna was produced at 775.0 MHz.

Results of SAR computations with the roof mounted antenna

The test conditions for VHF mobile radio requiring SAR computations are summarized in Table II, together with the antenna data and the SAR results. The conditions are for antenna mounted on the side of the roof. The seated human body model is located in the driver location. The model is surrounded by air, as the seat, which is made out of poorly conductive fabrics, is not included in the computational model. All the transmit frequencies and antenna lengths combinations reported in Table II have been simulated individually.

Table II: Results of the SAR computations for passenger exposure
from VHF mobile radio roof-mount antennas (50% talk time)

Mount location	Antenna Kit #	Antenna length (cm)	Freq [MHz]	P.D. (mw/cm^2)	Exposure location	SAR [W/kg]		
						1-g	10-g	WB
Roof	HAD4008A	47.3	150.8	0.27	Driver	0.321	0.237	0.0131
Roof	HAD4021A	53.5	145.9 **Fig 5&6**	0.29		0.974	0.585	0.0241
			150.8	0.28		0.307	0.223	0.0128

The SAR distribution in the passenger model in the exposure condition that gave highest 1-g SAR is reported in Figure 5 (145.9 MHz, driver exposure condition, HAD4021A antenna).

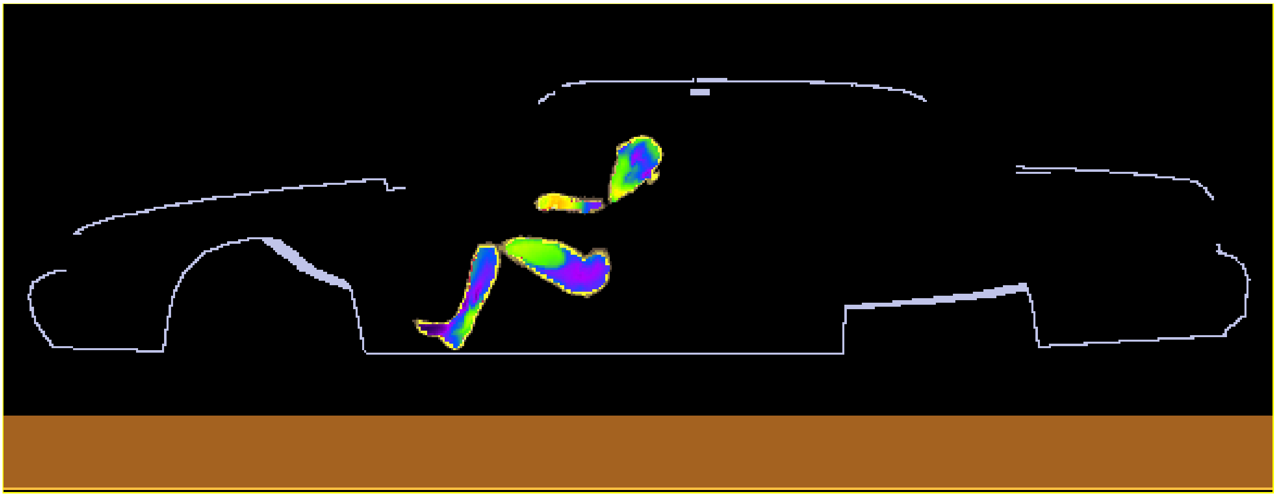

Figure 5. SAR distribution at 145.9 MHz in the driver model produced by the roof-mount HAD4021A antenna. The contour plot is relative to the plane where the peak 1-g average SAR for this exposure condition occurs.

The two pictures below in Figure 6 show the E and H field distributions in the plane of the antenna corresponding to the condition in Figure 3.

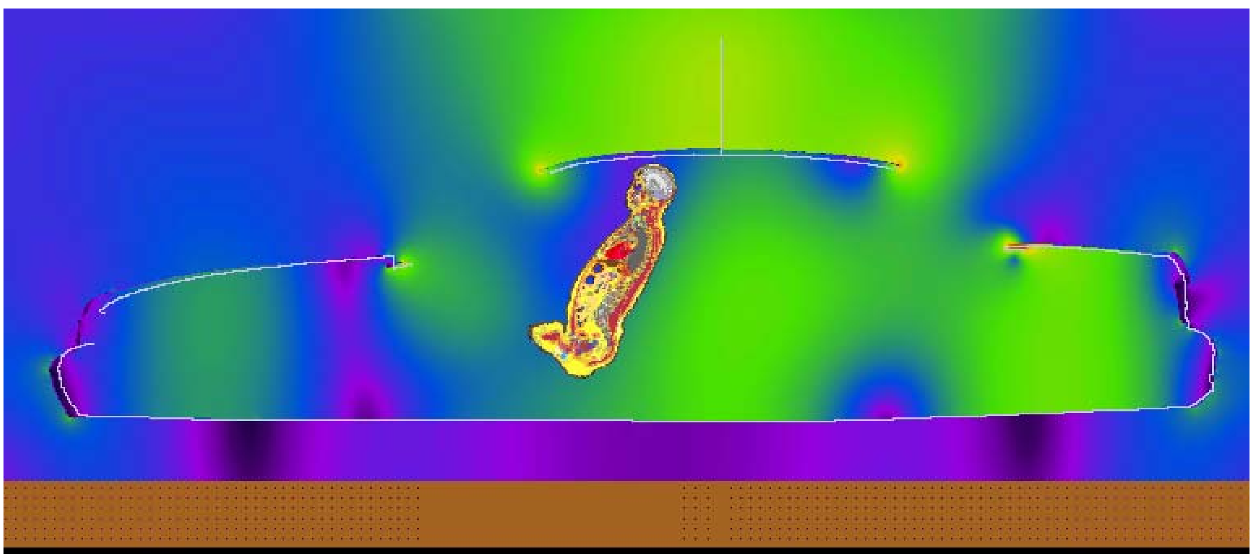

a)

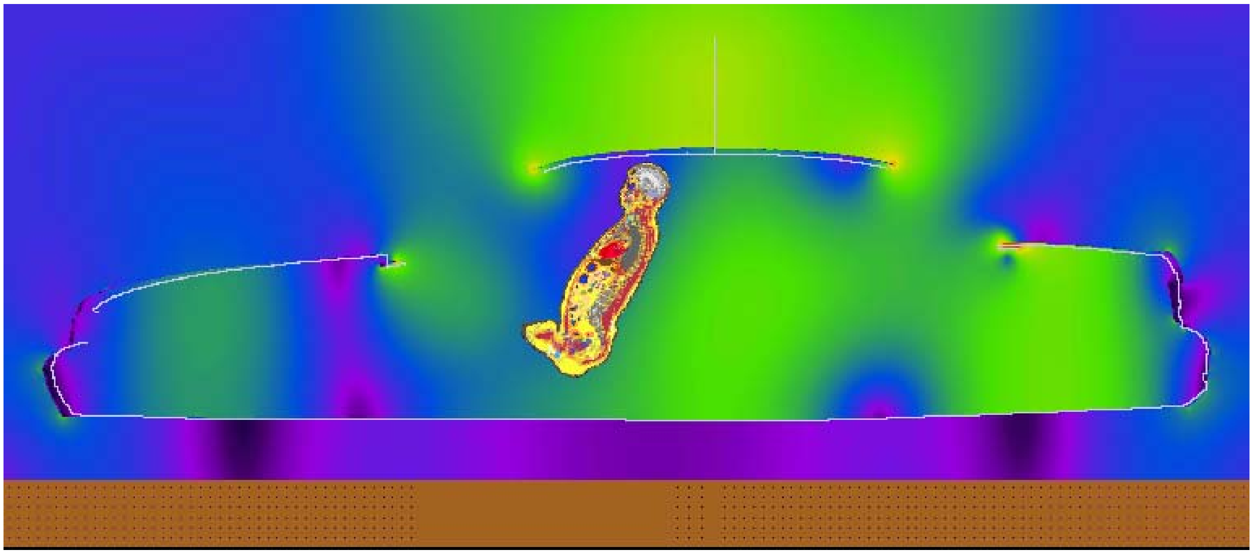

b)

Figure 6. (a) E-field distribution corresponding to exposure condition of Figure 3, and (b) H-field distribution corresponding to exposure condition of Figure 3.

For each location of the passenger on the front seat (driver and right side) the peak SAR values were identified for both DVR 700 and VHF mobile radio exposure and then combined to produce the composite peak SAR value. Table III and Table IV present those values.

Table III: Peak 1-g average SAR for both passenger locations on the front seat and composite 1-g average SAR from simultaneous exposure.

Passenger location	DVR 700 [W/kg]	VHF mobile radio [W/kg]	Total [W/kg]
Driver	0.07	0.97	1.04

Table IV: Peak whole body average SAR for both passenger locations on the front seat and composite whole body average SAR from simultaneous exposure.

Passenger location	DVR 700 [W/kg]	VHF mobile radio [W/kg]	Total [W/kg]
Driver	0.0015	0.0241	0.0256

From Table III and Table IV the maximum combined peak 1-g SAR is 1.04 W/kg, less than the 1.6 W/kg limit, while the maximum combined whole-body average SAR is 0.0256 W/kg, less than the 0.08 W/kg limit. The overall maximum combined peak 10-g SAR is 0.621 W/kg, less than the 2.0 W/kg limit.

Conclusions

Under the test conditions described for evaluating exposure to the RF electromagnetic fields emitted by vehicle-mounted antennas used in conjunction with these mobile radio products, the present analysis shows that the computed maximum SAR values are compliant with the FCC general public SAR limits. All maximum computed SAR values are compliant with the corresponding ICNIRP and IEEE Std. C95.1-2005 SAR limits.

References

[1] IEEE Standard C95.1-1999. *IEEE Standard for Safety Levels with Respect to Human Exposure to RF Electromagnetic Fields*, 3 kHz to 300 GHz.

[2] http://www.nlm.nih.gov/research/visible/visible_human.html

[3] ICNIRP (International Commission on Non-Ionising Radiation Protection). 1998. *Guidelines for limiting exposure to time-varying electric, magnetic and electromagnetic fields (up to 300 GHz)*. Health Phys. 74:494–522.

[4] IEEE. 2005. *IEEE standard for safety levels with respect to human exposure to radio frequency electromagnetic fields, 3 kHz to 300 GHz*, IEEE Std C95.1-2005

APPENDIX: SPECIFIC INFORMATION FOR SAR COMPUTATIONS

This appendix follows the structure outlined in Appendix B.III of the Supplement C to the FCC OET Bulletin 65. Most of the information regarding the code employed to perform the numerical computations has been adapted from the draft IEC/IEEE 62704-1 and 62704-2 standards, and from the XFDTD™ User Manuals. Remcom Inc., owner of XFDTD™, is kindly acknowledged for the help provided.

1) Computational resources

a) A multiprocessor system equipped with two Intel Xeon X5570 quad-core CPUs and four Tesla C1060 GPUs was employed for all simulations.

b) The memory requirement was from 7 GB to 12 GB. Using the above-mentioned system with 8-cores operating concurrently, the typical simulation would run for 6-10 hours and with all four GPUs activated by the XFDTD version 7.2 this time would be from 60-180 min.

2) FDTD algorithm implementation and validation

a) We employed a commercial code (XFDTD™ v7.2, by Remcom Inc.) that implements the Yee's FDTD formulation [1]. The solution domain was discretized according to a rectangular grid with an adaptive 3-10 mm step in all directions. Sub-gridding was not used. Seven-layer PML absorbing boundary conditions are set at the domain boundary to simulate free space radiation processes. The excitation is a lumped voltage generator with 50-ohm source impedance. The code allows selecting *wire objects* without specifying their radius. We used a wire to represent the antenna. The car body is modeled by solid metal. We did not employ the "thin wire" algorithm since within the adaptive grid the minimum resolution of 3 mm was specified and used to model the antenna and the antenna wire radius was never smaller than one-fifth of the voxel dimension. In fact, the XFDTD™ manual specifies that "In most cases, standard PEC material will serve well as a wire. However, in cases where the wire radius is important to the calculation and is less than 1/4 the length of the average cell edge, the thin wire material may be used to accurately simulate the correct wire diameter." The maximum voxel dimension in the plane normal to the antenna in all our simulations was 3 mm, and the antenna radius is always at least 1 mm (1 mm for the short quarter-wave antennas and 1.5 mm for the long gain antennas), so there was no need to specify a "thin wire" material.

Because the field impinges on the bystander or passenger model at a distance of several tens of voxels from the antenna, the details of antenna wire modeling are not expected to have significant impact on the exposure level.

Some antennas have inductive loading coils located in the mid section as shown in the picture below of the HAE 6010A and HAE 4011A antenna examples.

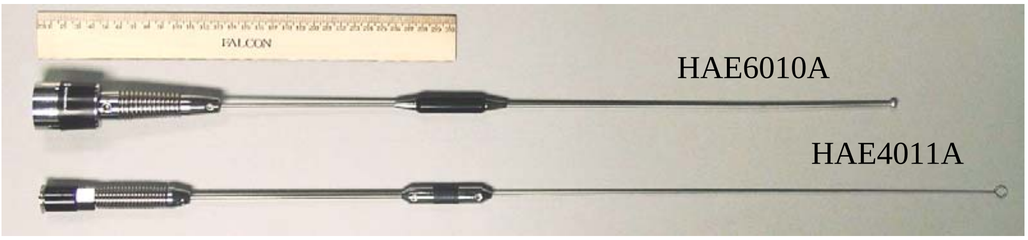

The X-ray of the reactive loads of the HAE4011A and HAE6010A antennas is also presented in the next pictures below. Those elements are significantly shorter than the length of the antenna and are about 1/40 of the wavelength at center operating frequency. They were modeled as lumped reactive elements. The comparison with measurements and validity of such simulation model has been summarized in [9].

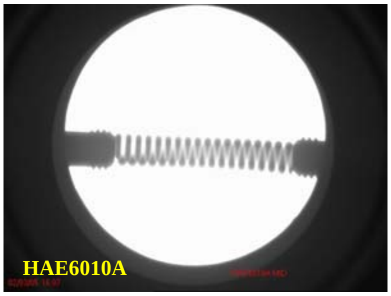

Some antennas, for example HAF4013A and HAF4017A, operating in 7/800 MHz band, may also be different from a simple wire monopoles. In those cases the XFDTD antenna models were validated against high resolution models simulated with alternative simulation tool as described [12] prior of conducting XFDTD exposure simulations.

b) XFDTD™ is one of the most widely employed commercial codes for electromagnetic simulations. It has gone through extensive validation and has proven its accuracy over time in many different applications. One example is provided in [3].

We carried out a validation of the code algorithm by running the canonical test case involving a half-wave wire dipole. The dipole is 0.475 times the free space wavelength at 160 MHz, i.e., 88.5 cm long. The discretization used to model the dipole was 5 mm. Also in this case, the “thin wire” model was not needed. The following picture shows XFDTD™ outputs regarding the antenna feed-point impedance (70.5 – j 6.0 ohm), as well as qualitative distributions of the total E and H fields near the dipole. The radiation pattern is shown as well (one lobe in elevation). As expected, the 3 dB beamwidth is about 78 degrees.

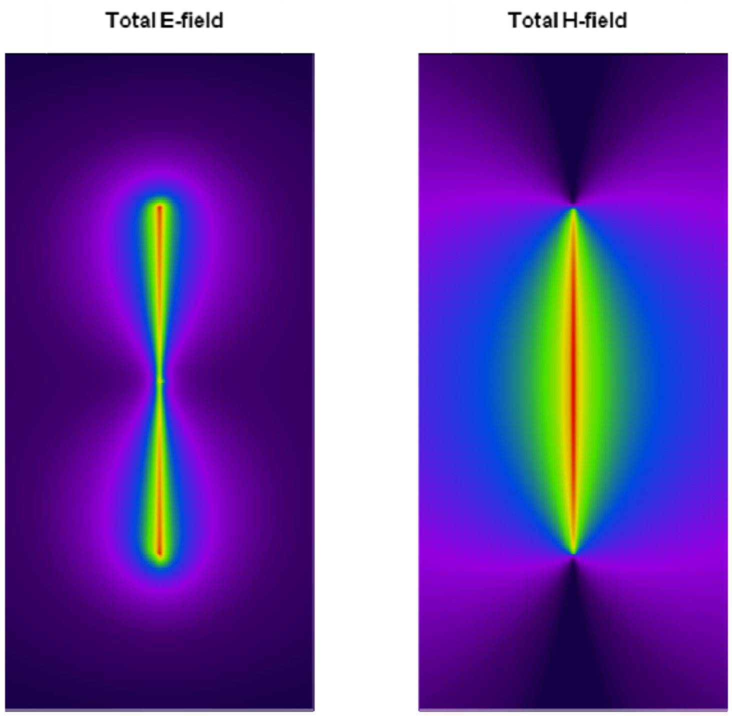

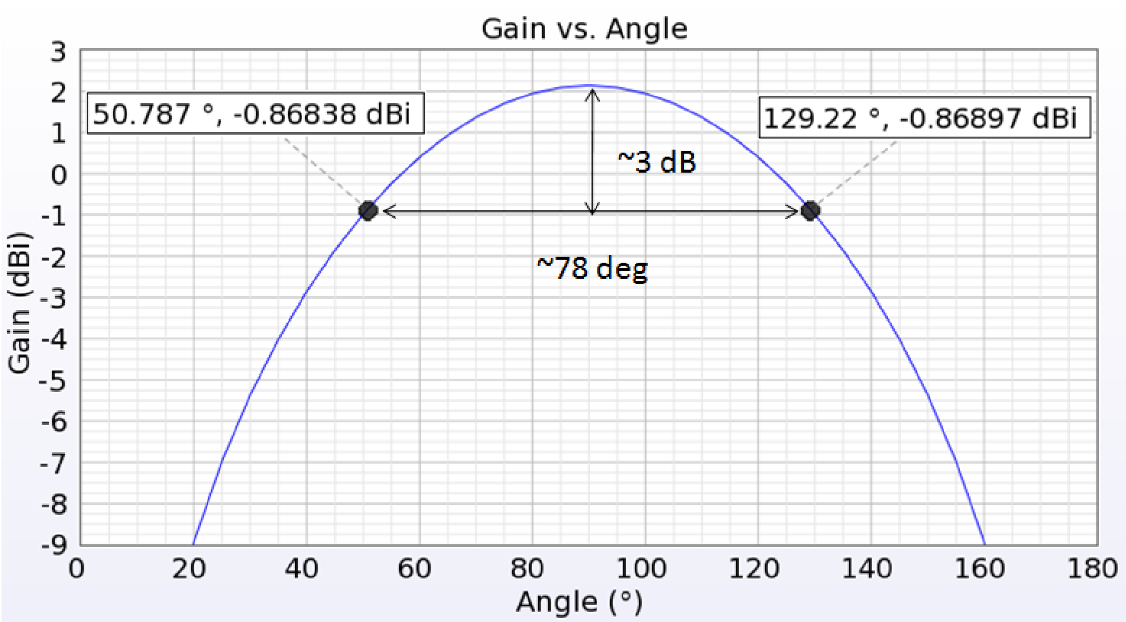

We also compared the XFDTD™ result with the results derived from NEC [4], which is a code based on the method of moments. In this case, we used a dipole with radius 1 mm, length 88.5 cm, and the discretization is 5 mm. The corresponding input impedance at 160 MHz is 69.5-j10.5 ohm. Its frequency dependence is reported in the following figure.

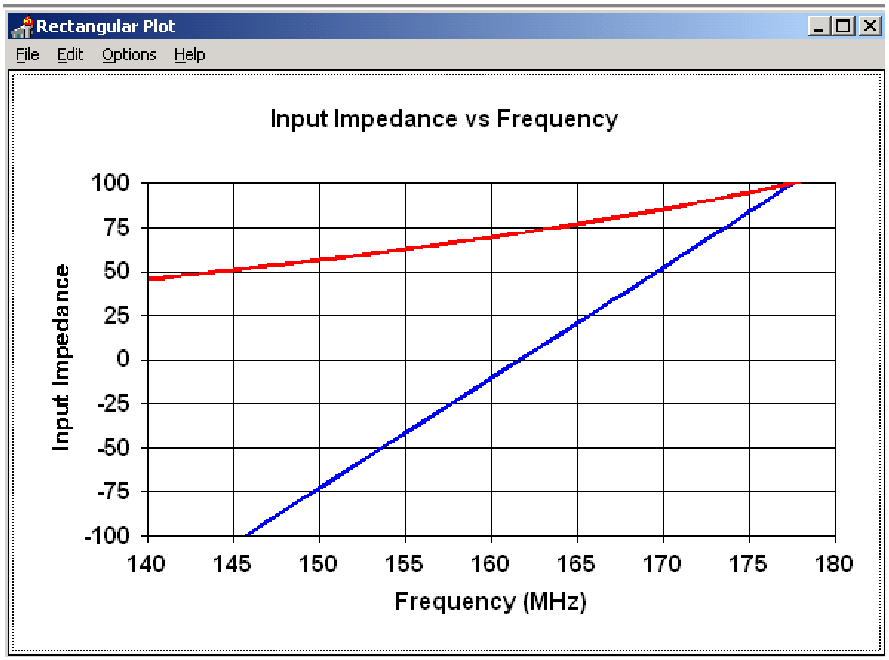

We also carried out similar validation at 400 MHz, i.e., about 35.5 cm long. The following picture shows XFDTD™ outputs regarding the antenna feed-point impedance (75.5 + j 11.9 ohm), as well as qualitative distributions of the total E and H fields near the dipole. The radiation pattern is shown as well (one lobe in elevation). As expected, the 3 dB beamwidth is about 78 degrees in this case as well. The computed results are in good agreement with the known analytical results for the half -wave dipole antenna which could be found in [10].

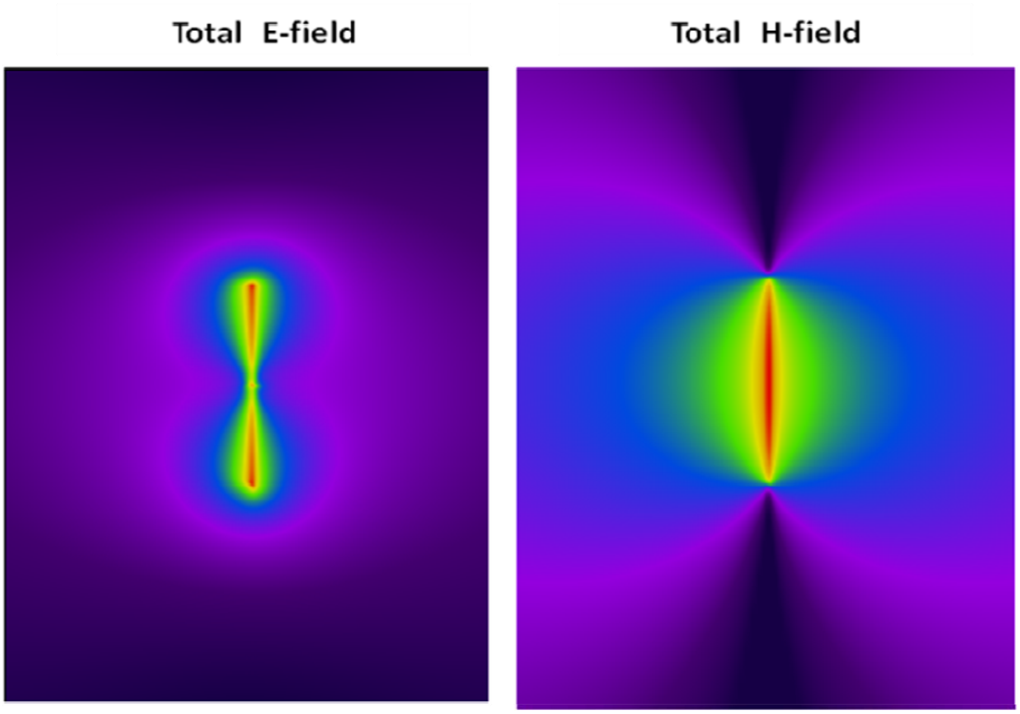

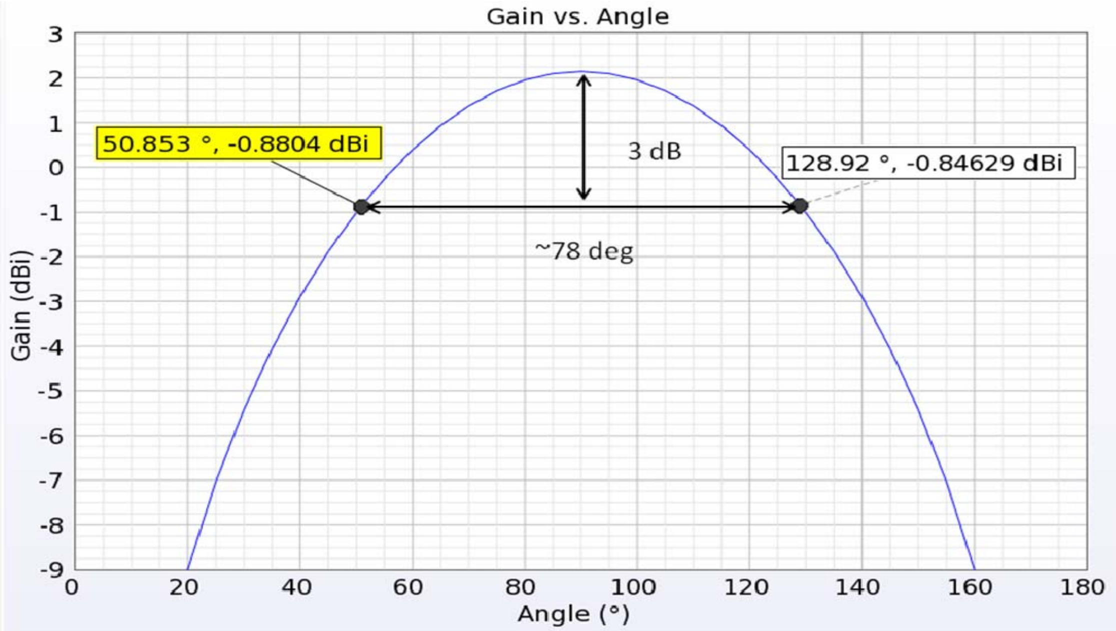

This validation ensures that the input impedance calculation is carried out correctly in XFDTD™, thereby enabling accurate estimates of the radiated power. It further ensures that the wire model employed in XFDTD™, which we used to model the antennas, produces physically meaningful current and fields distributions. Both these aspects ensure that the field quantities are correctly computed both in terms of absolute amplitude and relative distribution.

3) Computational parameters

a) The following table reports the main parameters of the FDTD model employed to perform our computational analysis:

PARAMETER	X	Y	Z
Voxel size	3-10 mm	3-10 mm	1-10 mm
Maximum domain dimensions employed for passenger computations with the trunk-mount antennas	397	910	559
Maximum domain dimensions employed for bystander computations with the trunk-mount antennas	449	791	709
Time step	About 0.7 of the Courant limit (typically 5 *ps*)		
Objects separation from FDTD boundary (mm)	>200	>200	>200
Number of time steps	Enough to reach at least -60 dB convergence		
Excitation	Sinusoidal (not less than 10 periods)		

4) Phantom model implementation and validation

a) The human body models (bystander and/or passenger) employed in our simulations are those defined in the draft IEEE 62704-2 standard. They are originally based on data from the *visible human project* sponsored by the National Library of Medicine (NLM)

(http://www.nlm.nih.gov/research/visible/visible_human.html). The original male data set consists of MRI, CT and anatomical images. Axial MRI images of the head and neck and longitudinal sections of the rest of the body are available at 4 mm intervals. The MRI images have 256 pixel by 256 pixel resolution. Each pixel has 12 bits of gray tone resolution. The CT data consists of axial CT scans of the entire body taken at 1 mm intervals at a resolution of 512 pixels by 512 pixels where each pixel is made up of 12 bits of gray tone. The axial anatomical images are 2048 pixels by 1216 pixels where each pixel is defined by 24 bits of color. The anatomical cross sections are also at 1 mm intervals and coincide with the CT axial images. There are 1871 cross sections. Dr. Michael Smith and Dr. Chris Collins of the Milton S. Hershey Medical Center, Hershey, Pa, created the High Fidelity Body mesh. Details of body model creation are given in the *methods* section in [5].
The final bystander and passenger model was generated for the IEEE 62704-2 standard from the above dataset using the Varipose softwar, Remocm Inc., The body mesh contains 39 tissues materials. Measured values for the tissue parameters for a broad frequency range are included with the mesh data. The correct values are interpolated from the table of measured data and entered into the appropriate mesh variables. The tissue conductivity and permittivity variation *vs.* frequency is included in the XFDTD™ calculation by a multiple-pole approximation to the Cole-Cole approximated tissue parameters reported in [11].

a) The XFDTD™ High Fidelity Body Mesh model correctly represents the anatomical structure and the dielectric properties of body tissues, so it is appropriate for determining the highest exposure expected for normal device operation.

b) One example of the accuracy of XFDTD™ for computing SAR has been provided in [6]. The study reported in [6] is relative to a large-scale benchmark of measurement and computational tools carried out within the IEEE Standards Coordinating Committee 34, Sub-Committee 2.

5) Tissue dielectric parameters

a) The following table reports the dielectric properties computed for the 39 body tissue materials in the employed human body models at 150 MHz.

#	Tissue	ε_r	σ (S/m)	Density (kg/m^3)
1	bile	85.3	1.60	928
2	body fluid	71.3	1.26	1050
3	eye cornea	69.0	1.07	1051
4	fat	12.2	0.07	911
5	lymph	65.7	0.81	1035
6	mucous membrane	59.2	0.56	1102
7	toe, finger, and nails	14.4	0.07	1908
8	nerve spine	42.3	0.36	1075
9	muscle	62.2	0.73	1090
10	heart	80.7	0.79	1081
11	white matter	50.3	0.35	1041
12	stomach	73.3	0.92	1088
13	glands	65.7	0.81	1028
14	blood vessel	54.0	0.49	1102
15	liver	61.7	0.53	1079
16	gall bladder	71.3	1.06	1071
17	spleen	78.8	0.86	1089
18	cerebellum	74.6	0.85	1045
19	cortical bone	14.4	0.07	1908
20	cartilage	51.4	0.50	1100
21	ligaments	50.8	0.50	1142
22	skin	61.5	0.54	1109
23	large intestine	73.8	0.72	1088
24	tooth	14.4	0.07	2180
25	grey_matter	70.1	0.60	1045
26	eye lens	41.7	0.32	1076
27	outer lung	61.9	0.59	1050
28	small intestine	83.4	1.72	1030
29	eye sclera	63.5	0.93	1032
30	inner lung	28.3	0.32	394
31	pancreas	65.7	0.81	1087
32	blood	71.3	1.26	1050
33	cerebro_spinal_fluid	81.2	2.16	1007
34	eye vitreoushumor	69.1	1.51	1005
35	kidneys	85.0	0.88	1066
36	bone marrow	13.2	0.16	1029
37	bladder	21.4	0.30	1086
38	testicles	70.3	0.94	1082
39	cancellous bone	25.5	0.19	1178

The following table reports the dielectric properties computed for the 39 body tissue materials in the employed human body models at 450 MHz.

#	Tissue	ε_r	σ (S/m)	Density (kg/m^3)
1	bile	72.2	1.71	928
2	body fluid	63.7	1.37	1050
3	eye cornea	58.5	1.21	1051
4	fat	11.6	0.08	911
5	lymph	61.2	0.89	1035
6	mucous membrane	49.2	0.69	1102
7	toe, finger, and nails	13.0	0.10	1908
8	nerve spine	34.9	0.46	1075
9	muscle	56.8	0.81	1090
10	heart	65.0	0.99	1081
11	white matter	41.5	0.46	1041
12	stomach	67.1	1.02	1088
13	glands	61.2	0.89	1028
14	blood vessel	46.6	0.57	1102
15	liver	50.4	0.67	1079
16	gall bladder	60.7	1.15	1071
17	spleen	62.1	1.05	1089
18	cerebellum	54.7	1.06	1045
19	cortical bone	13.0	0.10	1908
20	cartilage	45.0	0.60	1100
21	ligaments	47.0	0.57	1142
22	skin	45.8	0.71	1109
23	large intestine	61.7	0.88	1088
24	tooth	13.0	0.10	2180
25	grey_matter	56.6	0.76	1045
26	eye lens	37.2	0.38	1076
27	outer lung	54.0	0.70	1050
28	small intestine	64.9	1.93	1030
29	eye sclera	57.2	1.02	1032
30	inner lung	23.5	0.38	394
31	pancreas	61.2	0.89	1087
32	blood	63.7	1.37	1050
33	cerebro_spinal_fluid	70.5	2.26	1007
34	eye vitreoushumor	69.0	1.54	1005
35	kidneys	65.0	1.13	1066
36	bone marrow	11.8	0.19	1029
37	bladder	19.6	0.33	1086
38	testicles	62.9	1.04	1082
39	cancellous bone	22.2	0.24	1178

b) The tissue types and dielectric parameters used in the SAR computation are appropriate for determining the highest exposure expected for normal device operation, because they are derived from measurements performed on real biological tissues (XFDTD, Reference Manual Version 6.4, Remcom, Inc.).

c) The tabulated list of the dielectric parameters used in phantom models is provided at point 5(a). As regards the device (car plus antenna), we used perfect electric conductors.

6) Transmitter model implementation and validation

a) The essential features that must be modeled correctly for the particular test device model to be valid are:

- Car body. The car model is very similar to the car used for MPE measurements, so as to be able to correlate measured and simulated field values. This car model has been developed for the SAR computational draft standard IEC/IEEE 62704-2.
- Antenna. We used a straight wire, even when the gain antenna has a base coil for tuning. All the coil does is compensating for excess capacitance due to the antenna being slightly longer than half a wavelength. We do not need to do that in the model, as we used normalization with respect to the net radiated power, which is determined by the input resistance only. In this way, we neglect mismatch losses and artificially produce an overestimation of the SAR, thereby introducing a conservative bias in the model. This simulation model was also validated by comparing the computed and measured near-field distributions in the condition with antenna mounted on the reference ground plane and showed good agreement experimental data [9].
- Antenna location. We used the same location, relative to the edge of the car trunk, the backseat, or the roof, used in the MPE measurements. The following pictures show a lateral and a perspective view of the bystander and passenger model.

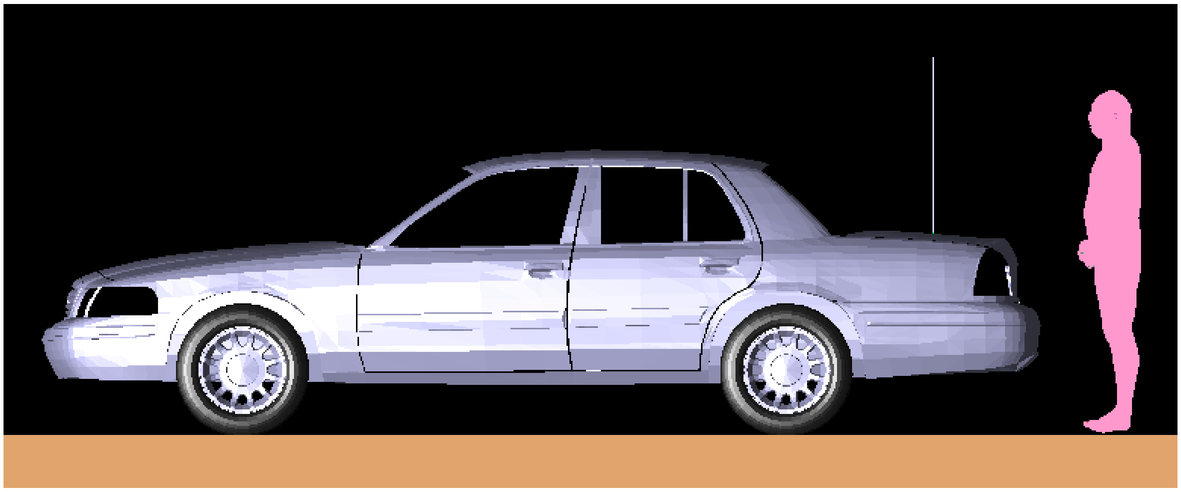

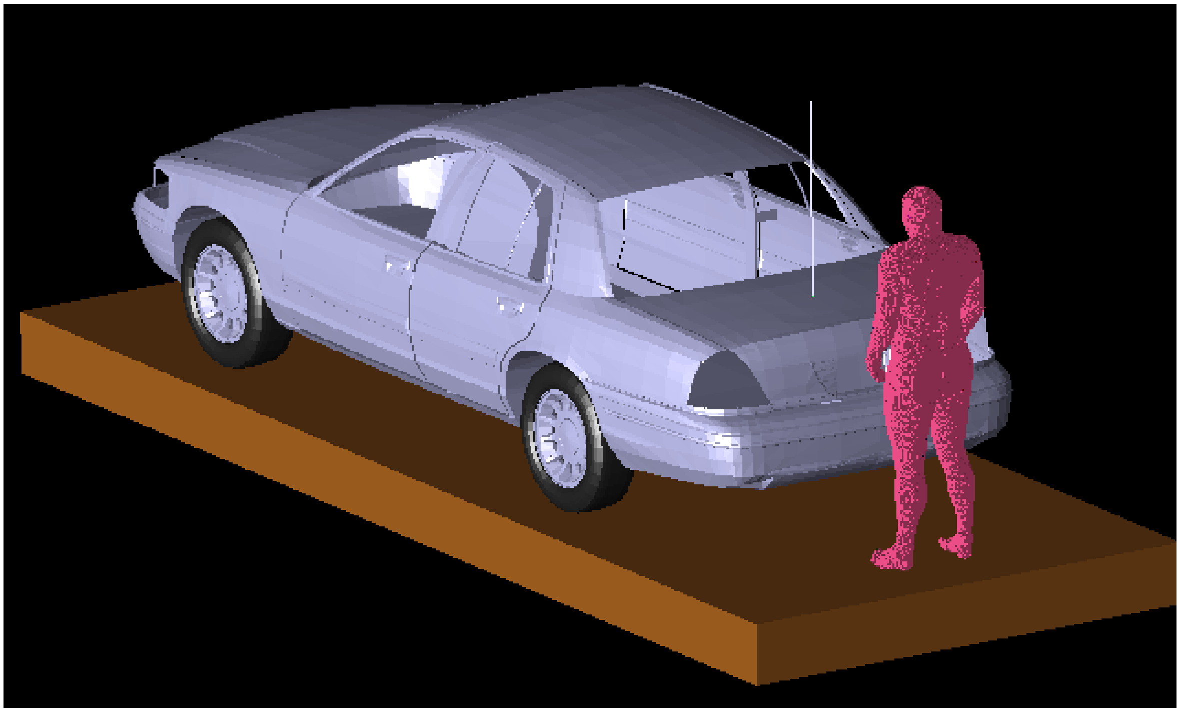

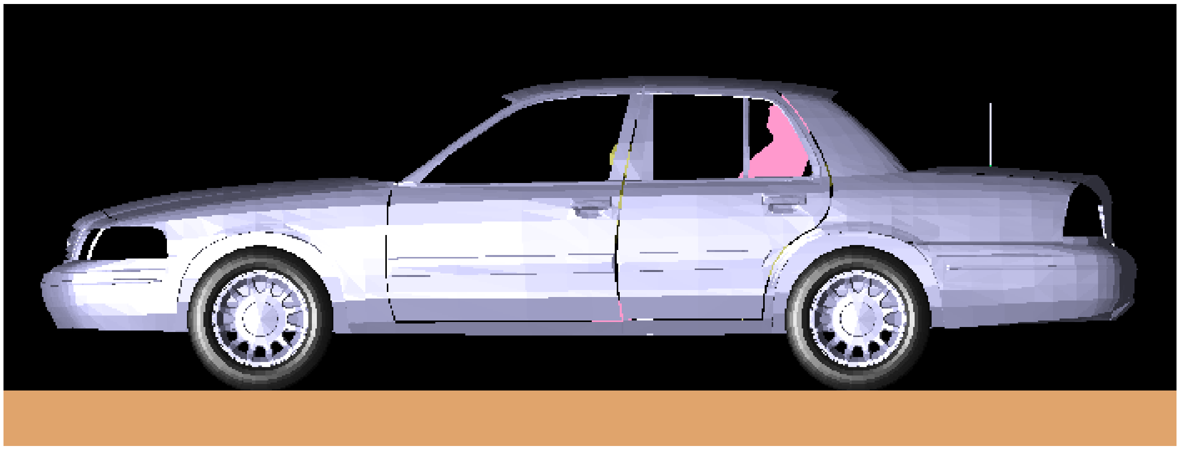

The car model is constituted by perfect electric conductor and does not include wheels in order to reduce its complexity. The passenger model is surrounded by air, as the seat, which is made out of poorly conductive fabrics, is not included in the computational model. The pavement has not been included in the model. The passenger and bystander models were validated for similar antenna and frequency conditions by comparing the MPE measurements at two VHF frequencies (146 MHz and 164 MHz) for antennas used for a VHF mobile radio analyzed previously in 2003 (FCC ID#ABZ99FT3046). The corresponding MPE measurements are reported in the compliance report relative to FCC ID#ABZ99FT3046. The comparison results are presented below, according to following definitions for the equivalent power densities (based on E or H-field):

$$S_E = \frac{|\mathbf{E}|^2}{2\eta}, \quad S_H = \frac{\eta}{2}|\mathbf{H}|^2, \quad \eta = 377\,\Omega$$

<u>Passenger with 43 cm monopole antenna (HAD4009A 164 MHz)</u>

The following figures of the test model show the empty car model, where the red dotted line represents the location of the passenger in the back seat, as it can be observed from the complete model picture above. The comparison has been performed by taking the computed steady-state field values at the red dots locations corresponding to the head, chest, and lower trunk area and comparing them with the corresponding measurements. Such a comparison is carried out at the same average power level (56.5 W) used in the measurements. Steady-state E-field and H-field distributions at a vertical crossing the passenger's head are displayed as well. Finally, a picture of the antenna is shown.

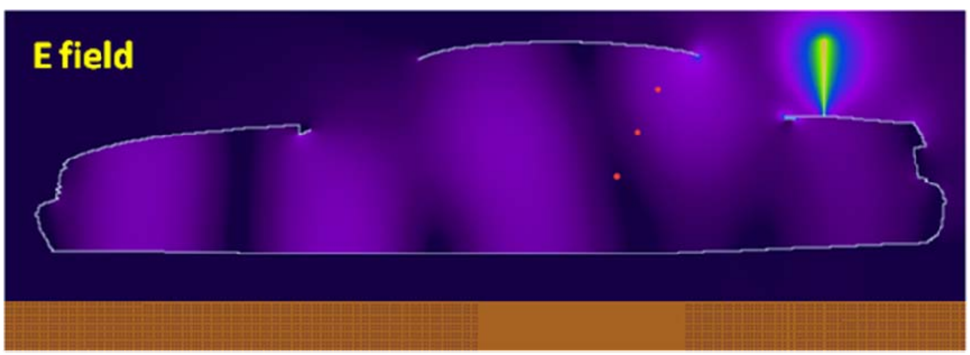

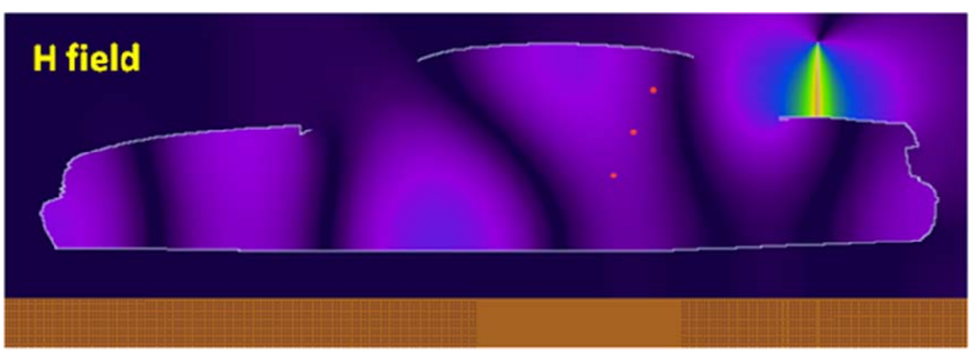

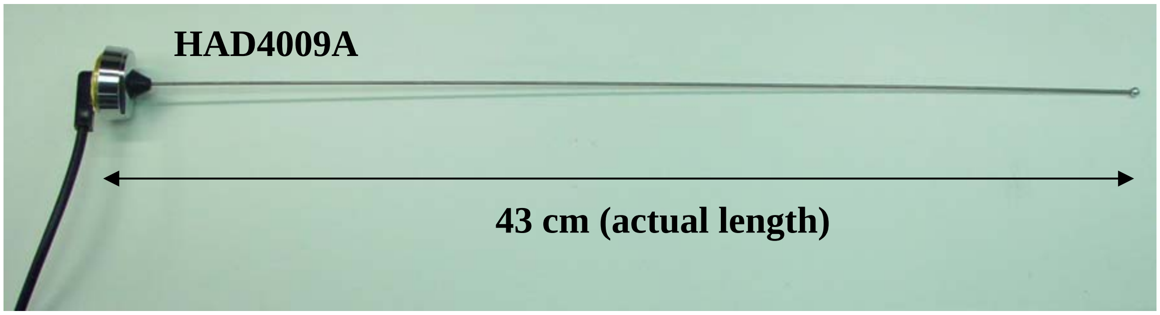

The highest exposure occurs in the middle of the backseat, which is also the case in the measurements. Therefore, the field values were determined on the yellow line centered at the middle of the backseat, approximately at the three locations that are shown by white dots. In actuality, the line is inclined so as to follow the inclination of the passenger's back, as shown previously.

Because the peak exposure occurs in the center of the back seat, that was where we placed the passenger model to perform the SAR evaluations presented in the report. However, it can be observed that the H-field distribution features peaks near the lateral edges of the rear window. That is the reason why we also carried out one SAR computation by placing the passenger laterally in the back seat, in order to determine whether the SAR would be higher in this case.

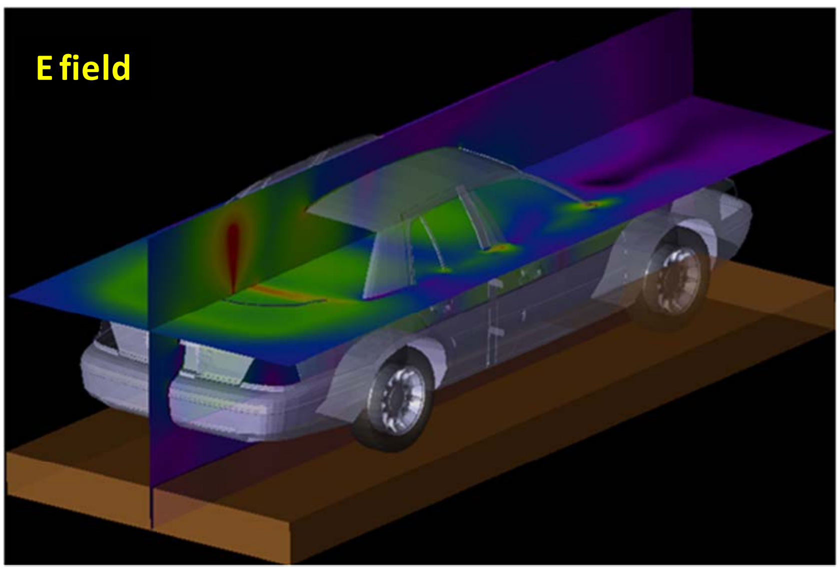

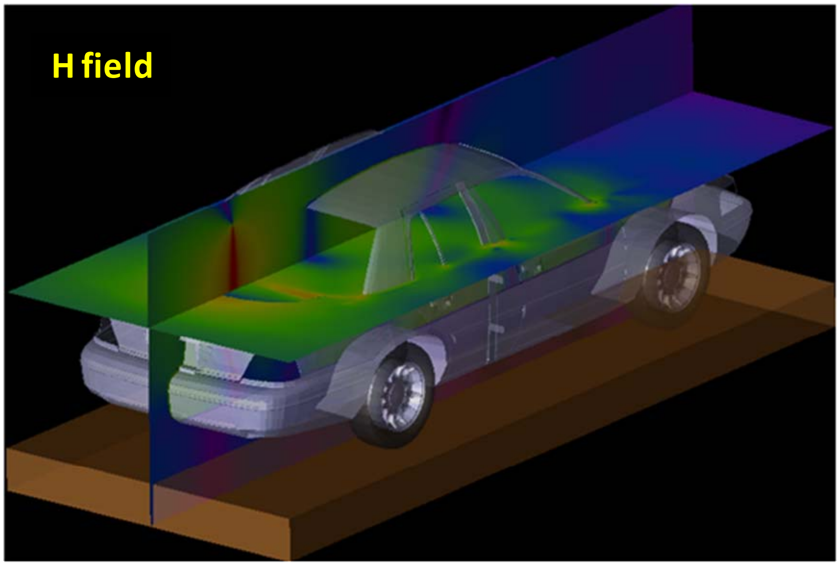

As done in the measurements, the equivalent power density (S) is computed from the E-field, the H-field being much lower. The following table reports the E-field values computed by XFDTD™ at the three locations, and the corresponding power density.

Location	E-field magnitude (V/m)	S (W/m^2)
Head	1.27	2.14E-03
Chest	0.70	6.55E-04
Lower Trunk area	0.20	7.70E-05
	Average S	**9.57E-04**

The input impedance is 24.8-j11.9 ohm, therefore the radiated power (considering the mismatch to the 50 ohm unitary voltage source) is 2.16E-3 W. The scaled-up power density for 56.5 W radiated power is 25.0 W/m^2, corresponding to 2.50 mW/cm^2. Measurements gave an average of 1.29 mW/cm^2, which is a reasonable overestimation considering conservativeness of simulations model. The following table and the graph show a comparison between the simulated power density and the measured one (see also MPE report in FCC ID#ABZ99FT3046, Table 43), normalized to 56.5 W radiated.

Position	SE (meas) mW/cm^2	SE (FDTD) mW/cm^2
Head	2.98	5.59
Chest	0.74	1.71
Lower Trunk	0.14	0.2

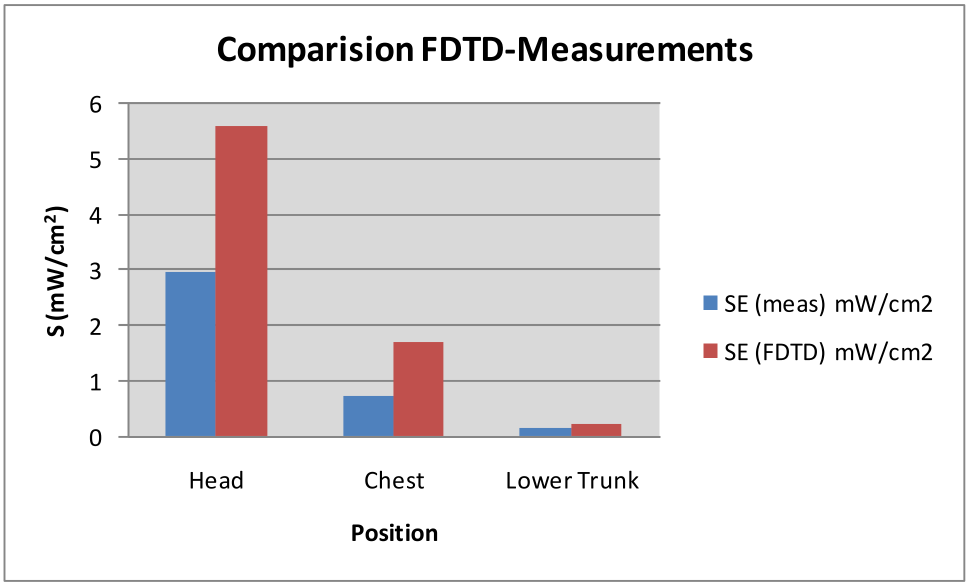

<u>Bystander with 48 cm monopole antenna (HAD4007A 146 MHz)</u>

The following figures show the E-field and H-field distributions across a vertical plane passing for the antenna and cutting the car in half. As done in the measurements, the MPE is computed from both E-field and H-field distributions, along the yellow dotted line at 10 points spaced 20 cm apart from each other up to 2 m in height. These lines and the field evaluation points are approximately indicated in the figures. The E-field and H-field distributions in the vertical plane placed at 60 cm from the antenna, are shown as well. The points where the fields are sampled to determine the equivalent power density (S) are approximately indicated by the white dots. A picture of the antenna is not reported because it is identical to the HAD4009A except for the length.


H field
60 cm
(0 mm, 200 mm, 0 mm)

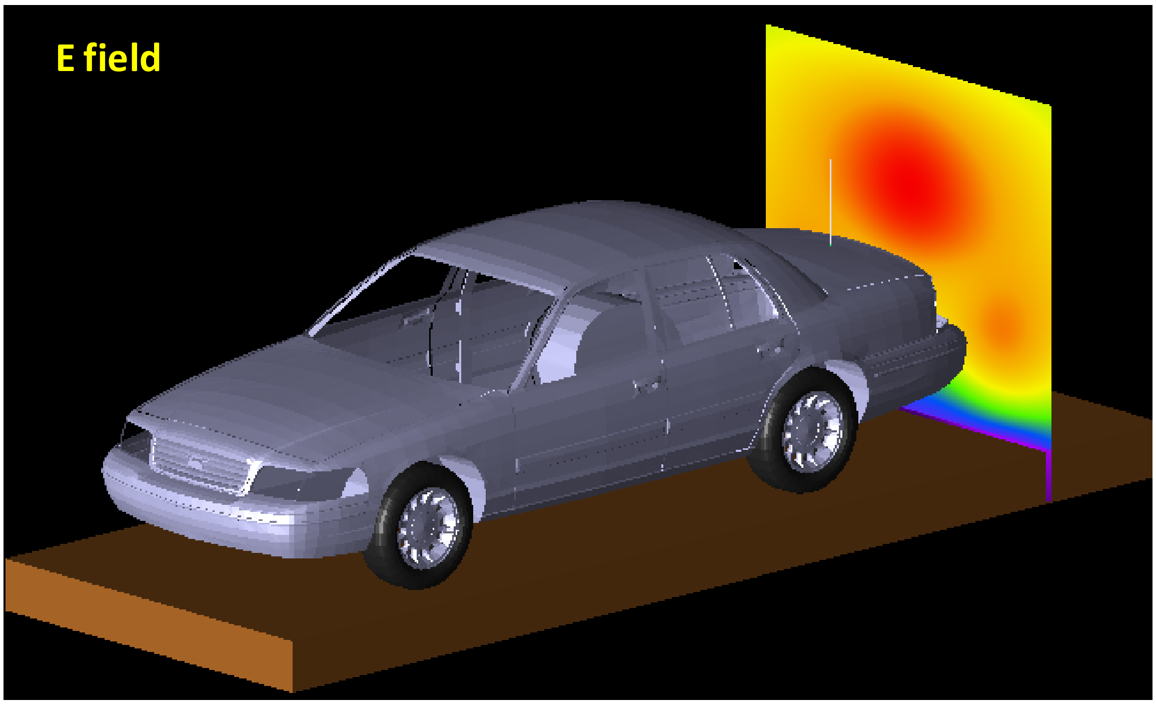
E field

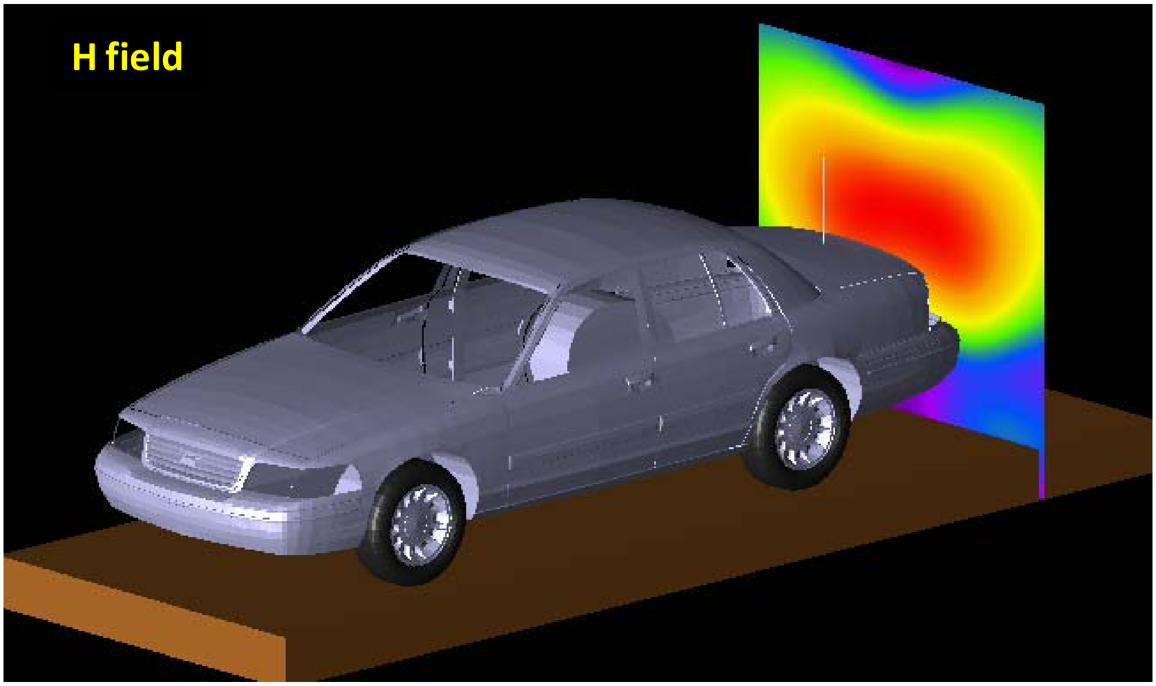

The following table reports the field values computed by XFDTD™ and the corresponding power density values. The average exposure levels are computed as well.

Height (cm)	E (V/m)	S_E (W/m^2)	H (A/m)	S_H (W/m^2)
20	1.84E-01	4.50E-05	5.10E-04	4.89E-05
40	2.71E-01	9.71E-05	6.38E-04	7.68E-05
60	3.58E-01	1.70E-04	1.08E-03	2.20E-04
80	4.42E-01	2.59E-04	1.54E-03	2.20E-04
100	5.85E-01	4.55E-04	1.82E-03	4.48E-04
120	6.86E-01	6.24E-04	1.85E-03	6.23E-04
140	6.82E-01	6.17E-04	1.58E-03	6.42E-04
160	5.93E-01	4.67E-04	1.16E-03	4.72E-04
180	4.63E-01	2.84E-04	7.67E-04	2.52E-04
200	3.41E-01	1.55E-04	4.94E-04	1.11E-04
	Average S_E	**3.17E-04**	**Average S_H**	**3.11E-04**

The input impedance is 33.7-j3.0 ohm, therefore the radiated power (considering the mismatch to the 50 ohm unitary voltage source) is 2.40E-3 W. The scaled-up power density values for 53.2 W radiated power are 7.03 W/m^2 (E), and 6.90 W/m^2 (H), that correspond to 0.70 mW/cm^2 (E), and 0.69 mW/cm^2 (H). Measurements yielded average power density of 0.664 mW/cm^2 (E), and 0.471 mW/cm^2 (H), i.e., which are in good agreement with the simulations. The following table and graph show a comparison between the simulated power density and the measured one, based on E (see MPE report in FCC ID#ABZ99FT3046, Table 1) or H fields (see MPE report in FCC ID#ABZ99FT3046, Table 13), normalized to 53.2 W radiated.

Height (cm)	SE (meas) mW/cm^2	SE (FDTD) mW/cm^2	SH (meas) mW/cm^2	SH (FDTD) mW/cm^2	Avg SE meas mW/cm^2	Avg SE FDTD mW/cm^2	Avg SH meas mW/cm^2	Avg SH FDTD mW/cm^2
20	0.19	0.10	0.2	0.11	0.664	0.703	0.471	0.690
40	0.37	0.22	0.23	0.17				
60	0.55	0.38	0.3	0.49				
80	0.68	0.57	0.56	0.49				
100	1.02	1.01	1.07	0.99				
120	1.15	1.38	1.1	1.38				
140	1.04	1.37	0.56	1.42				
160	0.79	1.03	0.24	1.05				
180	0.5	0.63	0.23	0.56				
200	0.35	0.34	0.22	0.25				

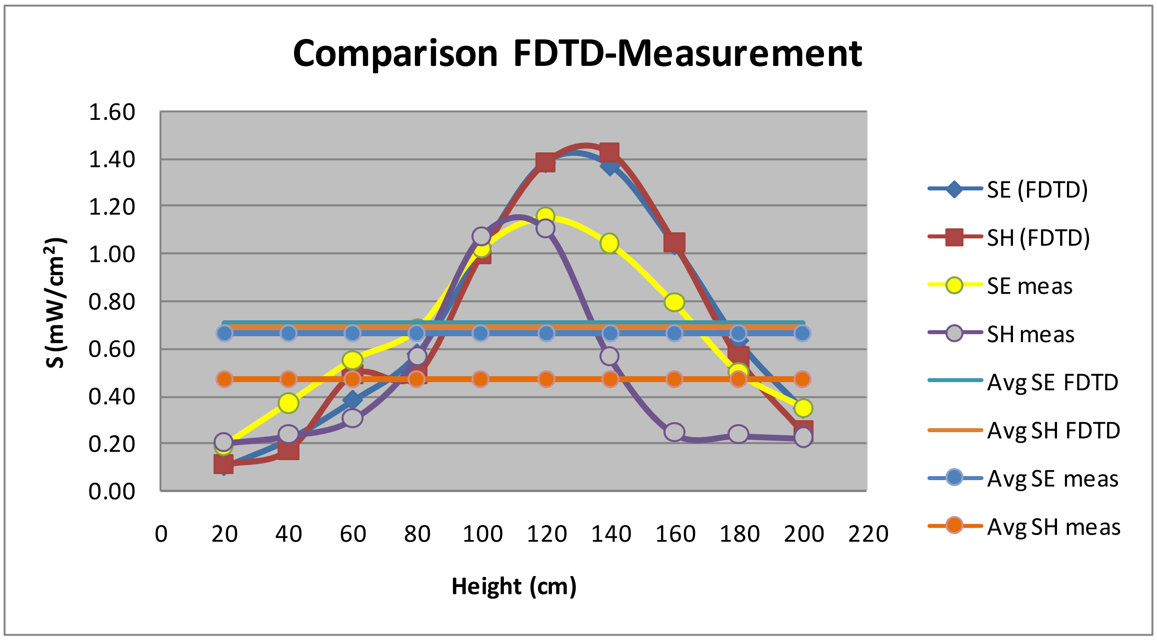

Passenger with 17.5 cm monopole antenna (HAE4002A 421.5 MHz)

The following figure of the test model shows the car model, where the red dots individuate the back seat, as it can be observed from the other figure showing the cross section of the passenger. The comparison has been performed by taking the average of the computed steady-state field values at the six dotted locations, corresponding to the head, chest, and legs along the red dots line, and comparing them with the average of the MPE measurements performed at the head, chest and legs locations. Such a comparison is carried out at the same average power level (22 W, including the 50% duty factor) used in the MPE measurements.

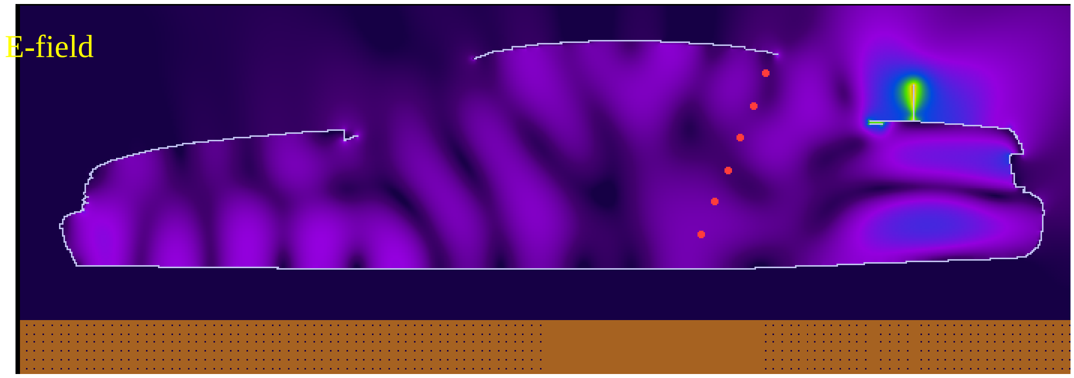

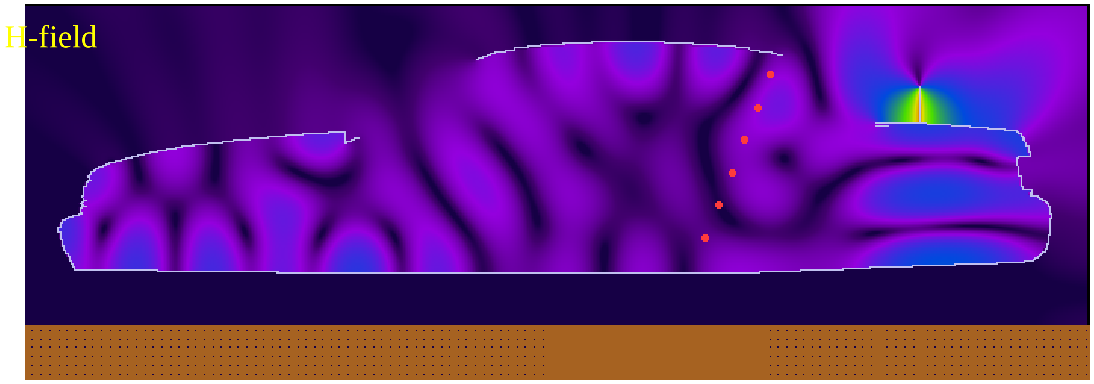

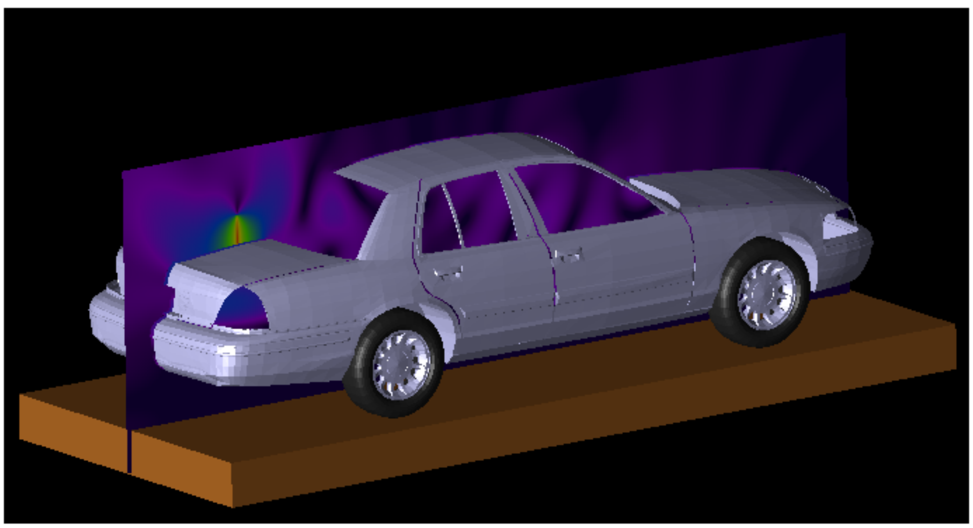

The equivalent power density (S) is computed from the E-field and the H-field separately. The following table reports the E-field values computed by XFDTD™ at the six locations, and the corresponding power density.

Location Number	E-field, V/m	Eq. Power Density 1.0 V source	Scaled Power Dens. 22 W output, mW/cm^2
1	3.11E-01	1.28E-04	1.56E-01
2	4.16E-01	2.29E-04	2.79E-01
3	5.25E-01	3.65E-04	4.45E-01
4	3.86E-01	1.98E-04	2.41E-01
5	3.84E-01	1.96E-04	2.39E-01
6	6.01E-01	4.80E-04	5.85E-01
Equivalent average Power Density			**3.24E-01**

Location Number	H-field, Weber/m2	Eq. Power Density 1.0 V source	Scaled Power Dens. 22 W output, mW/cm^2
1	1.34E-03	3.37E-04	4.11E-01
2	1.08E-03	2.21E-04	2.70E-01
3	5.59E-04	5.89E-05	7.18E-02
4	5.45E-04	5.60E-05	6.82E-02
5	5.45E-04	5.59E-05	6.82E-02
6	5.23E-04	5.16E-05	6.29E-02
Equivalent average Power Density			**1.59E-01**

The radiated power (considering the mismatch to the 50 ohm unitary voltage source) is 1.81E-3 W, therefore a factor equal to 12188 is required to scale up to 22 W radiated. The corresponding scaled-up power densities are reported in the tables above, which show that the simulation overestimates the average power density from the MPE measurements (0.297 mW/cm^2), as derived from the measured E-field reported in the following table:

Position	**SE (meas), 22 W output mW/cm^2**
Head	0.38
Chest	0.33
Lower Trunk	0.16

The simulations tend to overestimate the average power density levels, which is understandable since there are no ohmic losses and perfect impedance matching is enforced in the computational models. Based on these results, we conclude that the simulation will produce slight exposure overestimates (about 9%).

b) Descriptions and illustrations showing the correspondence between the modeled test device and the actual device, with respect to shape, size, dimensions and near-field radiating characteristics, are found in the main report.

c) Verification that the test device model is equivalent to the actual device for predicting the SAR distributions descends from the fact that the car and antenna size and location in the numerical model correspond to those used in the measurements.

d) The peak SAR is in the neck region for the passenger, which is in line with MPE measurements and predictions.

Passenger with 63.5 cm monopole antenna (HAE6010A 425 MHz)

The following figures show the car model with the field distribution in the horizontal planes where the MPE measurements have been performed. The comparison has been performed by taking the average of the computed steady-state field values at the three locations, corresponding to the head, chest, and lower trunk, and comparing them with the average of the MPE measurements performed at the head, chest and lower trunk locations. Such a comparison is carried out at the same average power level (61.5 W, including the 50% duty factor) used in the MPE measurements.

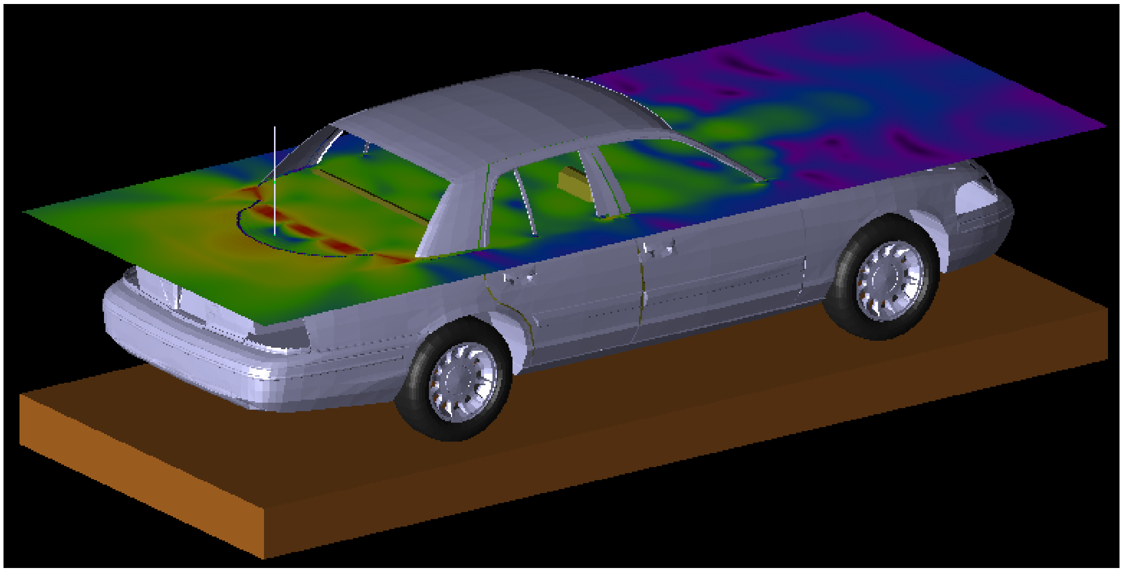

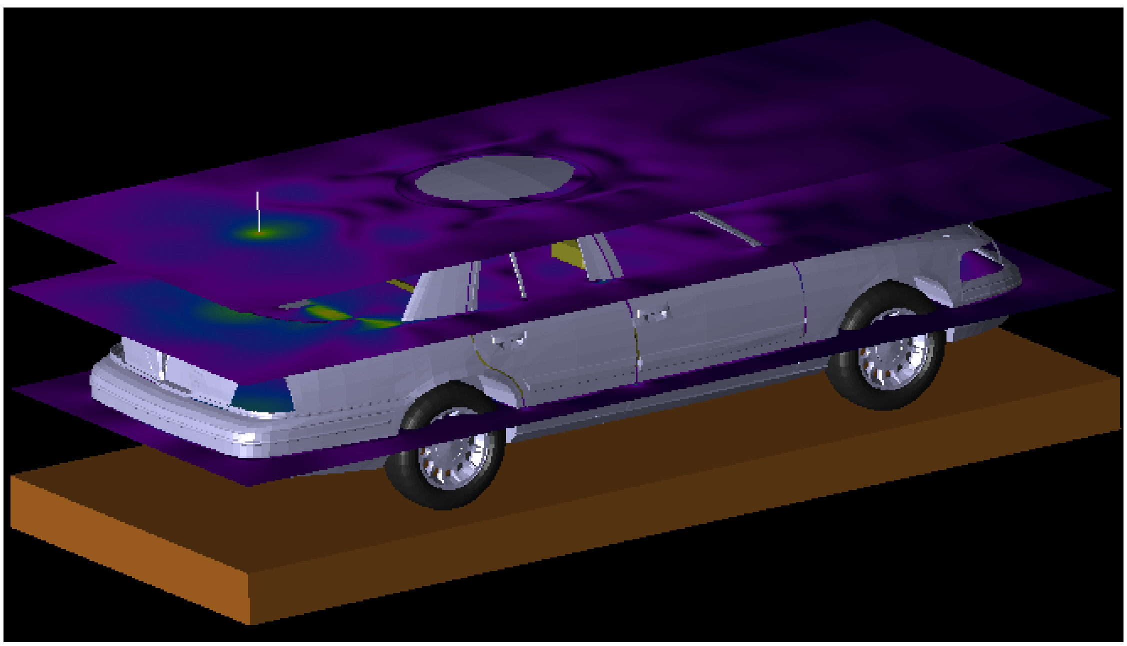

The equivalent power density (S) is computed from the E-field. The following table reports the E-field values computed by XFDTD™ at the three locations, and the corresponding power density.

Location Number	E-field, V/m	Eq. Power Density 1.0 V source	Scaled Power Dens. 61.5 W output, mW/cm^2
1	2.26E-01	6.76E-05	0.74
2	3.60E-01	1.72E-04	1.89
3	1.40E-01	2.59E-05	0.28
Equivalent average Power Density			**0.97**

The corresponding scaled-up power densities are reported in the tables above, which show that the simulation overestimates the average power density from the MPE measurements (0.52 mW/cm^2), as derived from the measured E-field reported in the following table:

Position	SE (meas), 60 W output mW/cm^2
Head	0.72
Chest	0.64
Lower Trunk	0.19

The simulations tend to overestimate the average power density levels, which is understandable since there are no ohmic losses and perfect impedance matching is enforced in the computational models. Based on these results, we conclude that the simulation will produce exposure overestimates (about 88%).

Bystander with 29 cm monopole antenna (HAE6013A 425 MHz)

The following figures show the E-field and H-field distributions across a vertical plane passing for the antenna and cutting the car in half. As done in the measurements, the MPE is computed from both E-field and H-field distributions, along the yellow dotted line at 10 points spaced 20 cm apart from each other up to 2 m in height. These lines and the field evaluation points are approximately indicated in the figures. The E-field and H-field distributions in the vertical plane placed at 90 cm from the antenna, behind the case, are shown as well. The points where the fields are sampled to determine the equivalent power density (S) are approximately indicated by the white dots. A picture of the antenna is not reported because it is identical to the HAE6013A.

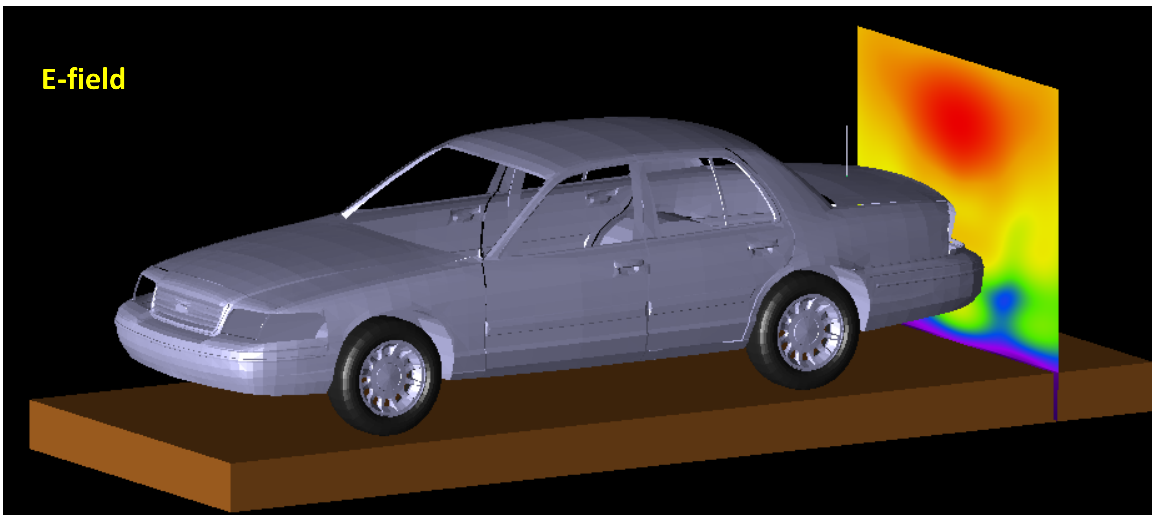

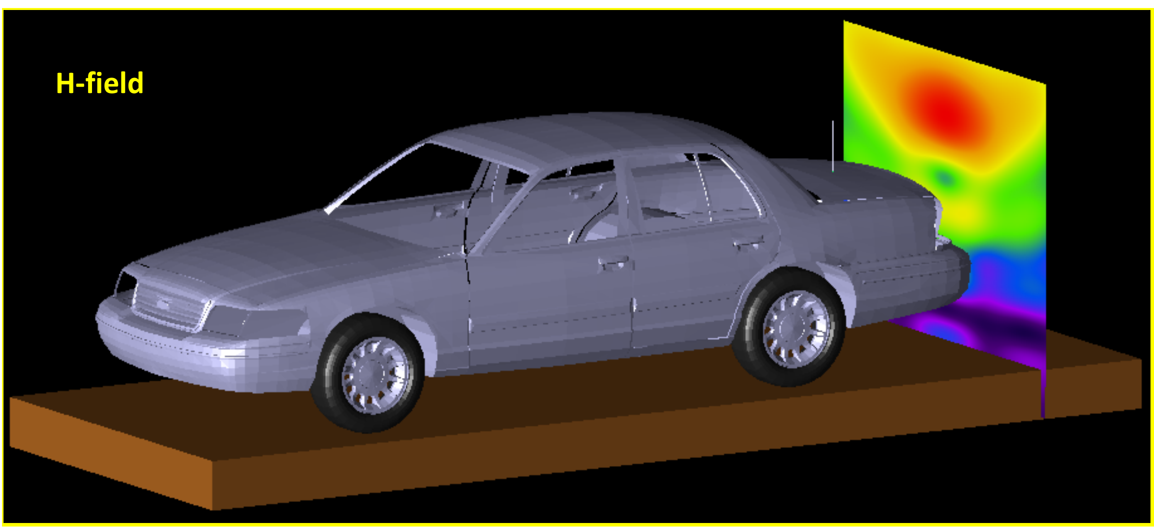

The following table reports the field values computed by XFDTD™ for the 1.0 V source and the corresponding power density values. The average exposure levels are computed as well.

Height (cm)	E (V/m)	S_E (W/m^2)	H (A/m)	S_H (W/m^2)
0	5.67E-02	4.27E-06	3.11E-04	1.83E-05
20	1.40E-01	2.59E-05	1.78E-04	5.96E-06

40	1.24E-01	2.03E-05	4.29E-04	3.47E-05
60	1.69E-01	3.79E-05	3.88E-04	2.84E-05
80	1.52E-01	3.08E-05	4.74E-04	4.24E-05
100	1.87E-01	4.65E-05	3.71E-04	2.59E-05
120	2.56E-01	8.67E-05	6.23E-04	7.31E-05
140	2.71E-01	9.73E-05	7.50E-04	1.06E-04
160	2.60E-01	8.94E-05	7.33E-04	1.01E-04
180	2.00E-01	5.31E-05	5.40E-04	5.50E-05
Average S_E		**4.92E-05**	**Average S_H**	**4.91E-05**

Since the conducted power during the MPE measurement was 123 W the calculated power density was then scaled up for 61.5 W radiated power (taking into account 50% talk time). This model does not include the mismatch loss, loss in the cable and finite conductivity of the car surface and as represents a conservative model for exposure assessment. The scaled-up power density values for 61.5 W radiated power are 6.03 W/m^2 (E), and 6.02 W/m^2 (H), that correspond to 0.603 mW/cm^2 (E), and 0.602 mW/cm^2 (H). Measurements yielded average power density of 0.309 mW/cm^2 (E), which shows that the calculated power density is overestimated. The following graph shows a comparison between the measured power density and the simulated one, based on E or H fields, normalized to 61.5 W radiated power.

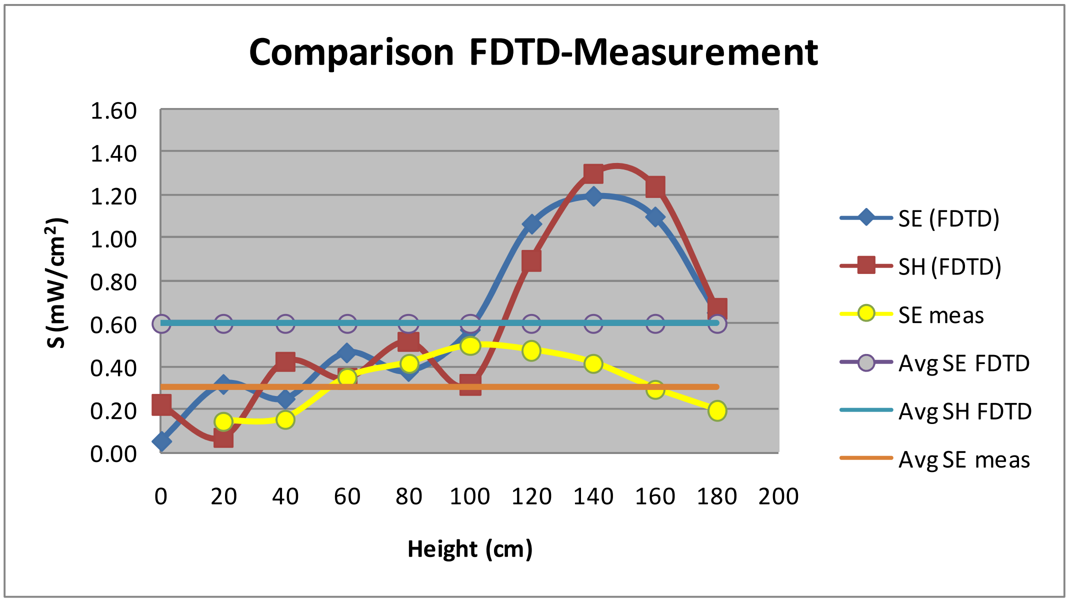

<u>Bystander with 63.5 cm monopole antenna (HAE6010A 425 MHz)</u>

The following figures show the E-field and H-field distributions across a vertical plane passing for the antenna and cutting the car in half. As done in the measurements, the MPE is computed from both E-field and H-field distributions, along the yellow dotted line at 10 points spaced 20 cm apart from each other up to 2 m in height. These lines and the field evaluation points are approximately indicated in the figures. The E-field and H-field distributions in the vertical plane placed at 90 cm from the antenna, behind the case, are shown as well. The points where the fields are sampled to determine the equivalent power density (S) are approximately indicated by the white dots. A picture of the antenna is not reported because it is identical to the HAE6010A.

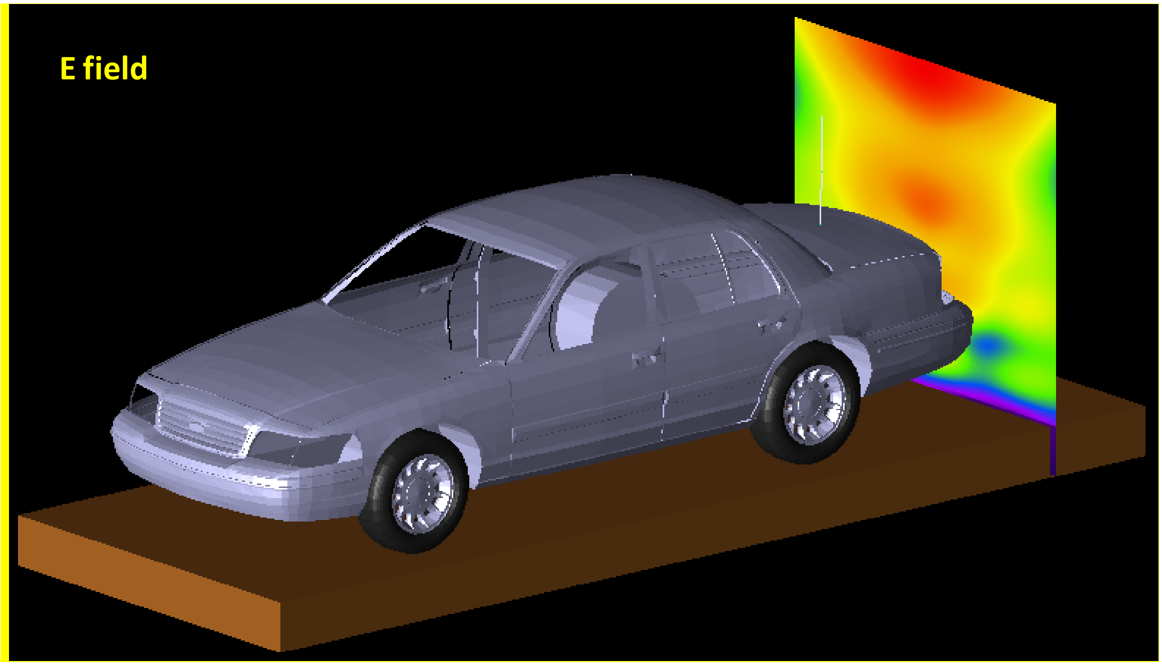

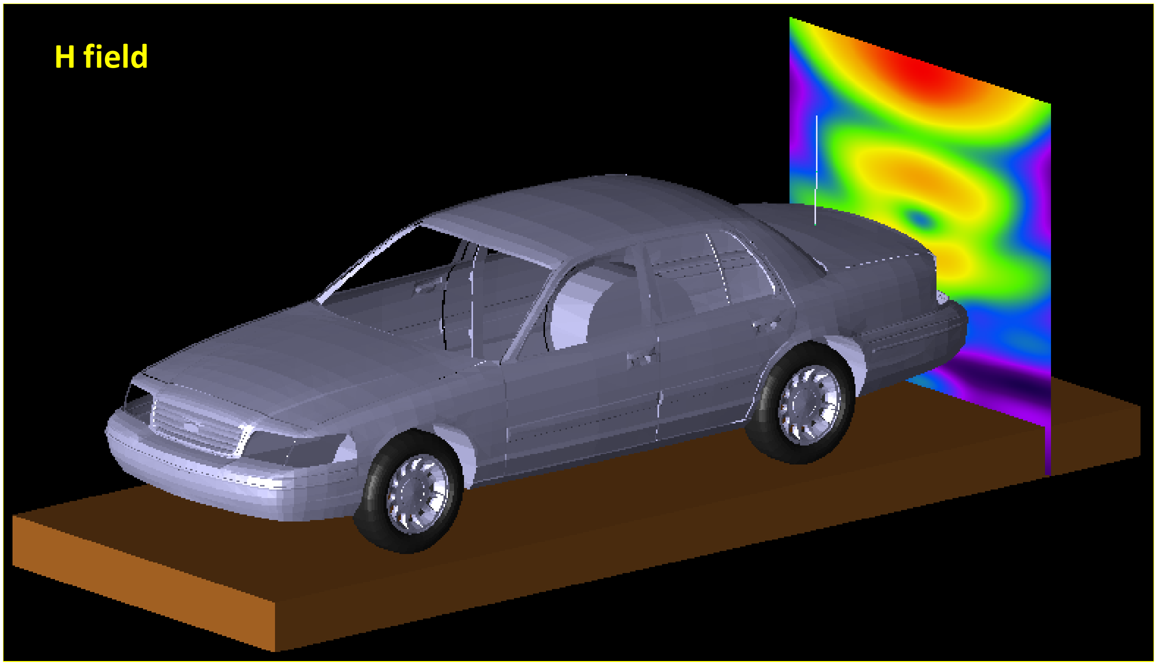

The following table reports the field values computed by XFDTD™ and the corresponding power density values. The average exposure levels are computed as well.

Height (cm)	E (V/m)	S_E (W/m^2)	H (A/m)	S_H (W/m^2)
0	7.55E-02	7.56E-06	4.13E-04	3.21E-05
20	1.79E-01	4.27E-05	2.37E-04	1.06E-05
40	1.56E-01	3.21E-05	5.49E-04	5.69E-05
60	2.12E-01	5.96E-05	4.84E-04	5.69E-05
80	1.78E-01	4.22E-05	5.65E-04	4.42E-05
100	2.07E-01	5.66E-05	3.43E-04	6.03E-05
120	1.99E-01	5.25E-05	5.34E-04	2.21E-05
140	1.70E-01	3.85E-05	4.20E-04	5.37E-05
160	2.18E-01	6.32E-05	5.10E-04	3.33E-05
180	1.80E-01	4.30E-05	8.15E-04	4.90E-05
Average S_E		**4.38E-05**	**Average S_H**	**4.19E-05**

Since the conducted power during the MPE measurement was 123 W the calculated power density was then scaled up for 61.5 W radiated power (taking into account 50% talk time). This model does not include the mismatch loss, loss in the cable and finite conductivity of the car surface and as represents a conservative model for exposure assessment. The scaled-up power density values for 61.5 W radiated power are 4.26 W/m^2 (E), and 4.07 W/m^2 (H), that correspond to 0.426 mW/cm^2 (E), and 0.407 mW/cm^2 (H). Measurements yielded average power density of 0.204 mW/cm^2 (E), which shows that the calculated power density is overestimated. The following graph shows a comparison between the measured power density and the simulated one, based on E or H fields, normalized to 61.5 W radiated power.

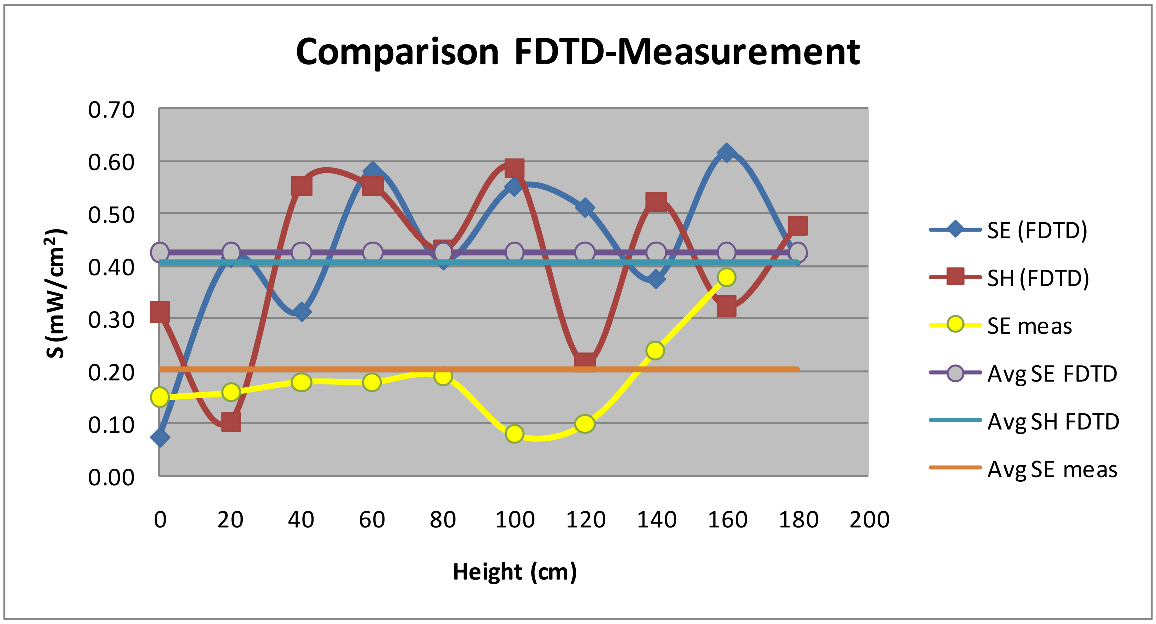
Comparison FDTD-Measurement
S (mW/cm²)
0.70
0.60
0.50
0.40
0.30
0.20
0.10
0.00
0
20
40
60
80
100
120
140
160
180
200
Height (cm)
SE (FDTD)
SH (FDTD)
SE meas
Avg SE FDTD
Avg SH FDTD
Avg SE meas

7) Test device positioning

a) A description of the device test positions used in the SAR computations is provided in the SAR report.

b) Illustrations showing the separation distances between the test device and the phantom for the tested configurations are provided in the SAR report.

8) Steady state termination procedures

a) The criteria used to determine that sinusoidal steady-state conditions have been reached throughout the computational domain for terminating the computations are based on the monitoring of field points to make sure they converge. The simulation projects were set to automatically track the field values throughout computational domain by means of XFDTD simulation control feature which ensures that "*convergence is reached when near-zone data shows a constant amplitude sine wave – when all transients have died down and the only variation left is sinusoidal. In this case "convergence" is tested on the average electric field in the space for its deviation from a pure sine wave. XFDTD automatically places points throughout the space for this purpose*." [XFDTD Reference Manual, version. 6.4 and version 7.2]. This convergence threshold was set to -50 dB.
In addition for at least one passenger and one bystander exposure condition, we placed one "field sensor" near the antenna, others between the body and the domain boundary at different locations, and one inside the head of the model. In all simulations, isotropic E-field sensors were placed at opposite sides of the computational domain. We used isotropic E and H field "sensors", meaning that all three components of the fields are monitored at these points. The following figures show an example of the time waveforms at the field point sensors in two points of the computational domain. We selected points close to antenna as well as furthest one. The highest field levels are observed for the higher index point, as it is closer to the antenna. In all cases, the field reaches the steady-state condition.

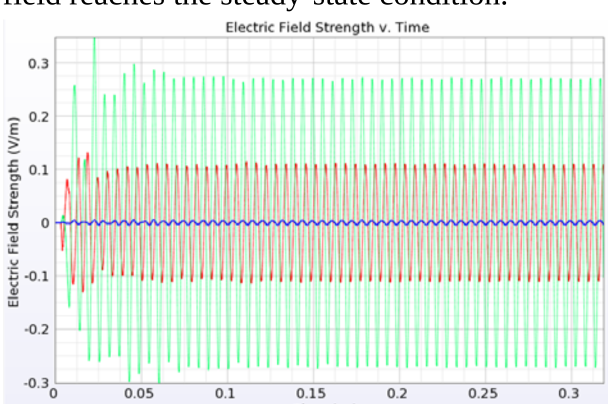

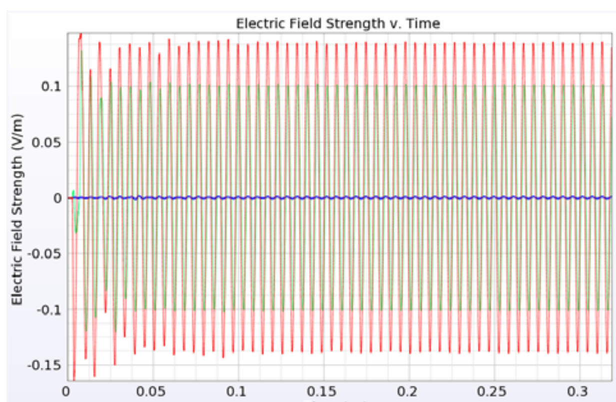

c) The XFDTD™ algorithm determines the field phasors by using the so-called "two-equations two-unknowns" method. Details of the algorithm are explained in [7].

9) Computing peak SAR from field components

a) The SAR for an individual voxel is computed according to the draft IEEE 62704-1 standard. In particular, the three components of the electric field are computed in the center of each voxel and then the SAR is computed as below:

$$SAR = \sigma_{voxel} \frac{|E_x|^2 + |E_y|^2 + |E_z|^2}{2\rho_{voxel}},$$

where σ_{voxel} and ρ_{voxel} are the conductivity and the mass density of the voxel.

10) One-gram and ten-gram averaged SAR procedures

a) XFDTD™ computes the Specific Absorption Rate (SAR) in each complete cell containing lossy dielectric material and with a non-zero material density. Using the SAR values computed for each voxel of the model the averaging calculation employs the method and specifications defined in the draft IEEE 62704-1 standard to generate one-gram and ten-gram average SAR.

11) Total computational uncertainty – We derived an estimate for the uncertainty of FDTD methods in evaluating SAR by referring to [6]. In Fig. 7 in [6] it is shown that the deviation between SAR estimates using the XFDTD™ code and those measured with a compliance system are typically within 10% when the probe is away from the phantom surface so that boundary effects are negligible. In that example, the simulated SAR always exceeds the measured SAR.

As discussed in 6(a), a conservative bias has been introduced in the model so as to reduce concerns regarding the computational uncertainty related to the car modeling, antenna modeling, and phantom modeling. The results of the comparison between measurements and simulations presented in 6(a) suggest that the present model produces an overestimate of the exposure between 4% and 36%. Such a conservative bias should eliminate the need for including uncertainty considerations in the SAR assessment.

12) Test results for determining SAR compliance

a) Illustrations showing the SAR distribution of dominant peak locations produced by the test transmitter, with respect to the phantom and test device, are provided in the SAR report.

b) The input impedance and the total power radiated under the impedance match conditions that occur at the test frequency are provided by XFDTD™. XFDTD™ computes the input impedance by following the method outlined in [8], which consists in performing the integration of the steady-state magnetic field around the feed point edge to compute the steady-state feed point current (*I*), which is then used to divide the feed-gap steady-state voltage (*V*). The net average radiated power is computed as

$$P_{XFDTD} = \frac{1}{2}\mathrm{Re}\left\{VI^{*}\right\}$$

Both the input impedance and the net average radiated power are provided by XFDTD™ at the end of each individual simulation.

We normalize the SAR to such a power, thereby obtaining SAR per radiated Watt (*normalized SAR*) values for the whole body and the 1-g SAR. Finally, we multiply such normalized SAR values times the max power rating of the device under test. In this way, we obtain the exposure metrics for 100% talk-time, i.e., without applying source-based time averaging.

c) For mobile radios, 50% source-based time averaging is applied by multiplying the SAR values determined at point 12(b) times a 0.5 factor.

REFERENCES

[1] K. S. Yee, "Numerical Solution of Initial Boundary Value Problems Involving Maxwell's Equations in Isotropic Media," *IEEE Transactions on Antennas and Propagation*, vol. 14, no. 3, 302-307, March 1966.

[2] Z. P. Liao, H. L. Wong, G. P. Yang, and Y. F. Yuan, "A transmitting boundary for transient wave analysis," Scientia Sinica, vol. 28, no. 10, pp 1063-1076, Oct. 1984.

[3] Validation exercise: Mie sphere. Remcom Inc. (enclosed PDF)

Remcom.pdf

[4] NEC-Win PRO ™ v 1.1, Nittany Scientific, Inc., Riverton, UT.

[5] C. M. Collins and M. B. Smith, "Calculations of B1 distribution, SNR, and SAR for a surface coil against an anatomically-accurate human body model," *Magn. Reson. Med.*, 45:692-699, 2001. (enclosed TIF)

Collins & Smith.pdf

[6] Martin Siegbahn and Christer Törnevik, "Measurements and FDTD Computations of the IEEE SCC 34 Spherical Bowl and Dipole Antenna," Report to the IEEE Standards Coordinating Committee 34, Sub-Committee 2, 1998. (enclosed PDF)

Ericsson.pdf

[7] C. M. Furse and O. P. Gandhi, “Calculation of electric fields and currents induced in a millimeter-resolution human model at 60 Hz using the FDTD method with a novel time-to-frequency-domain conversion**,”** Antennas and Propagation Society International Symposium, 1996. (enclosed PDF)

Furse & Gandhi.pdf

[8] *The Finite Difference Time Domain Method for Electromagnetics*, Chapter 14.2, by K. S. Kunz and R. J. Luebbers, CRC Press, Boca Raton, Florida, 1993.

[9] *Validation of Mobile Antenna Modeling by Comparison with Near-field Measurements*,” Report to the IEEE Standards Coordinating Committee 34, Sub-Committee 2, 2006. (enclosed PDF)

IEEE1528_2_vld.pdf

[10] *Antenna Theory: analysis and design*, Chapter 4, by C. A. Balanis, 2nd ed. John Wiley & Sons, Inc.

[11] S. Gabriel, R. W. Lau, and C. Gabriel. 1996. The dielectric properties of biological tissues: III. Parametric models for the frequency spectrum of tissues. Phys. Med. Biol. 41:2271–2293.

[12] "Validation of the HAF4013A and HAF4017A antenna Models", Internal report, G. Bit-Babik, 2012

HAF4013A_and_HAF4017A models.pdf